Advanced spacecraft attitude control and dynamics

Anton V. Doroshin
doran@inbox.ru

Samara National Research University

Outline

- **Part 1 -** Introduction to the attitude dynamics and control

- **Part 2 -** Research results:
  - the variable structure/mass/inertia dual-spin spacecraft attitude motion
  - regular and chaotic dynamics of Dual-Spin Cpacecraft (DSSC)

- Conclusion

Part 1 - Introduction to Attitude Dynamics and Control

Most of the spacecraft have instruments or antennas that must be pointed in specific directions:

– The Hubble must point its main telescope

– Communications satellites must point their antennas

The orientation of the spacecraft in the space is called its attitude

To control the attitude, the spacecraft operators must have the ability to

– Determine the current attitude (sensors…)

– Determine the error between the current and desired attitudes

– Apply torques to remove the error (with the help of actuators…)

The Spacecraft Attitude Stabilization:

- — Spin Stabilization methods
- — Gravity Gradient Stabilization methods
- — Magnetic Stabilization methods
- — Aerodynamic Stabilization methods

Actuators:

- — Reaction Wheel Assemblies (RWAs)
- — Control Moment Gyros (CMGs)
- — Thrusters

Spin stabilization

Spin-stabilization is a method of SC stabilizing in a fixed orientation using rotational motion around SC axis (usually symmetry axis) – “**the gyroscopic effect**”.

The Top

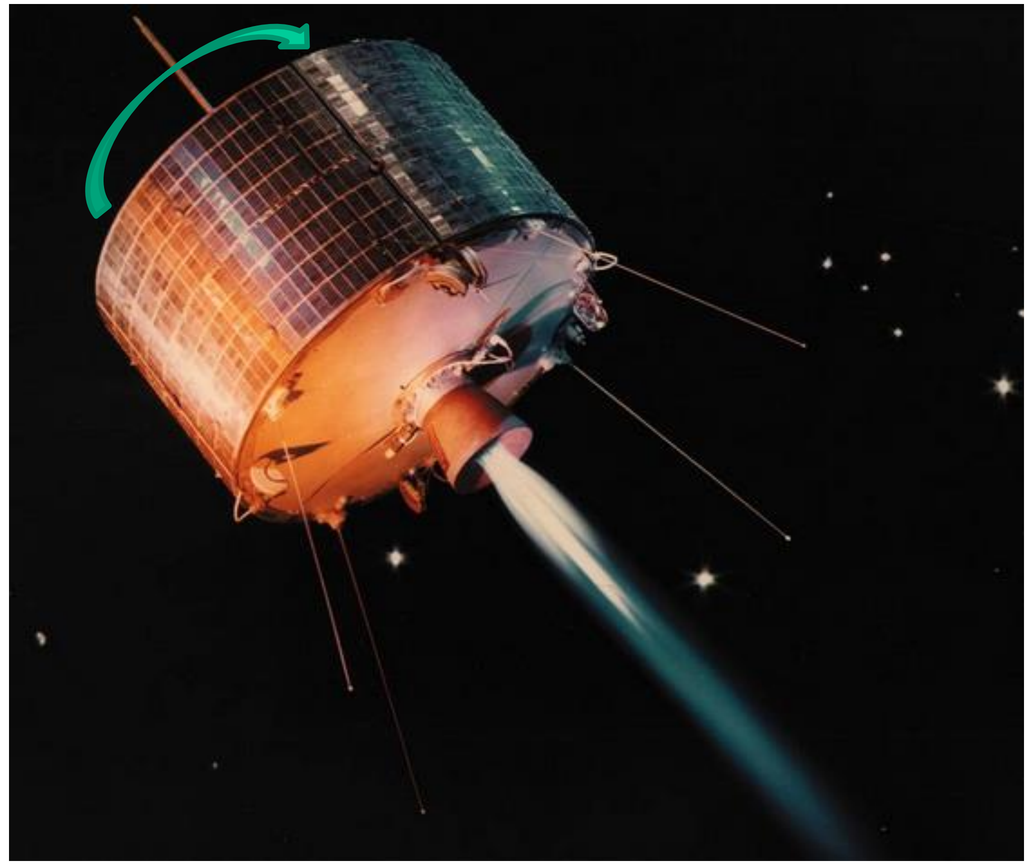

Spin stabilized spacecraft

Spin stabilization

Spin-stabilization is a method of SC stabilizing in a fixed orientation using rotational motion around SC axis (usually symmetry axis) – "**the gyroscopic effect**".

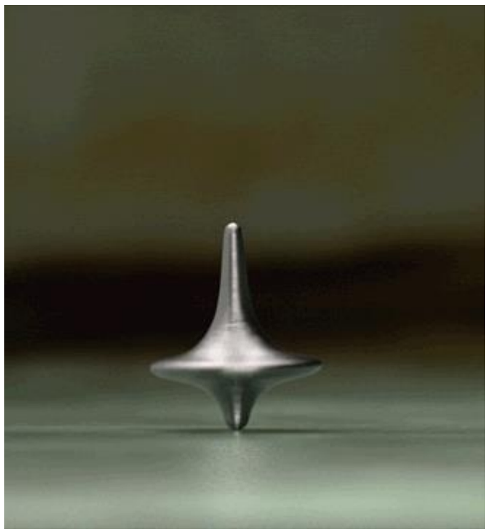

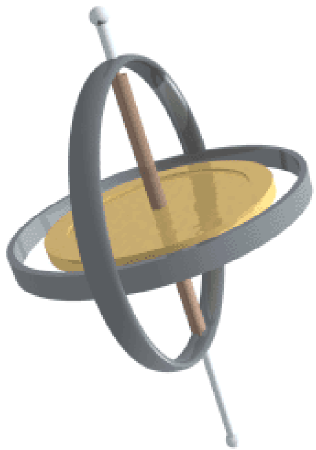

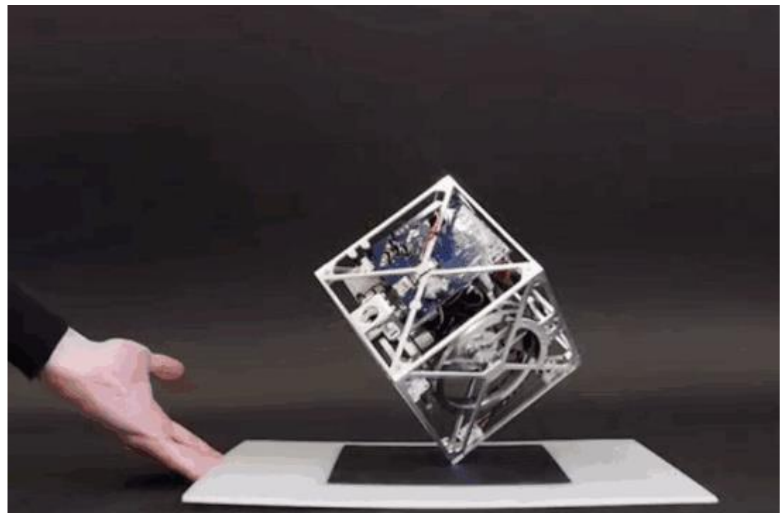

The gyrostats

John L. Junkins, J.D. Turner "Optimal spacecraft rotational maneuvers" (Studies in astronautics; v.3) © Elsevier Science Publishers B.V., 1986

Peter C. Hughes "Spacecraft attitude dynamics".
© John Wiley & Sons. New York, 1986

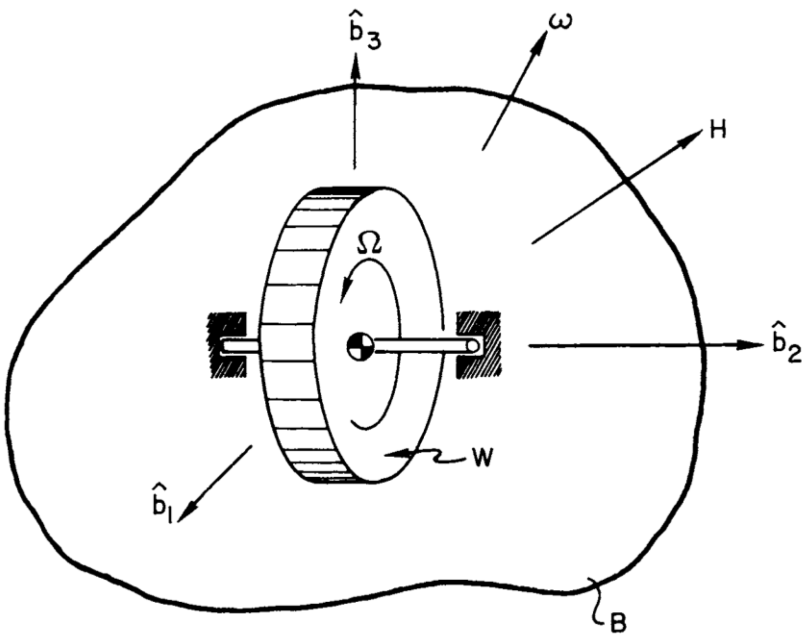

«A Dual-Spin Spacecraft Configuration»

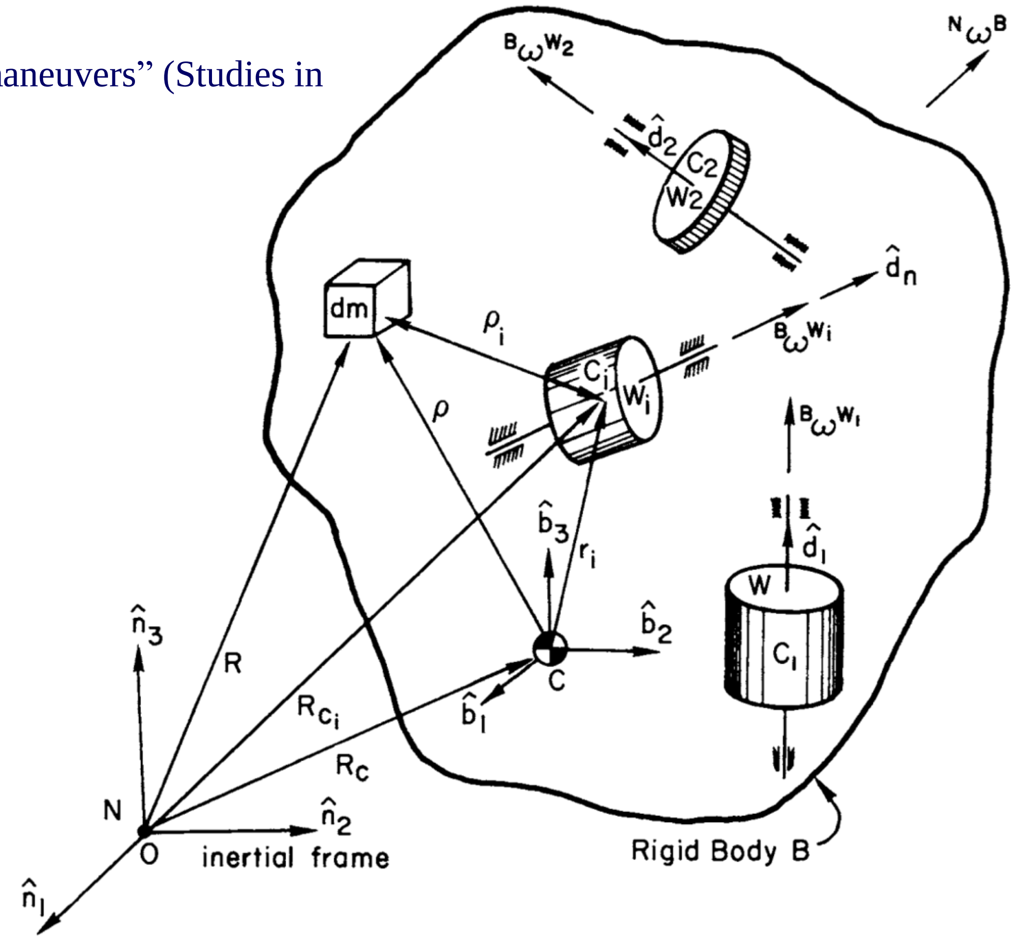

«A General Multi-Spin Spacecraft Configuration»

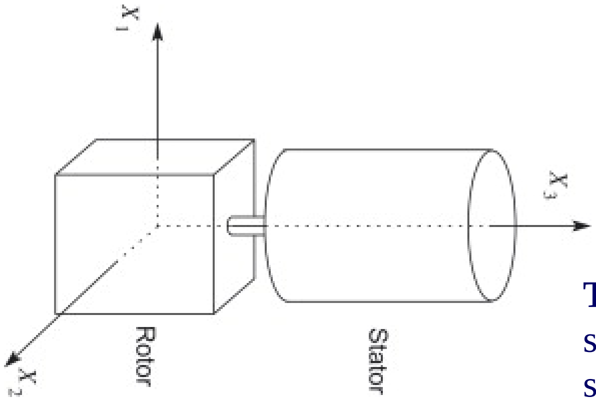

Spin Stabilization
Dual-Spin Spacecraft

TACSAT I : The antenna is the platform, and is intended to point continuously at the Earth, spinning at one evolution per orbit. The cylindrical body is the rotor, providing gyroscopic stability through its 60 RPM spin

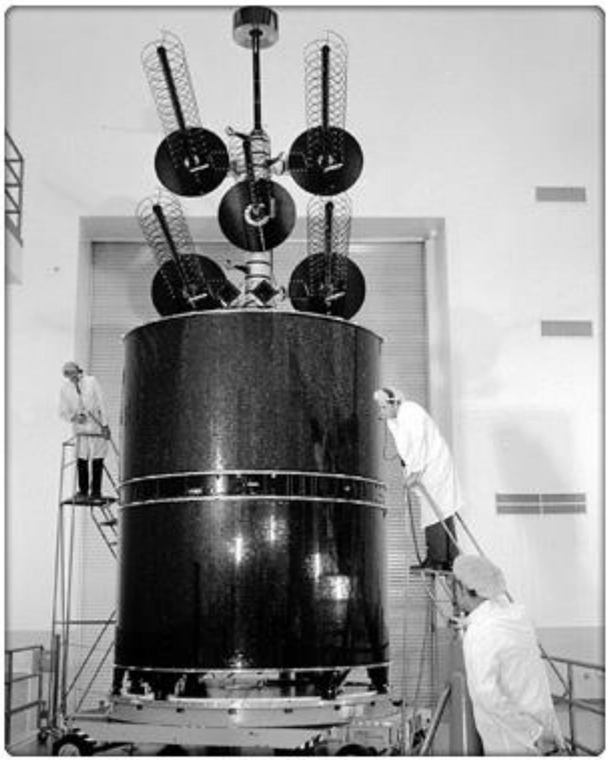

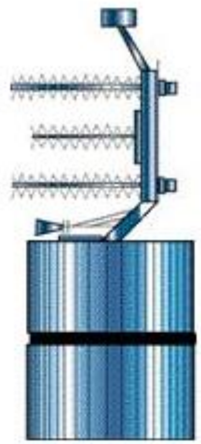

Diameter:
2.81 m (9 ft 3 in)

Overall Height
7.62 m (25 ft)

Weight in orbit
645 kg (1424 lb)

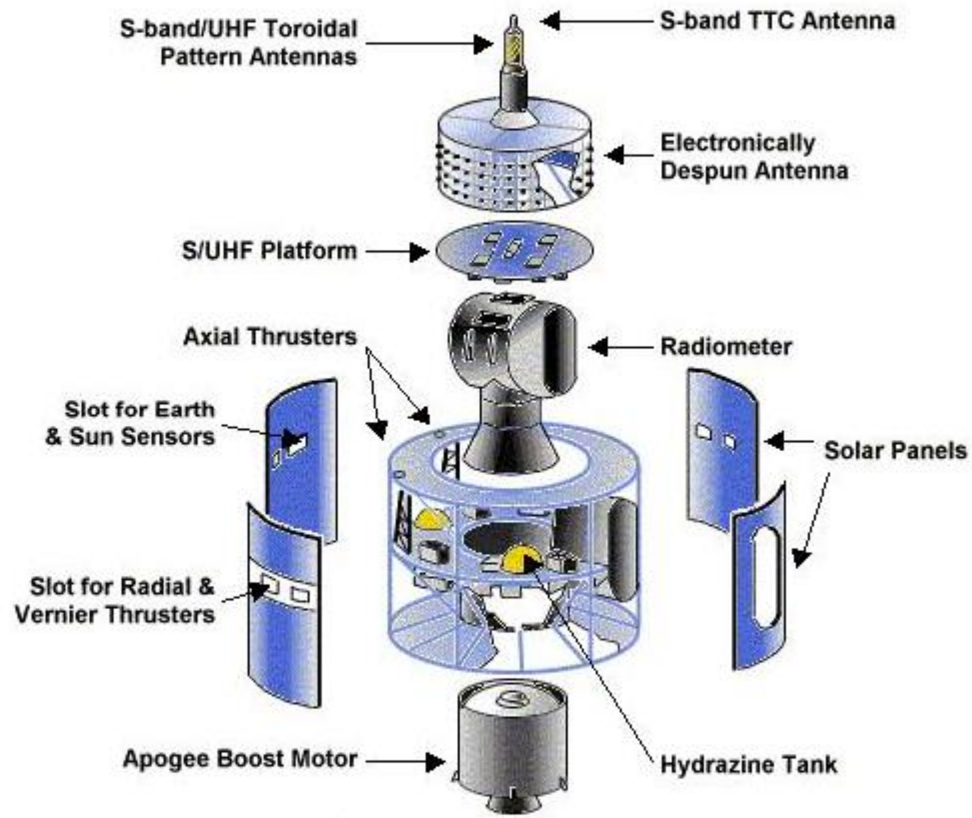

EUMETSAT

TACSAT I was the largest and most powerful communications satellite at the time when it was launched into synchronous orbit by a Titan IIIC booster 9 February 1969, from Cape Canaveral, Florida.

Spin Stabilization
Dual-Spin Spacecraft

The DSSC usually is used for the attitude stabilization by partial twist method: only one of the DSSC's coaxial bodies (**the «rotor»-body) has rotation at the «quiescence» of the second body (the «platform»-body**) – it allows to place into the «platform»-body some exploratory equipment and to perform of space-mission tests without rotational disturbances.

The dual-spin construction-scheme is quite useful in the practice during all **history of space flights realization**; and it is possible to present some examples of the DSSC, which was used in real space-programs (most of them are communications satellites and observing geostationary satellites):

- This is long-continued and well successful project "**Intelsat**" (the Intelsat II series of satellites first launched in 1966) including 8th generation of geostationary communications satellites and Intelsat VI (1991) designed and built by Hughes Aircraft Company.
-The "**Meteosat**"-project by European Space Research Organization (initiated with Meteosat-1 in 1977 and operated until 2007 with Meteosat-7) also used dual-spin configuration spacecraft.
-Spin-stabilized spacecraft with mechanically despun antennas was applied in the framework of **GEOTAIL** (a collaborative mission of Japan JAXA/ISAS and NASA, within the program "International Solar-Terrestrial Physics") launched in 1992; the GEOTAIL spacecraft and its payload continue to operate in 2013.
-Analogously the construction scheme with despun antenna was selected for **Chinese communications satellites DFH-2** (STW-3, 1988; STW-4, 1988; STW-55, 1990).
-Well-known **Galileo mission's spacecraft** (the fifth spacecraft to visit Jupiter, launched on October 19, 1989) was designed by dual-spin scheme.
-Of course, we need to indicate one of the world's most-purchased commercial communications satellite models such as **Hughes / Boeing HS-376 / BSS-376** (for example, Satellite Business Systems with projects SBS 1, 2, 3, 4, 5, 6 / HGS 5, etc.): they have spun section containing propulsion system, solar drums, and despun section containing the satellite's communications payload and antennas.
-Also very popular and versatile **dual-spin models are Hughes HS-381 (Leasat project), HS-389 (Intelsat project), HS-393 (JCSat project).**

Spin Stabilization
Dual-Spin Spacecraft

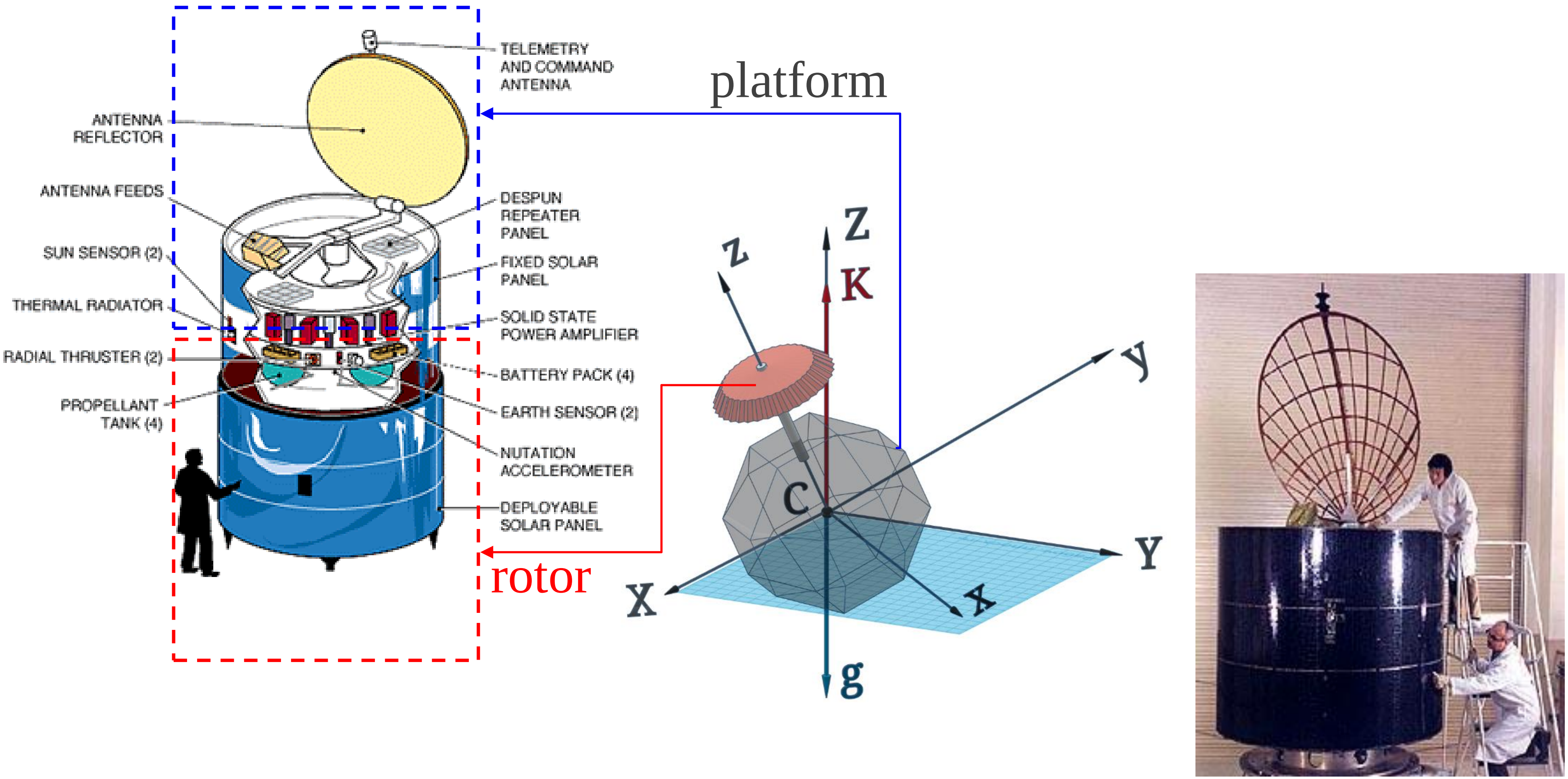

Spin Stabilization
Dual-Spin Spacecraft

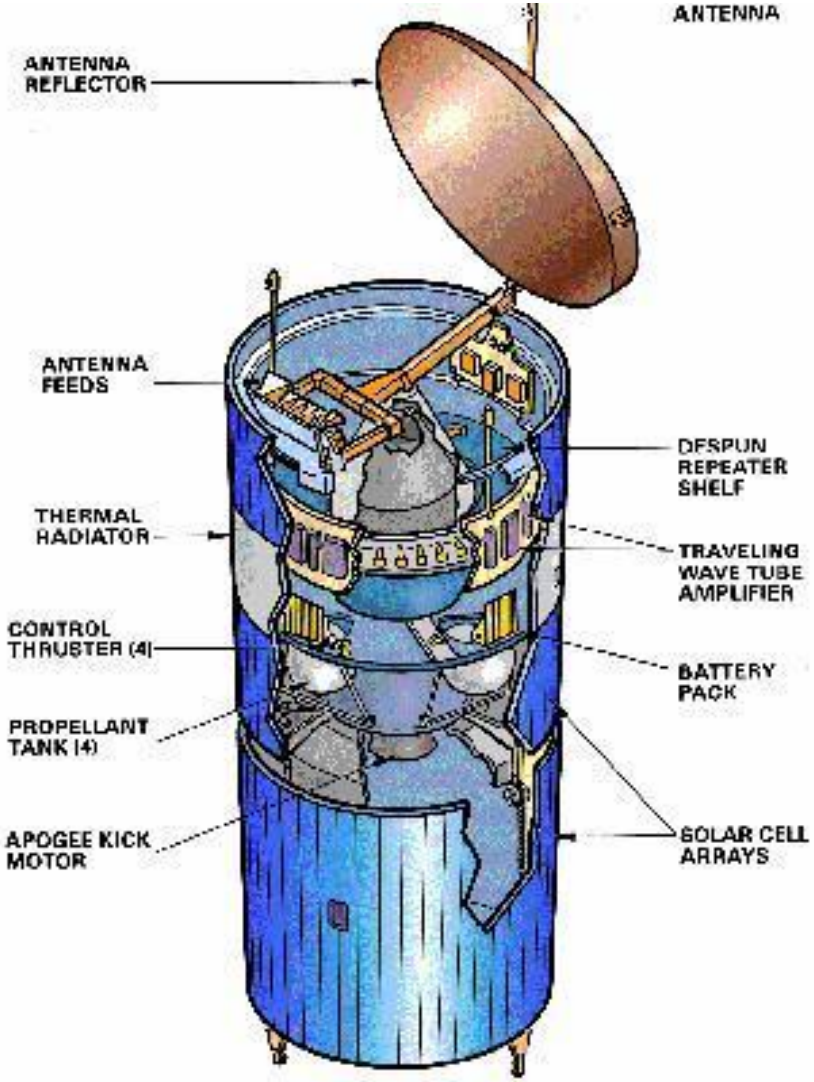

HS 376
SPACECRAFT CONFIGURATION

HS 376
Class: Communications.
Nation: USA.

Mass 654 kg at beginning-of-life in geosynchronous orbit.

Spin stabilized at 50 rpm by 4 hydrazine thrusters with 136 kg propellant.
Star 30 apogee kick motor.
Solar cells mounted on outside of cylindrical satellite body provide 990 W of power and recharge two NiCd batteries. 24 + 6 backup 9 W transmission beams.

HS 376 Chronology:
-15 November 1980 SBS 1 Program
-…
-22 November 1998 BONUM-1 Program

Spin Stabilization
Dual-Spin Spacecraft

Intelsat-6 [Boeing]

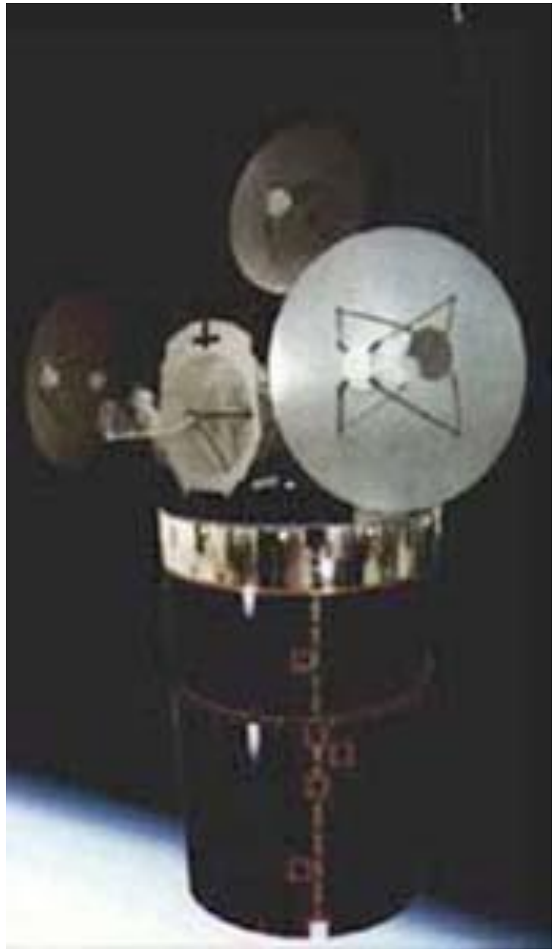

SDS-2 [NRO]

Hughes: HS-389

Ordered	Date	
Intelsat 601	1982	29.10.1991
Intelsat 602	1982	27.10.1989
Intelsat 603	1982	14.03.1990
Intelsat 604	1982	23.06.1990
Intelsat 605	1982	14.08.1991
SDS-2 1		08.08.1989
SDS-2 2		15.11.1990
SDS-2 3		02.12.1992
SDS-2 4		03.07.1996

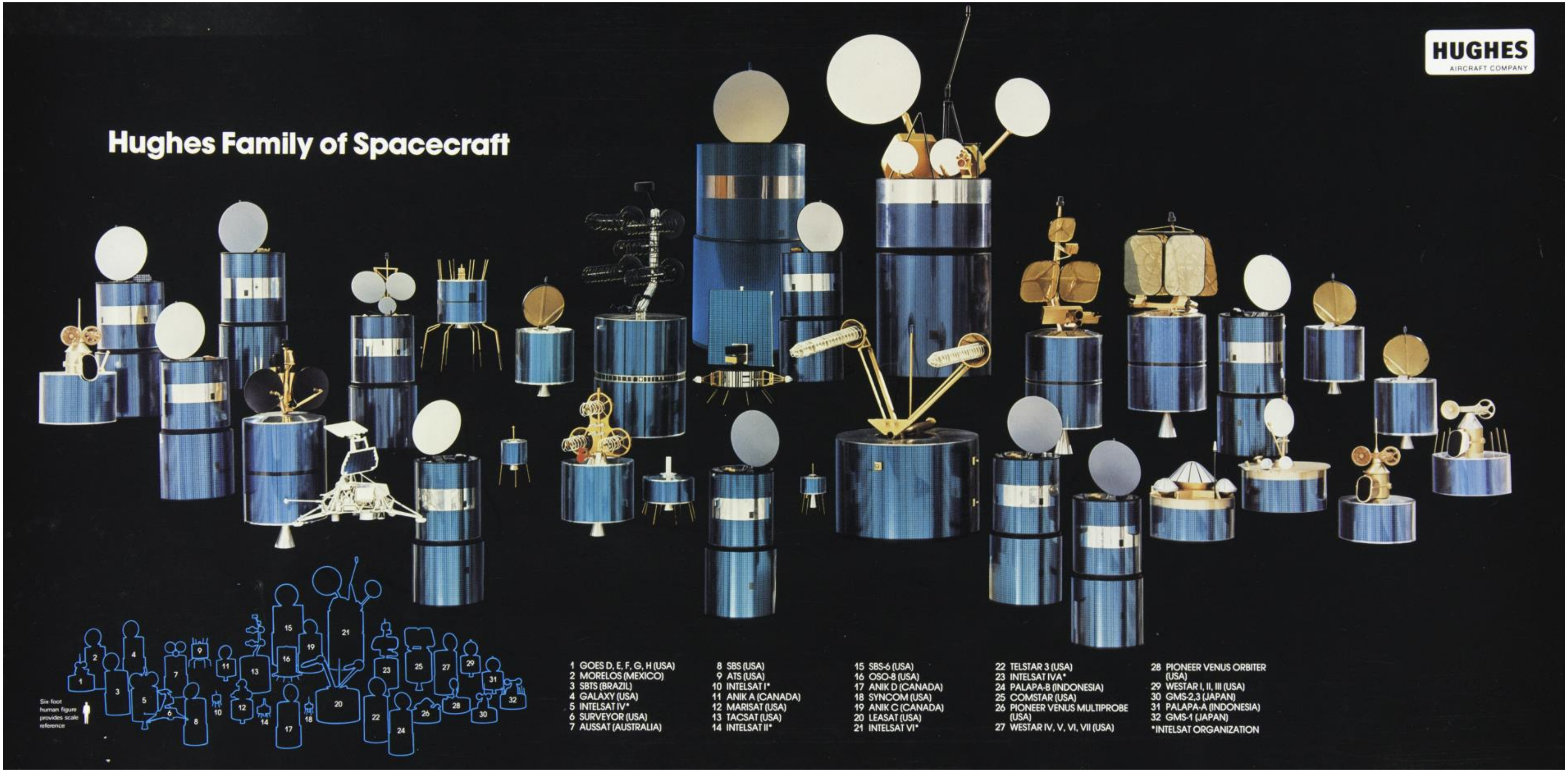

https://www.hughes.com/

The DSSC Missions

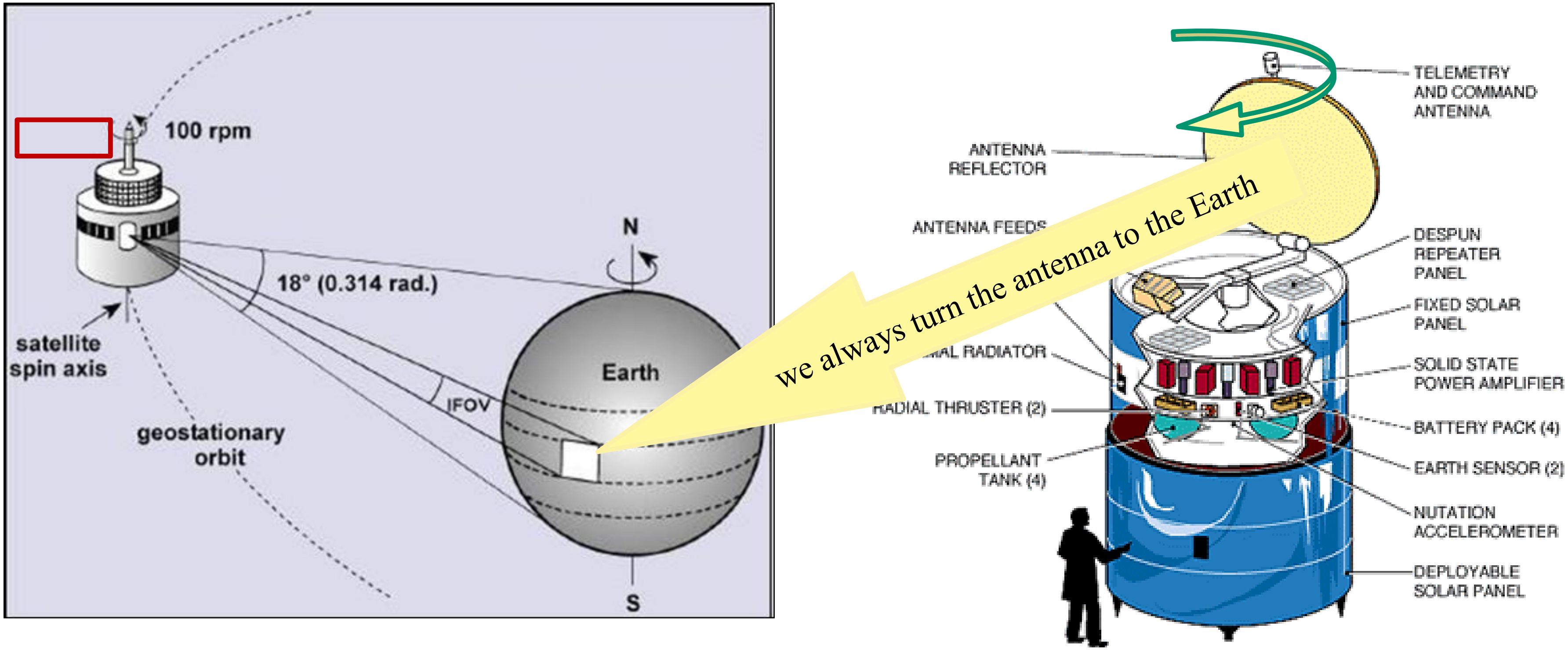

Geostationar satellite:

$\boldsymbol{\Omega}_{\mathbf{rotor}}$=100 rpm=10.47 rad/s

$\boldsymbol{\Omega}_{\mathbf{platform}}$=7.27 $\cdot 10^{-5}$ rad/s ≈ 0

SOLAR SENTINELS

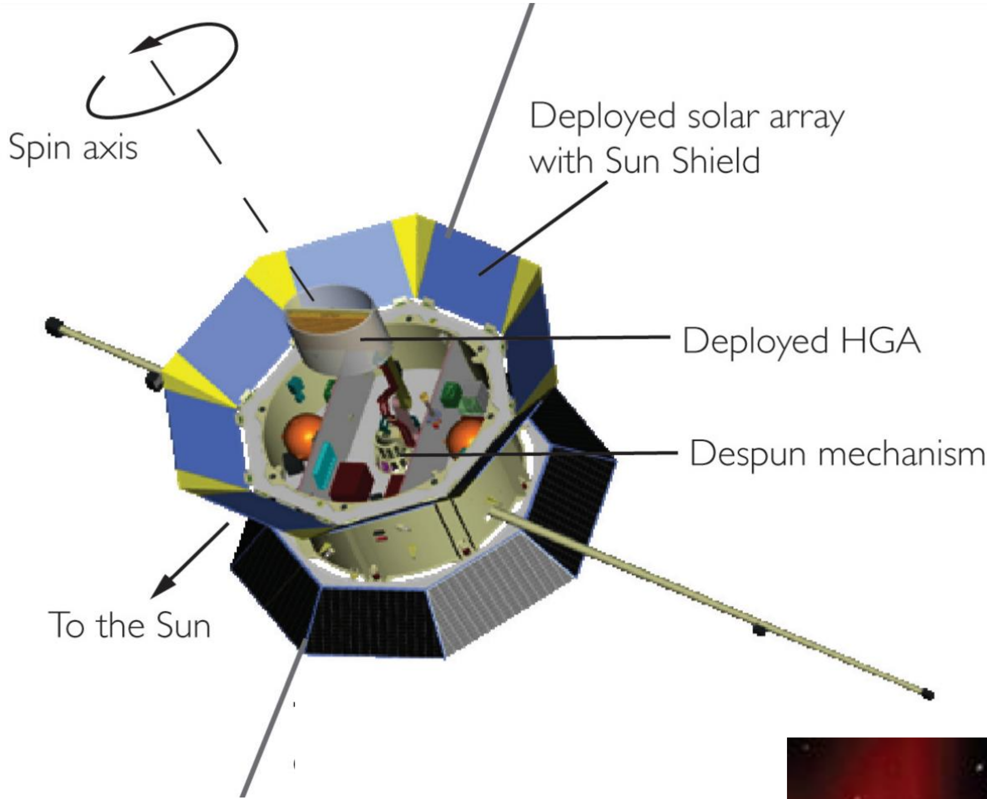

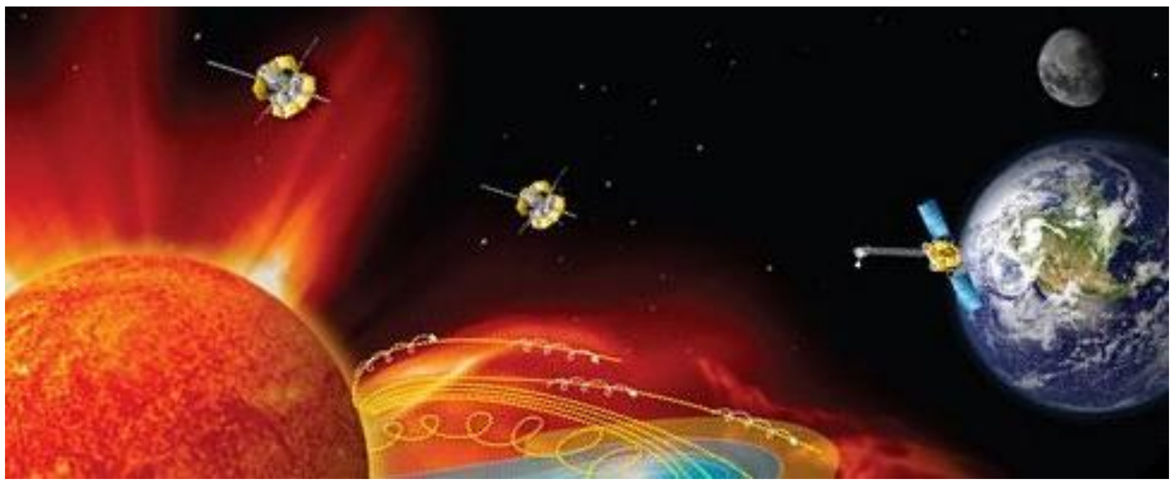

https://science.nasa.gov/science-news/science-at-nasa/2006/01sep_sentinels

NANOsatellites
MicroMAS-1 и MicroMAS-2A

(Micro-sized Microwave Atmospheric Satellite)

Massachusetts Institute of Technology, Lincoln Laboratory

MicroMAS-1 **04.03.2015**.
MicroMAS-2A **12.01.2019**

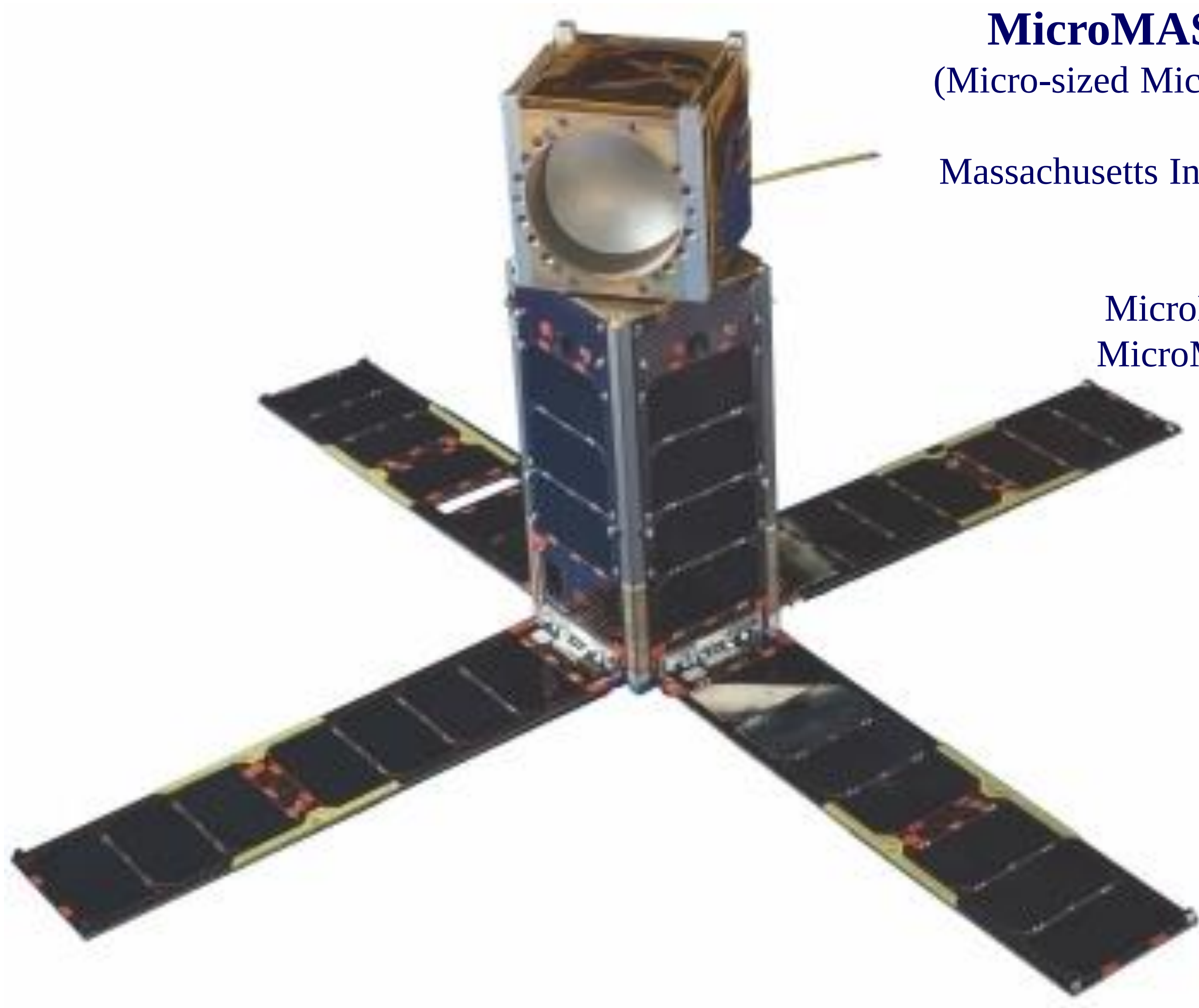

https://directory.eoportal.org/web/eoportal/satellite-missions/content/-/article/micromas-1
http://digitalcommons.usu.edu/cgi/viewcontent.cgi?article=3292&context=smallsat

https://www.ll.mit.edu/news/micromas-cubesat-technology-provides-fresh-approach-weather-forecasting

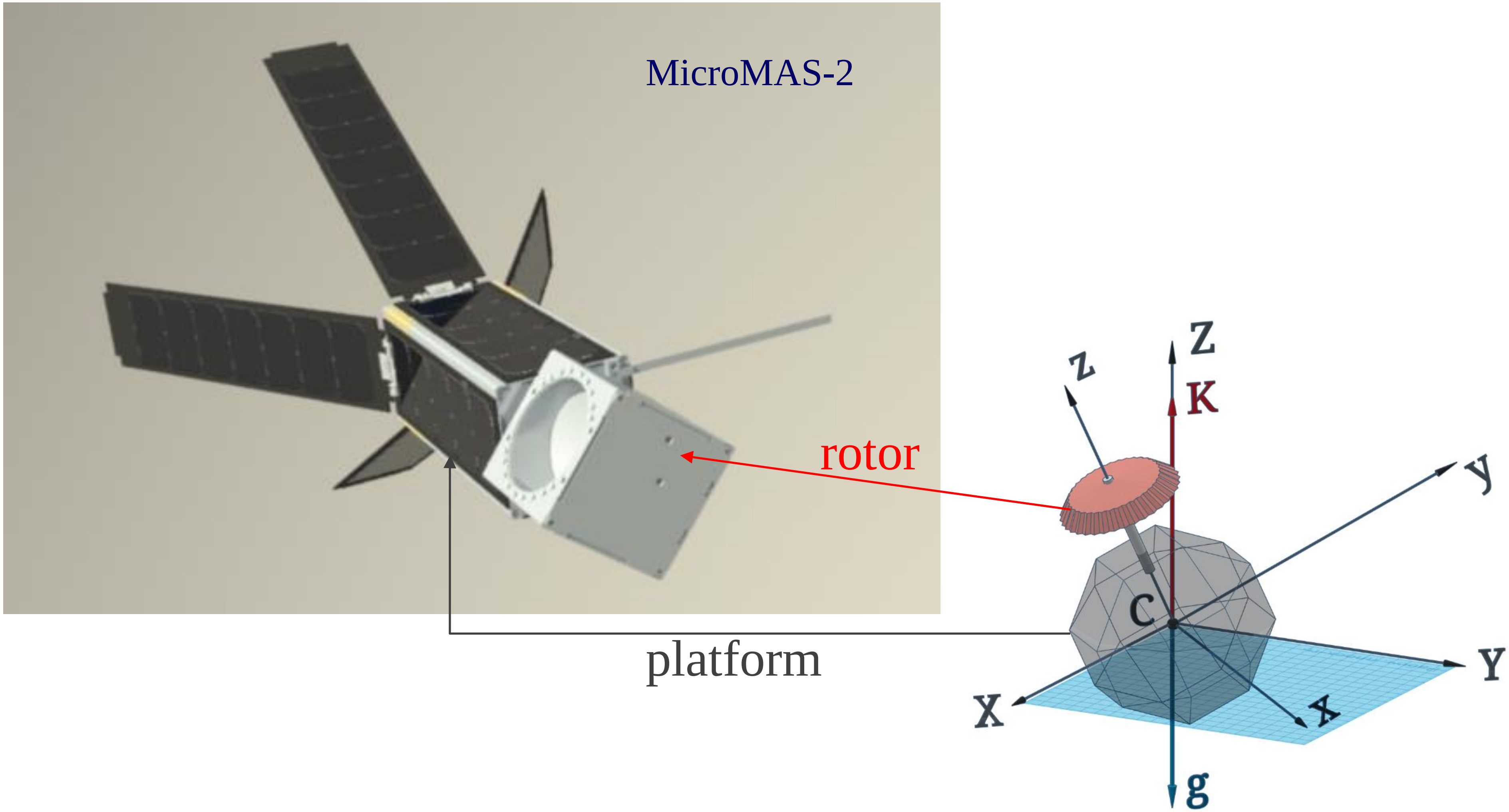

https://directory.eoportal.org/web/eoportal/satellite-missions/content/-/article/micromas-1
http://digitalcommons.usu.edu/cgi/viewcontent.cgi?article=3292&context=smallsat

https://www.ll.mit.edu/news/micromas-cubesat-technology-provides-fresh-approach-weather-forecasting

Variable composition of DSSC-gyrostats

GPS

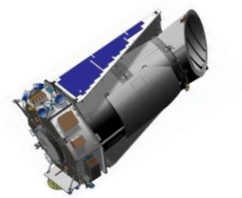

Kepler

Mars Polar Lander

ICESat-2

Delta II
ULA-United Launch Alliance
(Boeing BDS)

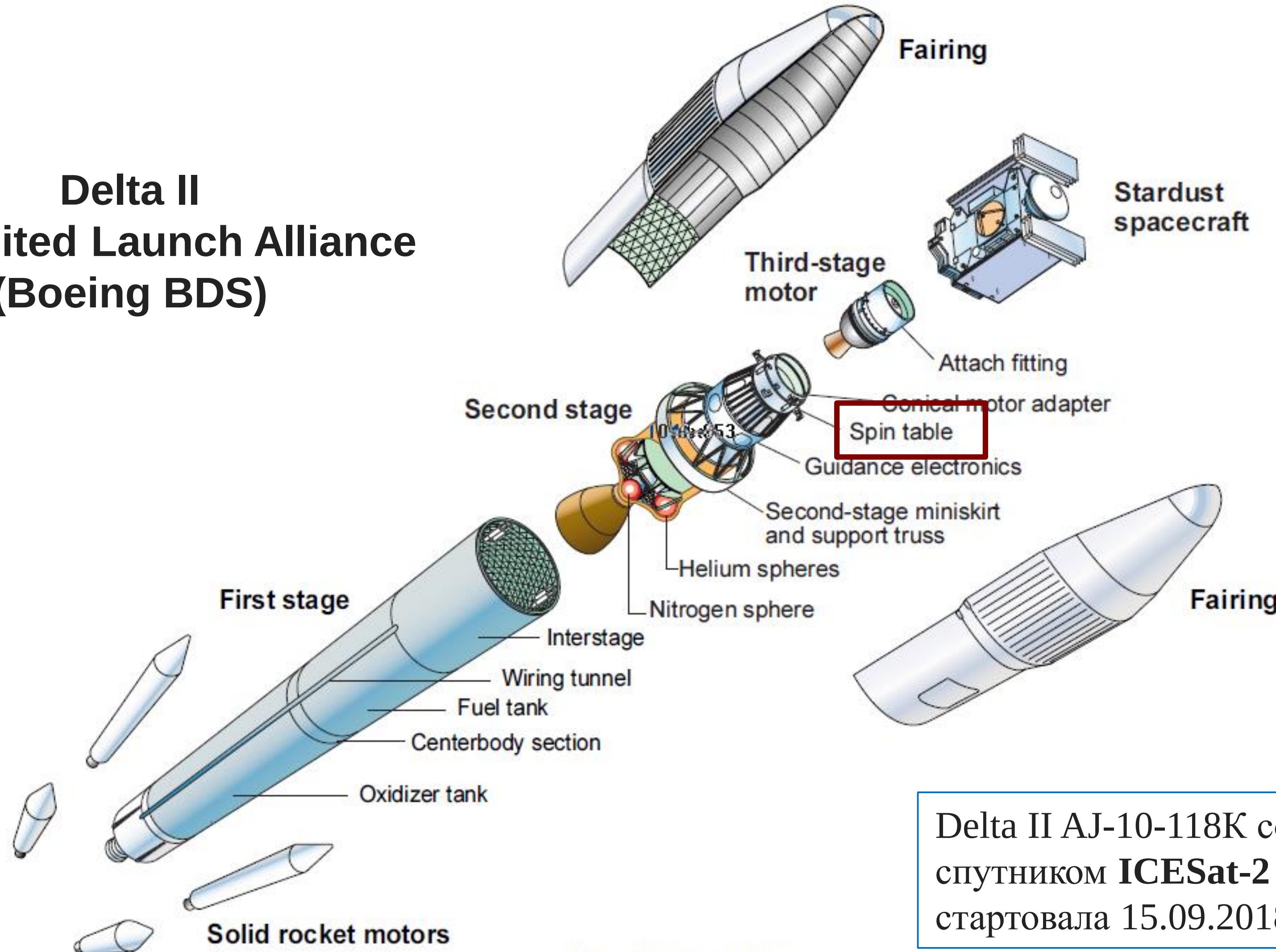

Delta launch vehicle

Delta II AJ-10-118K со спутником **ICESat-2** стартовала 15.09.2018

https://www.ulalaunch.com/rockets/delta-ii

Variable composition of DSSC-gyrostats

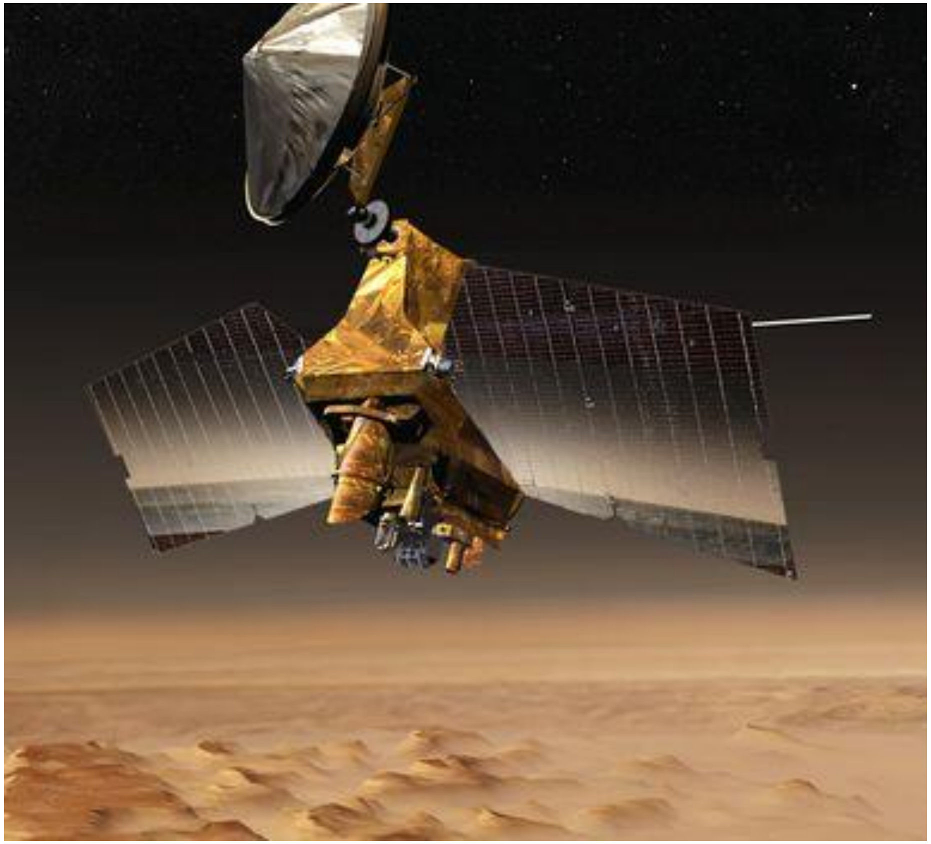

The second stage of Delta II with Mars Polar Lander (03.01.1999)

https://www.ulalaunch.com/rockets/delta-ii

Gravity Gradient Stabilization

The Gravity-gradient stabilization is a method of SC stabilizing in a fixed orientation using only the orbited body's mass distribution and the Earth's gravitational field.

SC is placed along the radius-vector of the Earth

Physical pendulums

Tether-satellites

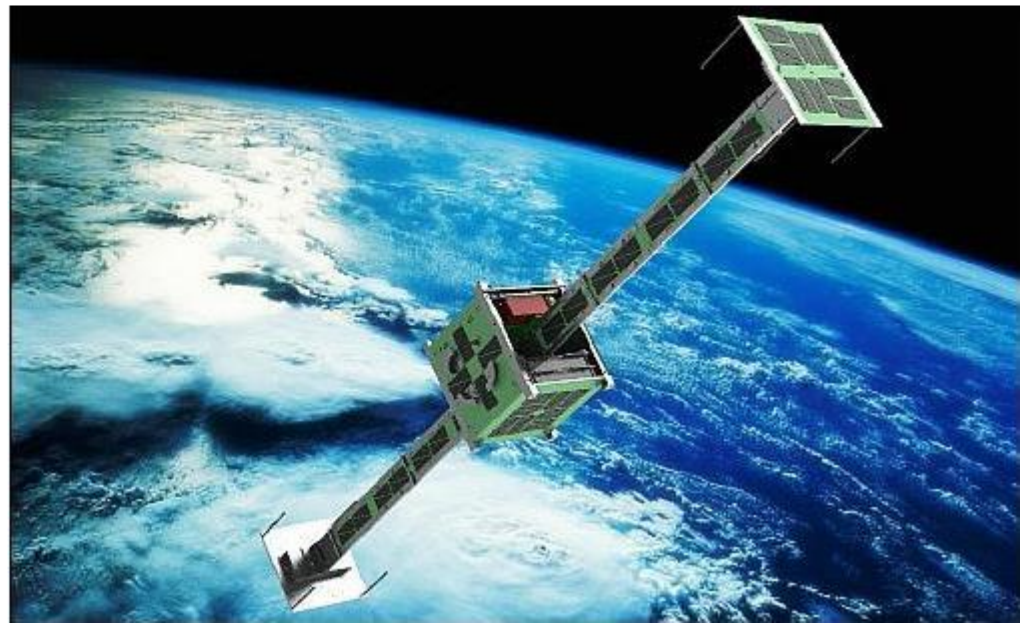

UniCubeSat-GG is the first CubeSat mission of GAUSS (Gruppo di Astrodinamica dell' Universita degli Studi “la Sapienza”) at the University of Rome (Universita di Roma “La Sapienza”, Scuola di Ingegneria Aerospaziale), Italy.

Magnetic Stabilization

Magnetic stabilization is a method of SC stabilizing using geomagnetic field of the Earth

SC is positioned along the magnetic lines of the geomagnetic field ("magnetic compass")

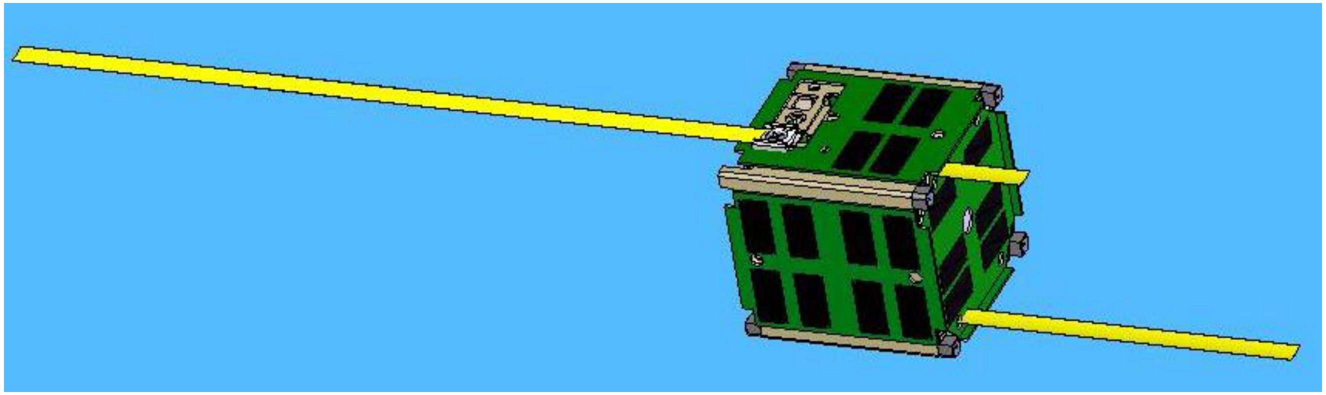

KySat-1 Passive Magnetic Stabilization System is used for antenna orientation and coarse camera pointing

KySat-1, the first satellite project by Kentucky Space, is a 1-U CubeSat scheduled to launch in 2010 on a NASA mission.

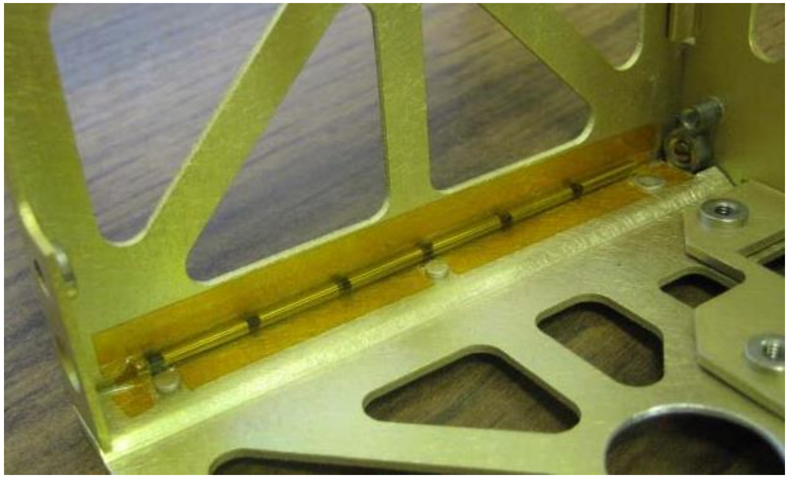

← One of Four Alinco-5 Permanent Magnet sets on board KySat-1.

Aerodynamic Stabilization

The Aerodynamic stabilization is a method of SC stabilizing using aerodynamic force in rarefied atmosphere of low earth orbit .

SC is positioned along the orbital velocity vector

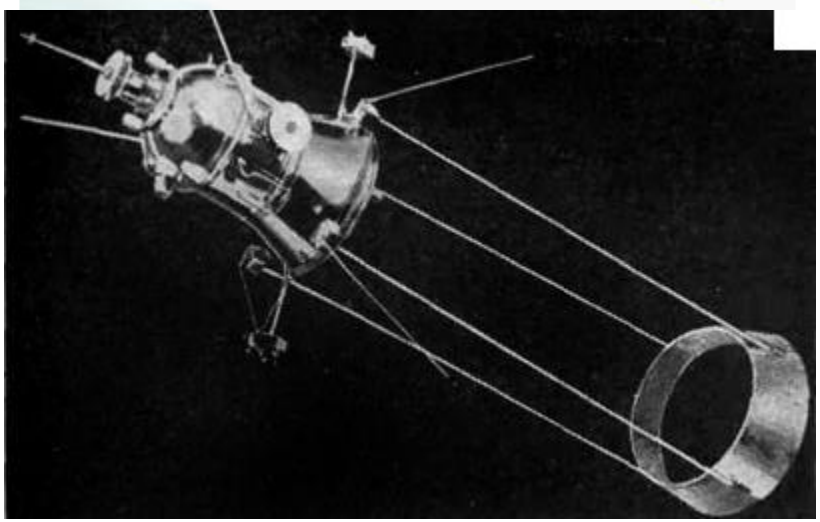

SC with tail unit

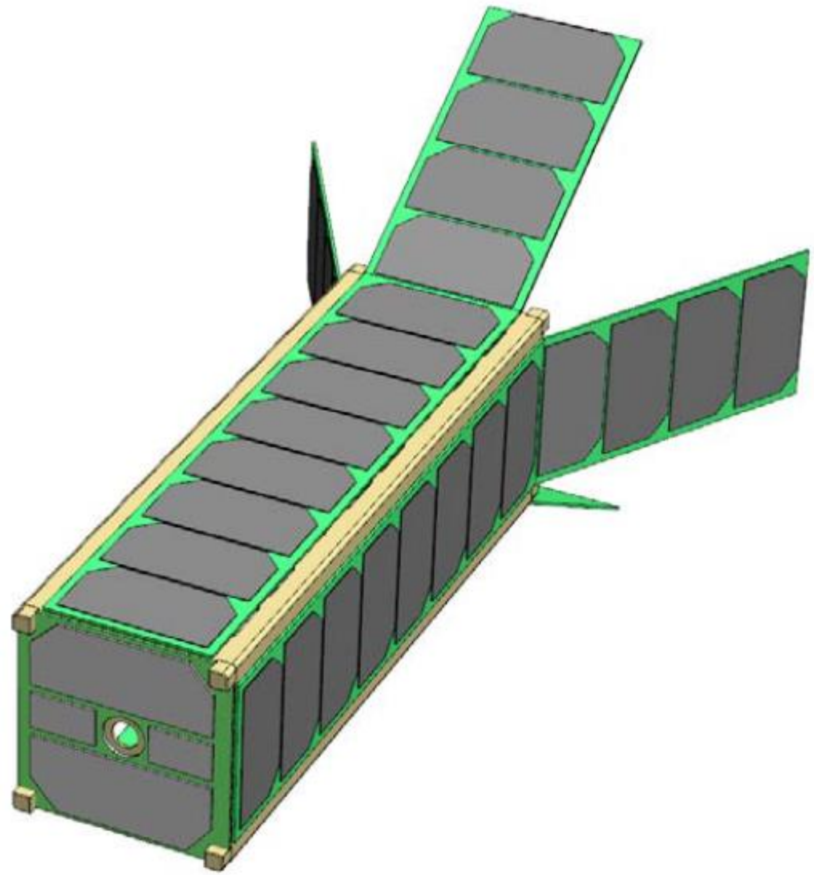

Aerodynamically Stable CubeSat Design Concept

Actuators

Reaction Wheel Assemblies (RWAs)

RWAs are particularly useful when the spacecraft must be rotated by very small amounts, such as keeping a telescope pointed at a star.

This is accomplished by equipping the spacecraft with an electric motor attached to a **flywheel, which when rotated increasingly fast causes the spacecraft to spin the other way** in a proportional amount by conservation of angular momentum.

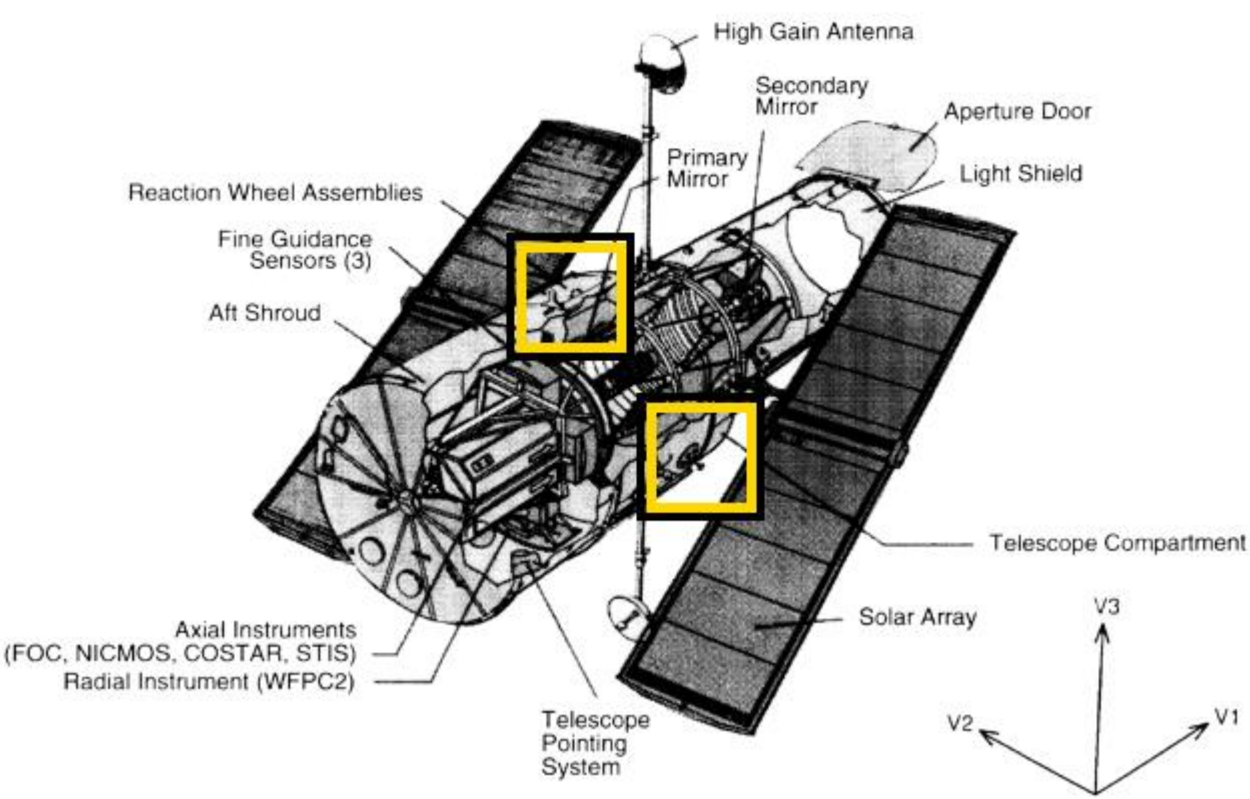

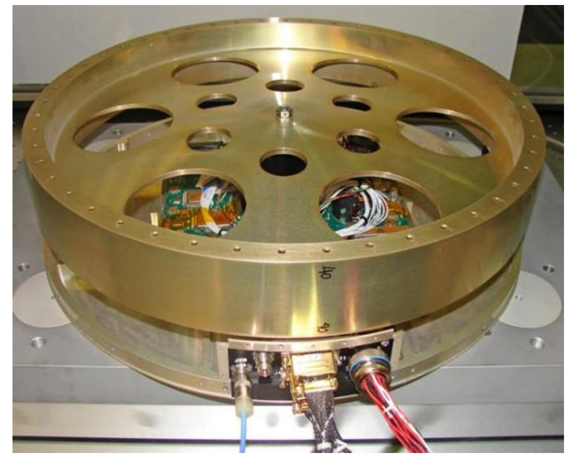

Actuators

Control Moment Gyros (CMGs)

A CMG consists of a spinning rotor and one or more motorized gimbals that tilt the rotor’s angular momentum. As the rotor tilts, the changing angular momentum causes a gyroscopic torque that rotates the spacecraft.

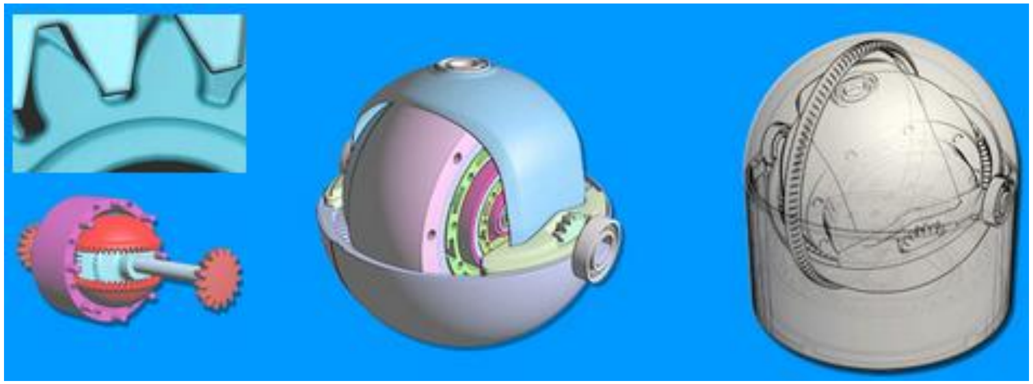

Microsatellite with four control moment gyroscopes

Actuators

Thrusters

A **thruster** is a small propulsive device used by spacecraft for attitude control, in the reaction control system, or long-duration, low-thrust acceleration

Cyclone-3 LV thruster of 30 N thrust

Liquefied gases in high-pressure balloons

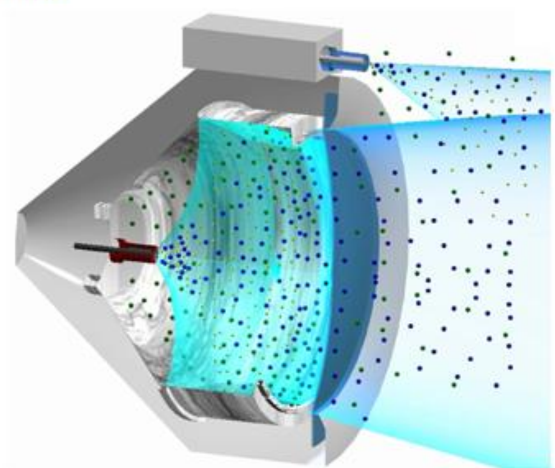

Main Equations of Angular Motion of Rigid Body (Attitude Motion of SC)

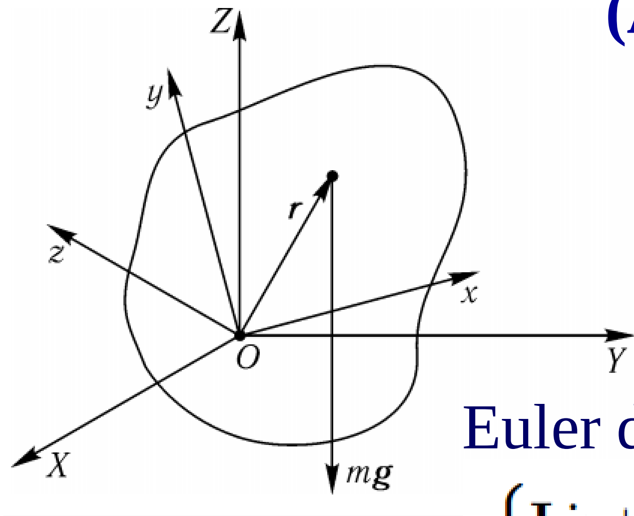

The study of the angular motion of the SC attitude dynamics is one of the main problems of rigid body systems dynamics in the classical mechanics.

And vice versa

Tasks of analysis and synthesis of the rigid bodies' motion have important applications in the space-flight dynamics.

Euler dynamical equations:

$$\begin{cases} \mathbf{I}\dot{\boldsymbol{\omega}} + \boldsymbol{\omega} \times \mathbf{I}\boldsymbol{\omega} = \mu \boldsymbol{r} \times \boldsymbol{\gamma}, \\ \dot{\boldsymbol{\gamma}} = \boldsymbol{\gamma} \times \boldsymbol{\omega}, \end{cases}$$

Euler kinematical equations:

$$\omega_1 = \dot{\psi} \sin\theta \sin\varphi + \dot{\theta} \cos\varphi,$$
$$\omega_2 = \dot{\psi} \sin\theta \cos\varphi - \dot{\theta} \sin\varphi,$$
$$\omega_3 = \dot{\psi} \cos\theta + \dot{\varphi}.$$

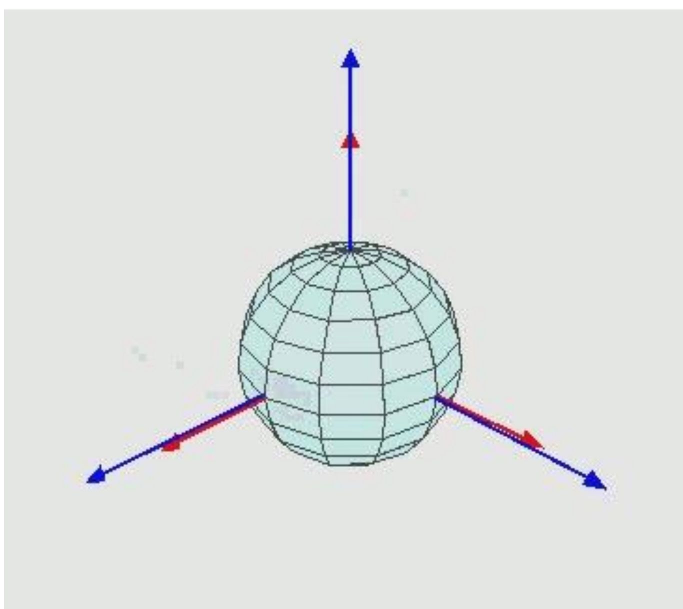

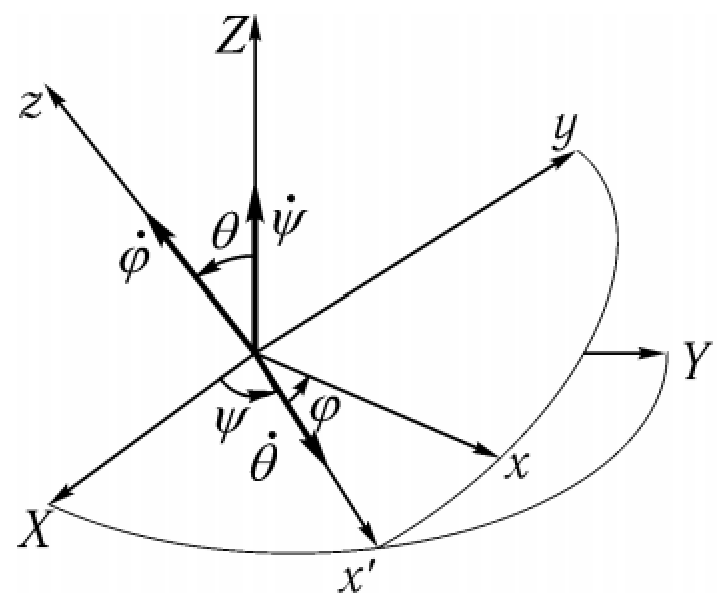

Main Properties of the Free Angular Motion of Rigid Body (Attitude Motion of SC)

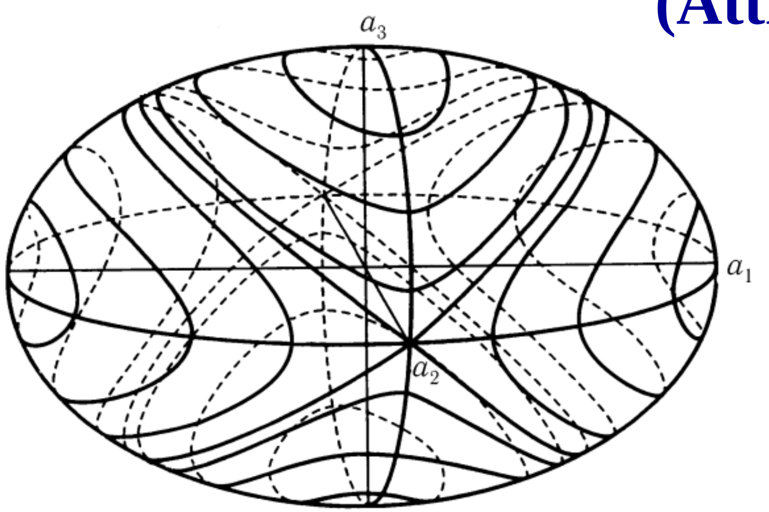

Inertia tensor with polhodes

Louis Poinsot interprétation

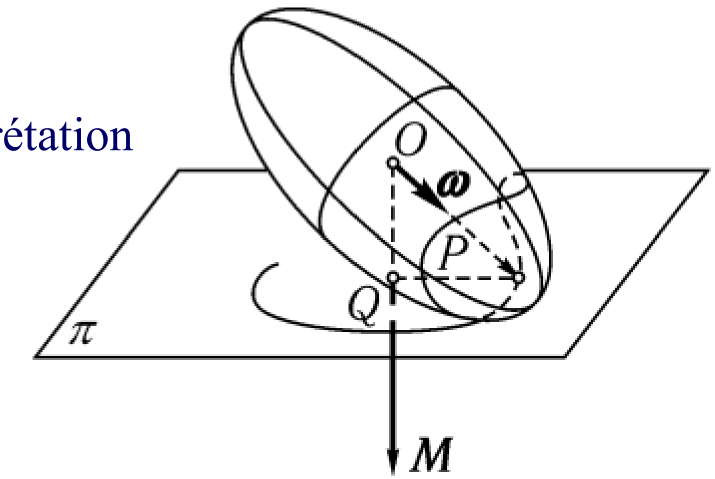

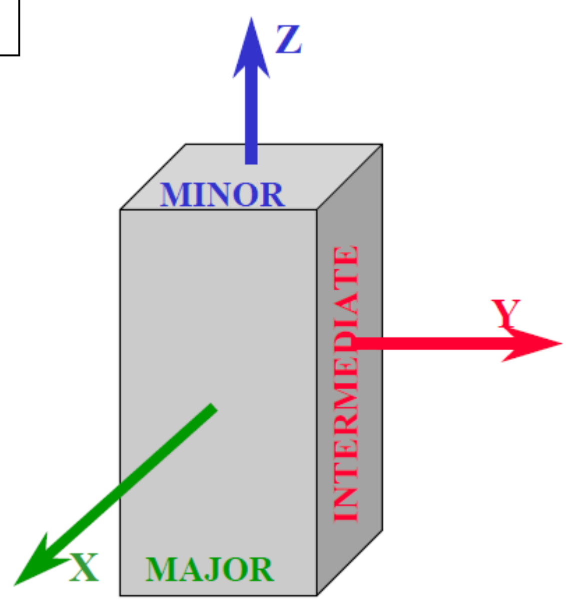

- $I_{xx} > I_{yy} > I_{zz}$
- Major axis spin is stable
- Minor axis spin is stable
- Intermediate axis spin is unstable
- Energy dissipation changes these results
  → Minor axis spin becomes unstable
- This is called the Major-Axis Rule

--- notation by C.D.Hall

Main Properties of the Free Angular Motion of Rigid Body (Attitude Motion of SC)

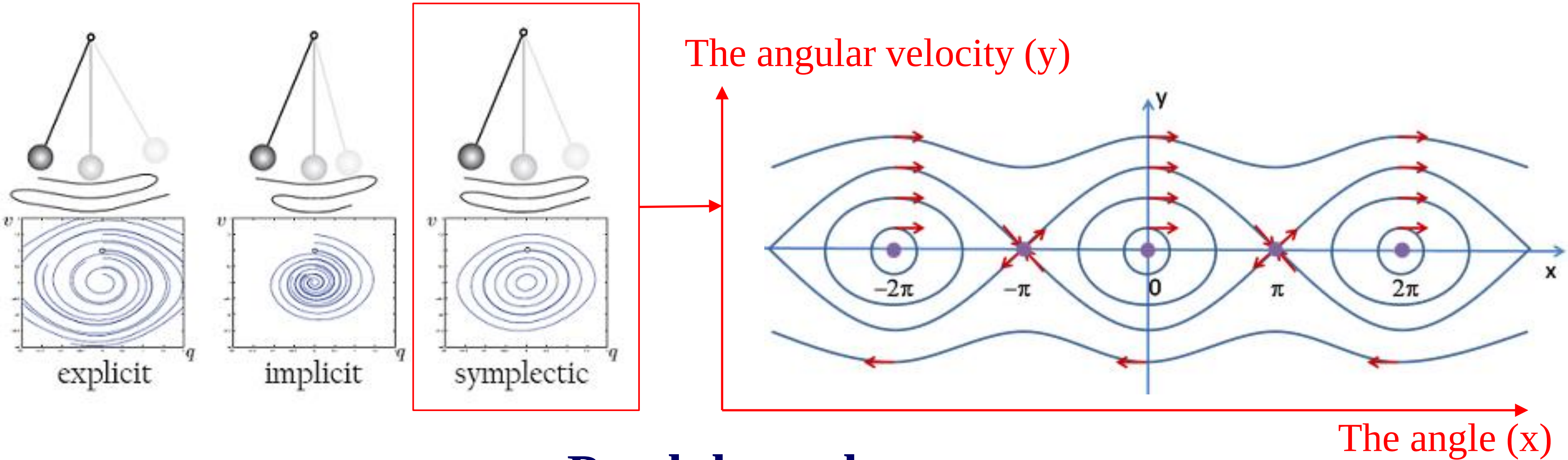

Pendulum phase space

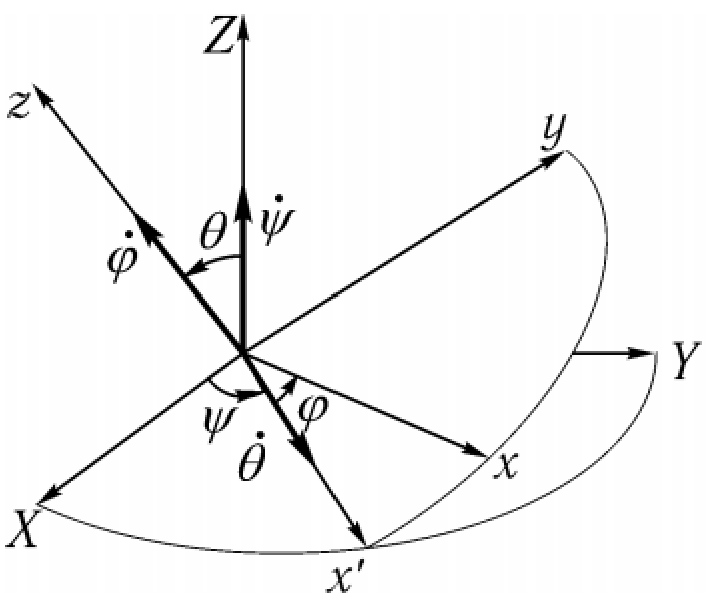

If we consider rigid body angular motion on the base of Hamilton dynamics, than for rigid body motion we take pendulum phase structure:

x=θ (nutation)

and

y = impulse (θ) ~ dθ/dt

Part 2 – Research Results

1. Constructions of mechanical models of spider-type multirotor systems (and spacecrafts) and mathematical models of the systems angular motion.

2. The analysis of the angular motion multirotor spacecrafts (gyrostats-spacecrafts, dual-spin spacecrafts) and the spacecrafts spatial reorientation synthesis.

3. The analysis of the chaotic motion at presence of small harmonic perturbations

Mechanical models of multiple-rotor systems

Let's consider an angular motion (about point O) of spider-type multiple rotor rigid bodies systems and coaxial bodies systems

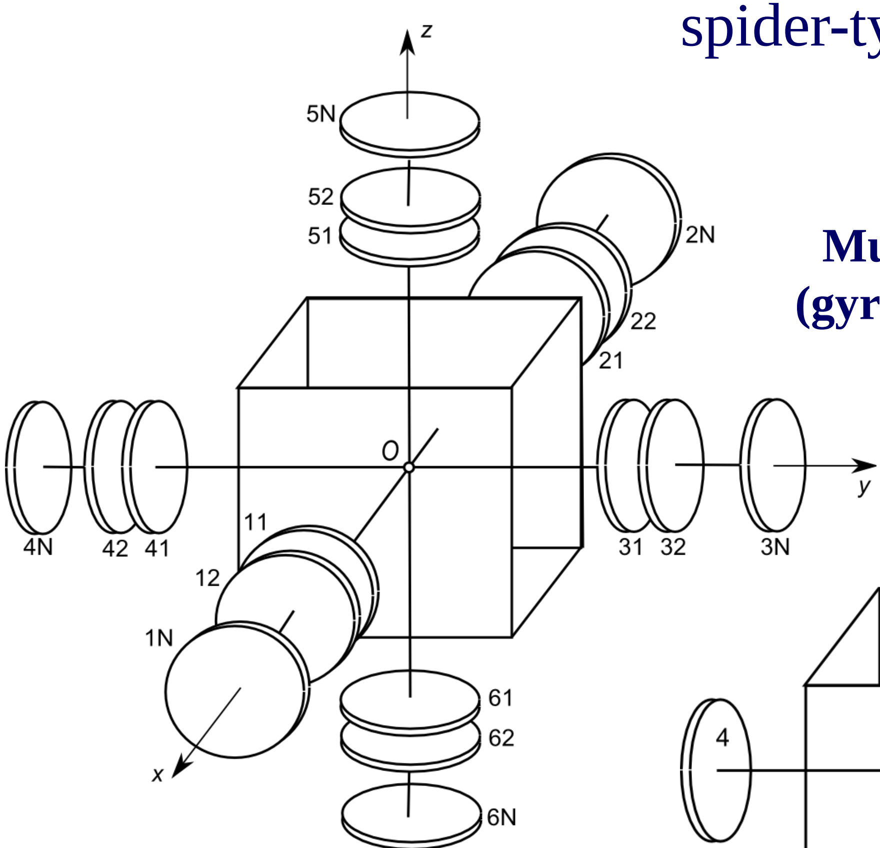

Number of rotors = N

Multirotor spiders (gyrostat-spacecrafts)

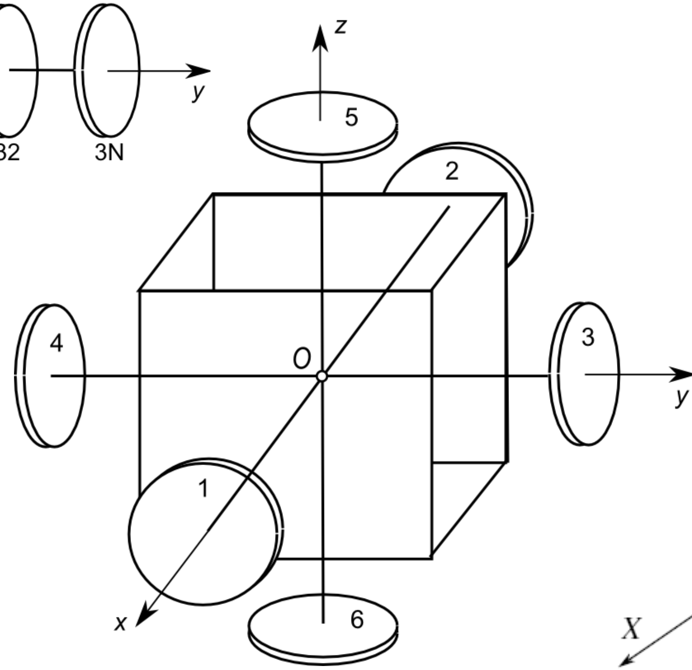

Number of rotors = 6

Coaxial bodies system (dual-spin spacecraft)

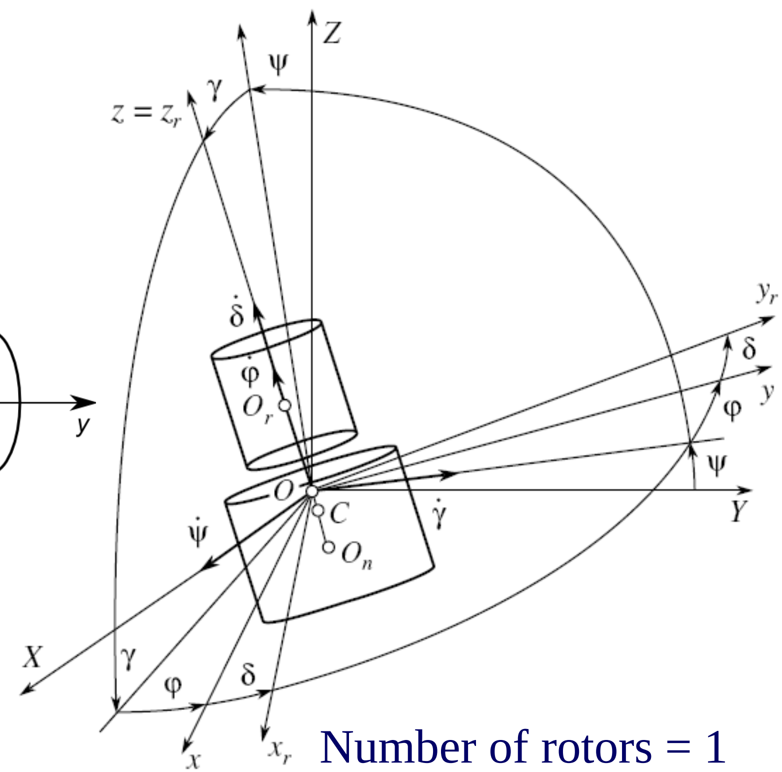

Number of rotors = 1

I. The coaxial bodies system with variable composition

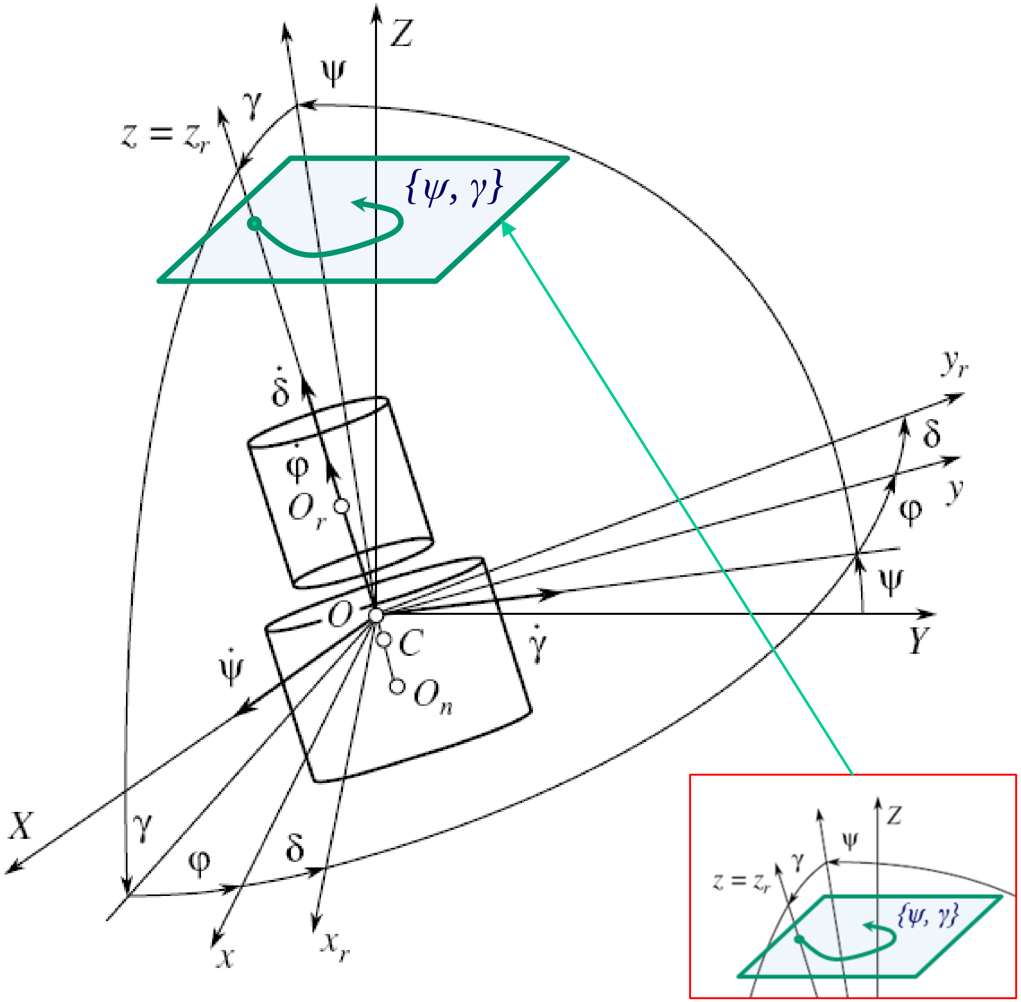

I.1 The angular motion general equations:

$$\begin{cases} A(t)\dot{p}+\left(C(t)-A(t)\right)qr+C_r(t)q\sigma=M_x^e \\ A(t)\dot{q}-\left(C(t)-A(t)\right)pr-C_r(t)p\sigma=M_y^e \\ C(t)\dot{r}+C_r(t)\dot{\sigma}=M_z^R+M_z^e \\ C_r(t)\left(\dot{r}+\dot{\sigma}\right)=M_r+M_z^R+M_{z,r}^e \end{cases} \qquad (1)^*$$

$$\begin{cases} \dot{\psi}=\dfrac{1}{\cos\gamma}\left(p\cos\varphi-q\sin\varphi\right) \\ \dot{\gamma}=p\sin\varphi+q\cos\varphi, \qquad \dot{\delta}=\sigma \\ \dot{\varphi}=r-\dfrac{\sin\gamma}{\cos\gamma}\left(p\cos\varphi-q\sin\varphi\right) \end{cases} \qquad (2)$$

•- Doroshin A.V. Analysis of attitude motion evolutions of variable mass gyrostats and coaxial rigid bodies system, Int. J. Non-Linear Mech. 45 (2010) 193–205

Second stage of DELTA II

Delta II AJ-10-118K with **ICESat-2** 15.09.2018.

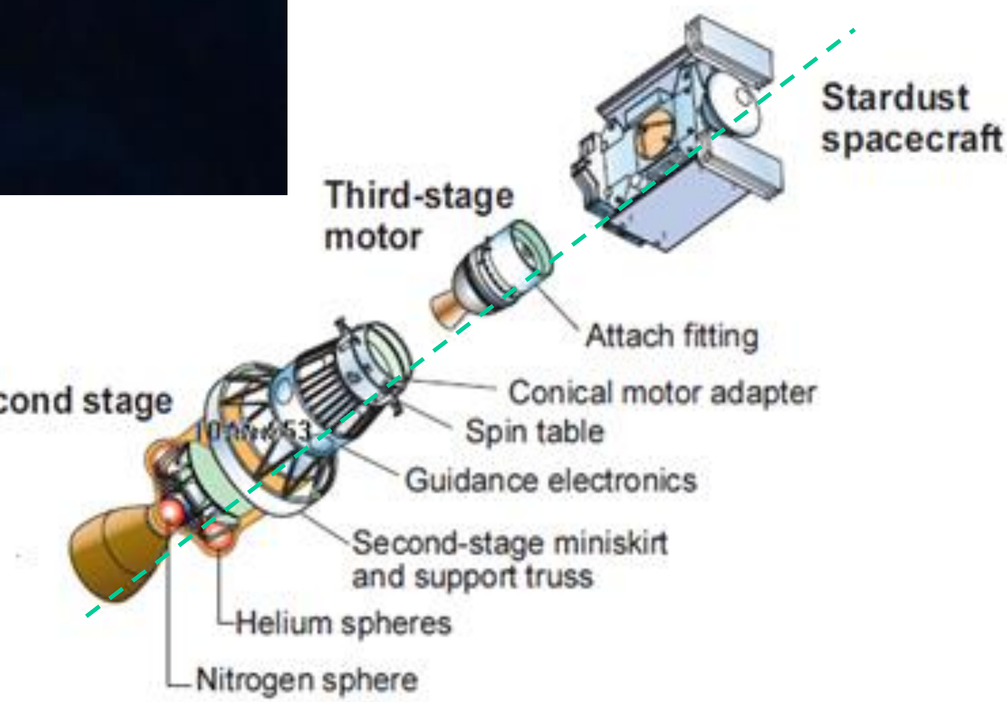

GPS

Kepler

Mars Polar Lander

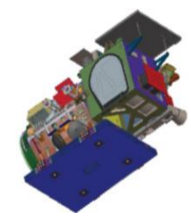

ICESat-2

I.2. Applications in space flight mechanics

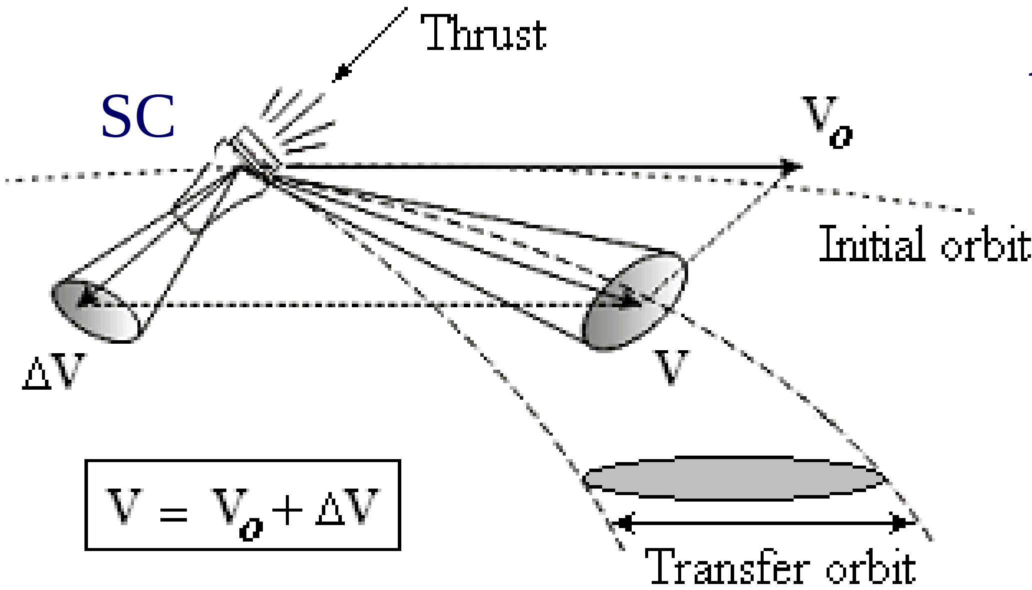

Realization of active maneuvers for inter-orbital transfers

A reason of transfer orbit "**Scattering**"

1. Spacecraft (SC) makes two motions:
   - -trajectory motion
   - -angular motion

2. SC angular motion obviously changes a thrust direction.

Precession motion of the thrust vector is the reason of the inter-orbital transfer impulse deviation and "**Scattering**".

I.3. Transformations of the equations

$$p(t) = G(t)\sin F(t), \quad q = G(t)\cos F(t) \qquad \left(G \geq 0\right). \qquad (3)$$

Angular motion dynamical equations (1) in new variables:

$$\begin{cases} \dot{F} = -\dfrac{1}{A(t)}\left[\left(C(t) - A(t)\right)r + C_r(t)\sigma + f_F\left(G,F\right)\right], \qquad \dot{G} = \dfrac{f_G\left(G,F\right)}{A(t)} \\ \dot{r} = \dfrac{M^e_{z,c} - M_r}{C_m}, \qquad \dot{\sigma} = \dfrac{C(t)M_r}{C_r(t)C_m} + \dfrac{M^R_z + M^e_{z,r}}{C_r(t)} - \dfrac{M^e_{z,m}}{C_m} \end{cases} \qquad (4)$$

$$f_G\left(G,F\right) = \left(M^e_x \sin F + M^e_y \cos F\right), \quad f_F\left(G,F\right) = \frac{1}{G}\left(M^e_x \cos F - M^e_y \sin F\right)$$

Relative value of a transversal angular velocity of main body is small.

Angles ψ and γ are small:

$$\varepsilon = \sqrt{p^2 + q^2} / \left|\sigma\right| << 1, \qquad \gamma = O\left(\varepsilon\right), \quad \psi = O\left(\varepsilon\right)$$

Kinematical equations (2) :

$$\dot{\gamma} \cong G\cos\Phi(t), \quad \dot{\psi} \cong G\sin\Phi(t), \quad \dot{\varphi} \cong r, \quad \dot{\delta} = \sigma, \quad \Phi(t) = F(t) - \varphi(t) \qquad (5)$$

I.4. The phase trajectory configuration analysis

The Phase space: $\gamma,\ \psi$

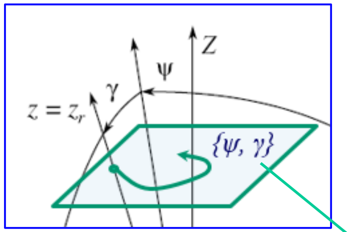

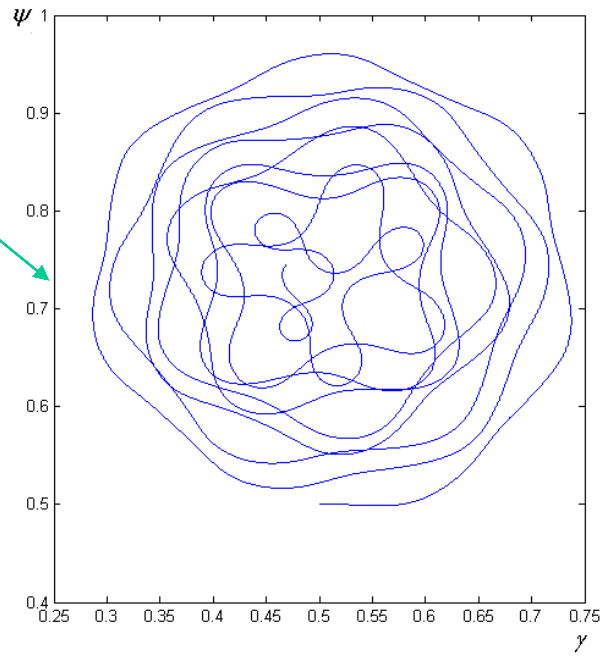

Example of phase trajectory (Trajectory of direct-axis SC)

The Phase velocities: $V_\gamma = \dot{\gamma},\ V_\psi = \dot{\psi}$ (6)

ThePhase accelerations: $W_\gamma = \ddot{\gamma},\ W_\psi = \ddot{\psi}$ (7)

The Trajectory's curvature (k):

$$k^2 = \frac{\left(\ddot{\gamma}\dot{\psi} - \ddot{\psi}\dot{\gamma}\right)^2}{\left(\dot{\gamma}^2 + \dot{\psi}^2\right)^3} = \frac{\dot{\Phi}^2}{G^2}. \qquad (8)$$

$$\frac{d}{dt}\left(k(t)^2\right) = 2\left(\dot{\Phi}\ddot{\Phi}G - \dot{G}\dot{\Phi}^2\right)/G^3. \qquad (9)$$

Function of phase trajectory evolutions:

$$P(t) = \dot{\Phi}\left(\ddot{\Phi}G - \dot{G}\dot{\Phi}\right). \qquad (10)$$

case "a" – the function $P(t)$ is positive;

case "b" – $P(t)$ has one zero;

case "c" – $P(t)$ has some zero.

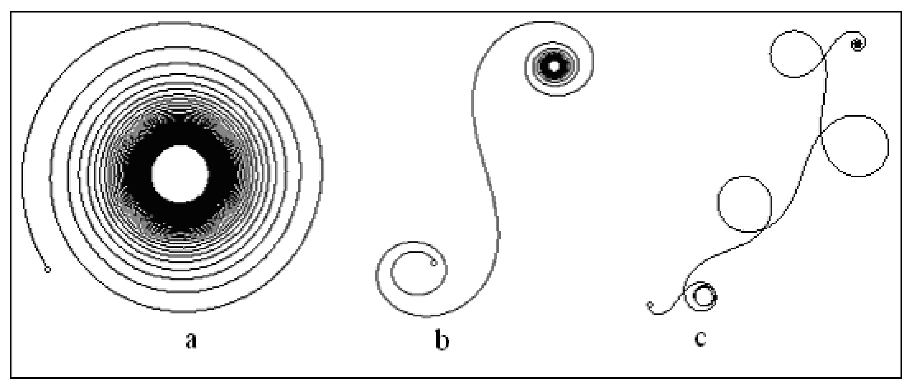

I.5. Analysis and synthesis of the motion behavior

$A(t), C(t) - linear(t)$

$M_r = const, \ \ M_z^R = const$

$r_0 = 0, \ \ \sigma_0 < 0, \ \ M_r > 0$

$$\begin{cases} \dot{G} = 0, \qquad \dot{F} = -\dfrac{\left(C_m + C_r - ct - A_m - A_r + at\right)r + (C_r - ct)\sigma}{A_m + A_r - at} \\ \dot{\sigma} = \dfrac{\left(C_m + C_r - ct\right)M_r}{(C_r - ct)C_m} + \dfrac{M_z^R}{(C_r - ct)}, \qquad \dot{r} = -M_r / C_m \end{cases} \tag{11}$$

Analytical solutions:

$$\begin{cases} r = r_0 - \dfrac{M_r}{C_n}t, \quad \sigma = \sigma_0 + s_1 t + s_2 \ln\left(1 - c_1 t\right), \quad \varphi = \varphi_0 + r_0 t - \dfrac{M_r}{2C_m}t^2 \\ \dot{F} = F_0 + \sum_{i=1}^{\infty} F_i t^i, \quad \dot{\Phi} = \dot{F} - \dot{\varphi} = f_0 + \sum_{i=1}^{\infty} f_i t^i \ f_1 = F_1 + M_r / C_m, \quad f_j = F_j \quad (j = 2..\infty) \\ s_1 = \dfrac{M_r}{C_n}, \quad s_2 = -\dfrac{1}{c}\left(M_r + M_z^R\right), \ \ c_1 = c / C_r \ f_0 = F_0 - r_0, \end{cases} \tag{12}$$

Approximation of the evolution function: $P(t) \approx f_1\left(f_0 + f_1 t\right) = f_1^2 t + f_1 f_0$ (13)

Polynom (13) is steady and trajectory is **twisted** if $f_1 f_0 > 0 \Rightarrow$

$$\left\{ \frac{c}{C_r} < \frac{a}{A_m + A_r}, \quad M_z^R < 0 \right\} (14) \qquad \left\{ \frac{c}{C_r} < \frac{a}{A_m + A_r}, \quad M_z^R > 0, \quad \frac{\sigma_0\left[c\left(A_m + A_r\right) - C_r a\right]}{\left(A_m + A_r\right)} > M_z^R \right\} (15)$$

I.6. Numerical check of motion behavior

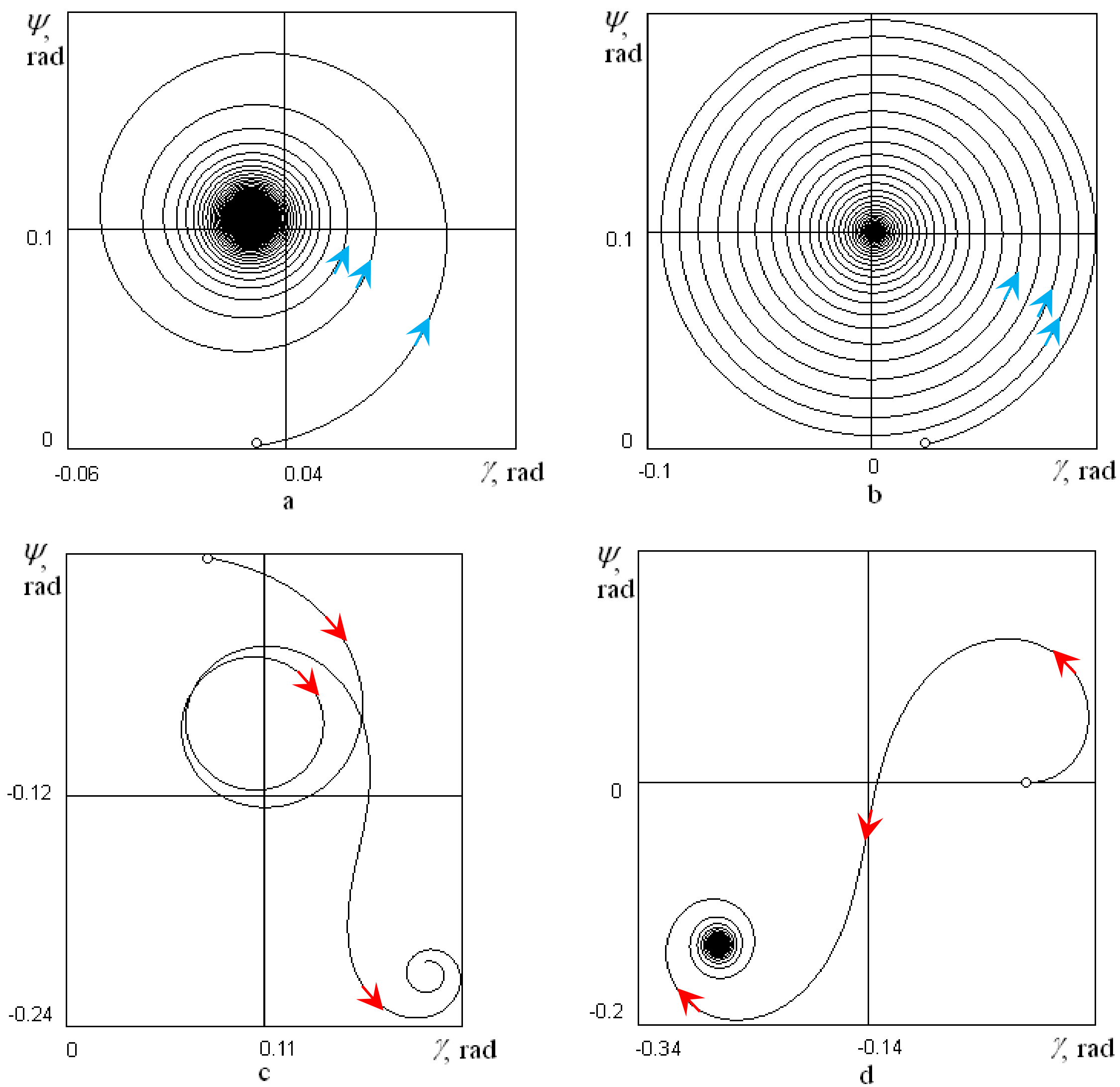

case "a" – the fulfillment of conditions (14);

case "b" – the non-fulfillment of conditions (14);

case "c" – the fulfillment of conditions (15);

case "d" – the non-fulfillment of conditions (15);

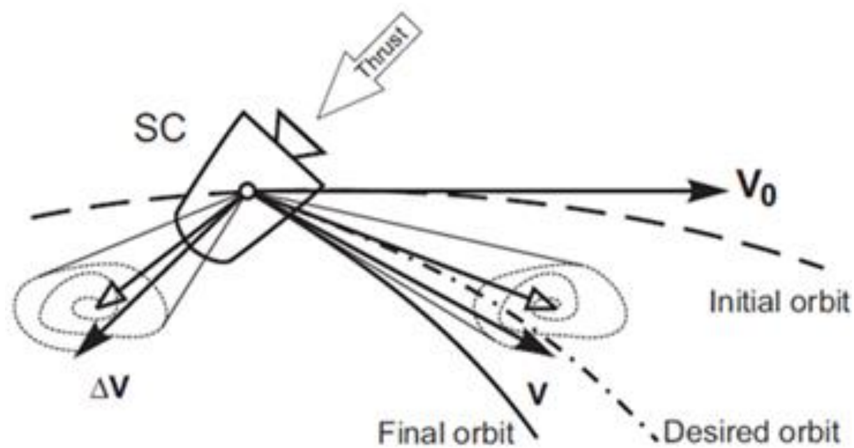

The liquid extruding

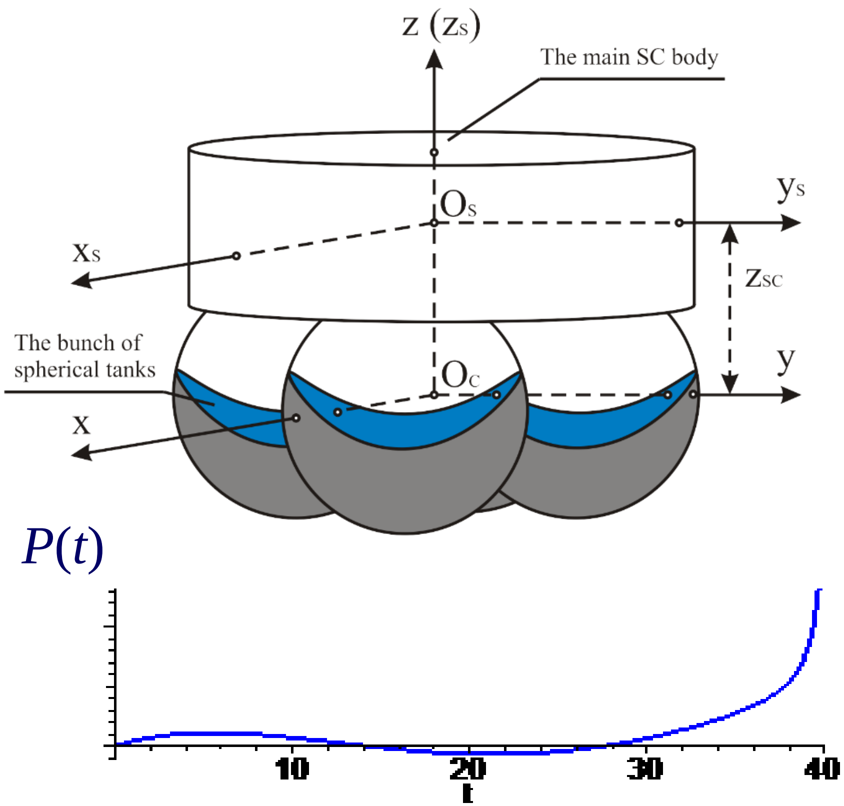

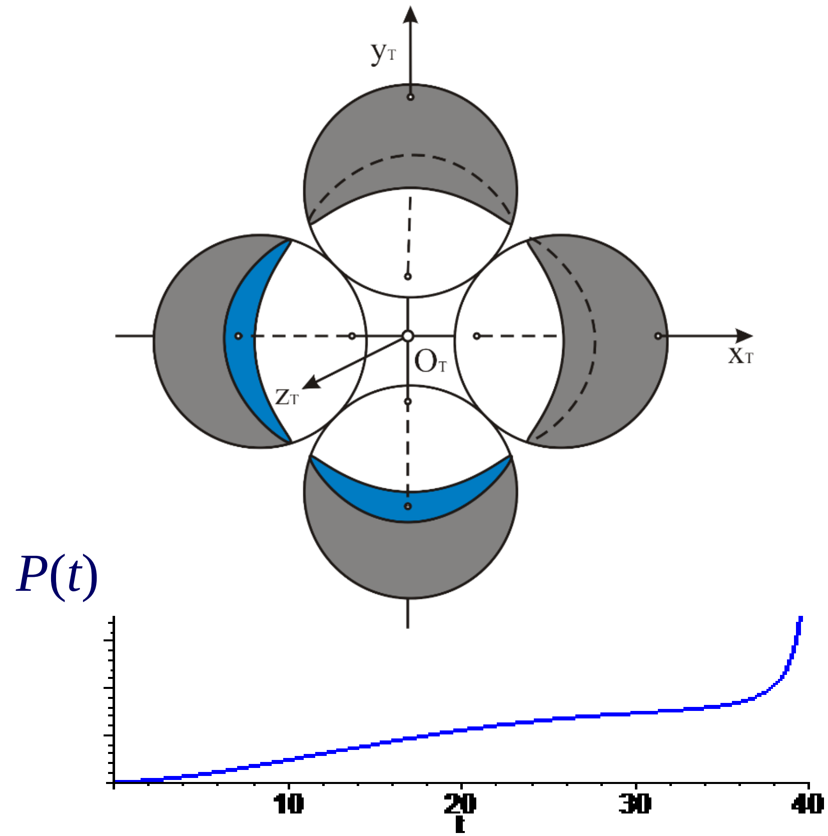

[Complex case]

Geomagnetic field and motion of spacecraft

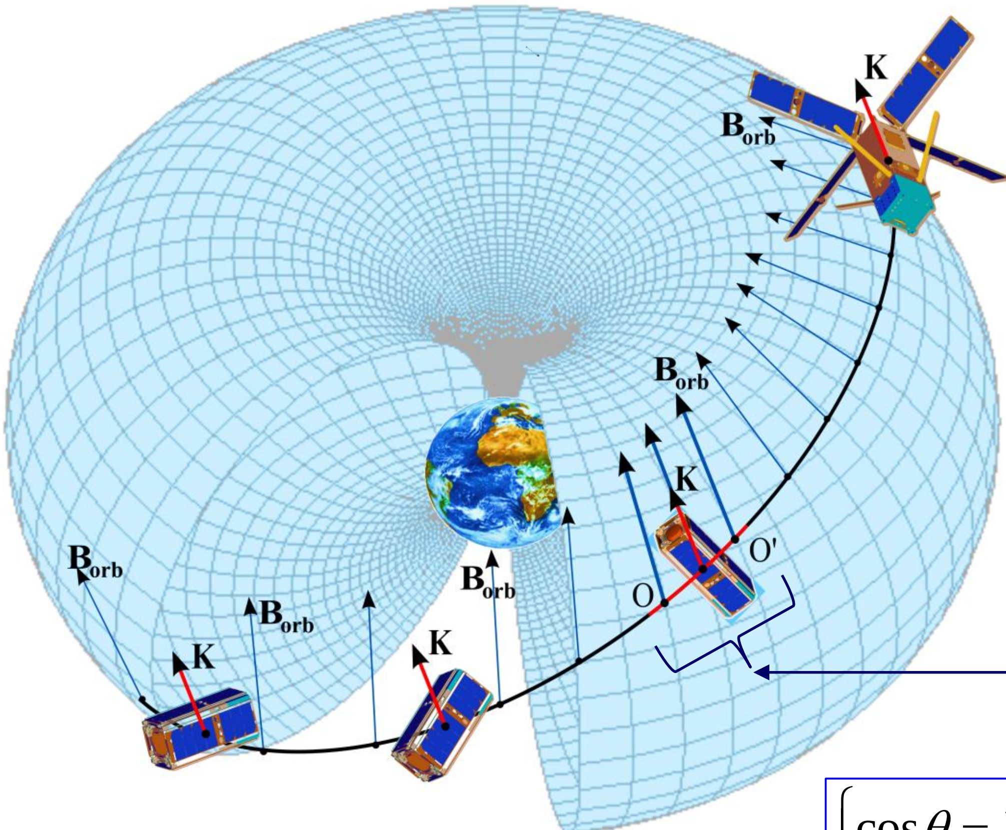

Magnetic torque

$$\mathbf{M}_m = \mathbf{m} \times \mathbf{B}_{\mathbf{orb}} \qquad (2.1)$$

(along OO'):

$$\left\{ \mathbf{K} \uparrow\uparrow \mathbf{B}_{\mathbf{orb}},\ A|\mathbf{m}||\mathbf{B}_{\mathbf{orb}}|/K^2 << 1 \right\} \Rightarrow$$

$$|\mathbf{K}| = K \cong K_Z \cong \text{const};\ \ \mathbf{B}_{\mathbf{orb}} \cong \mu\mathbf{K}$$

$$\boxed{\mathbf{m} = \mathbf{m}(\boldsymbol{\omega}, t) = \mathbf{m}(p, q, r, t)} \qquad (2.1')$$

$$\boxed{\mathbf{M}_m \cong \mathbf{m}(p, q, r, t) \times \mu\mathbf{K}} \qquad (2.1'')$$

$$\boxed{\begin{cases} \cos\theta = L/G;\ \sin\theta = \sqrt{G^2 - L^2}/G;\ \ \varphi_3 \equiv 0;\ \varphi_2 = \psi;\ l = \varphi; \\ \gamma_1 = Ap/K;\ \gamma_2 = Bq/K;\ \gamma_3 = \left(\bar{C}_2 r + \Delta\right)/K \end{cases}}$$

Geomagnetic field and motion of spacecraft

$\boxed{A_b > B_b > C_b}$

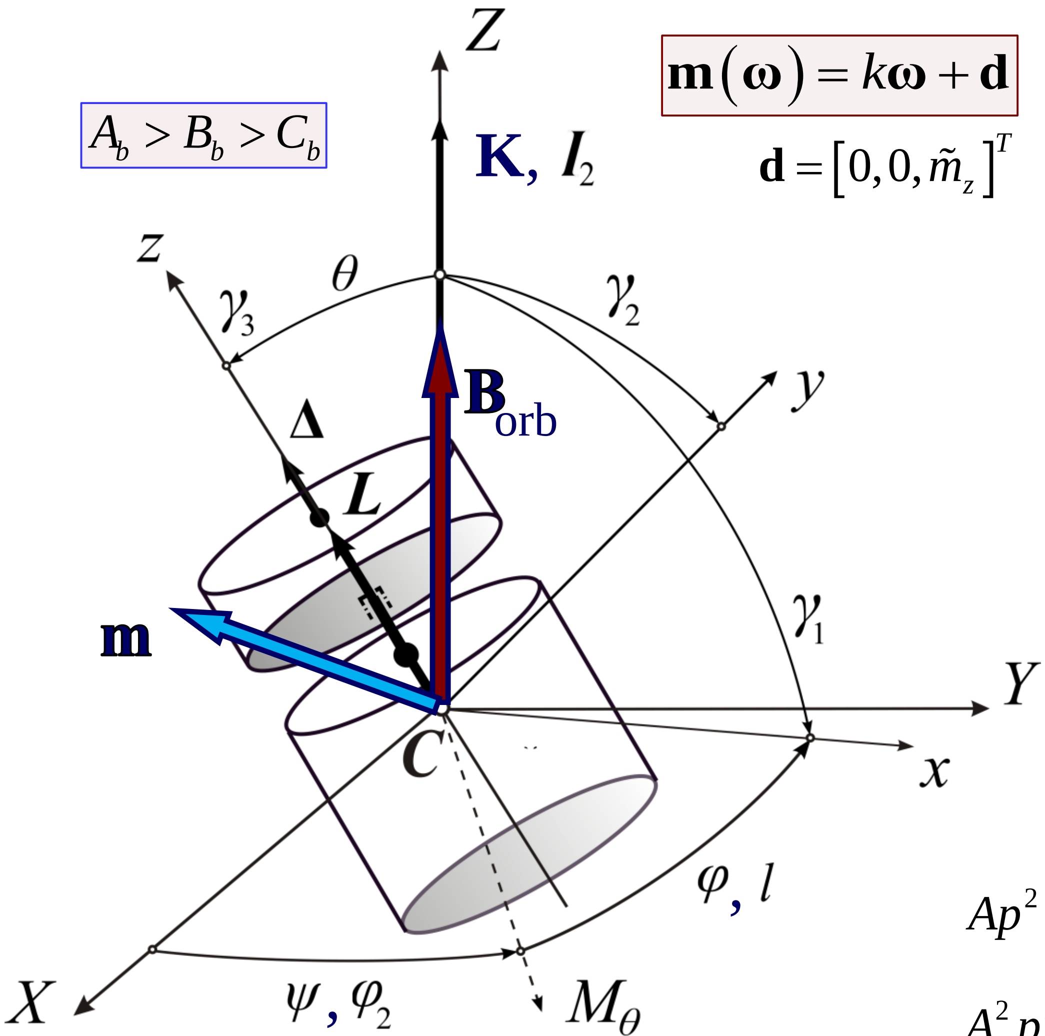

$$\boxed{\mathbf{m}(\boldsymbol{\omega}) = k\boldsymbol{\omega} + \mathbf{d}}$$

$$\mathbf{d} = [0, 0, \tilde{m}_z]^T$$

$$\mathbf{m} = k[p(t), q(t), r(t)]^T + [0, 0, \tilde{m}_z]^T \qquad (2.2)$$

$$\nu = kB_{orb}/K << 1; \quad \mu = \tilde{m}_z B_{orb}/K << 1$$

$$\mathbf{M}_m = [\nu\boldsymbol{\omega} + \mu\mathbf{e}_z] \times \mathbf{K}$$

$$\begin{cases} A\dot{p} + [(C_b - B)qr + q\Delta](1-\nu) = -B\mu q \\ B\dot{q} + [(A - C_b)pr - p\Delta](1-\nu) = A\mu p \\ C_b\dot{r} + \dot{\Delta} + pq(B - A)(1-\nu) = 0 \\ \dot{\Delta} = 0 \end{cases} \qquad (2.3)$$

First integrals

$$Ap^2 + Bq^2 + C_b r^2 + \frac{\Delta^2}{C_r} - \frac{2\mu}{(1-\nu)}[C_b r + \Delta] = 2\tilde{T}$$

$$A^2p^2 + B^2q^2 + [C_b r + \Delta]^2 = \text{const} = K^2 = 2D\tilde{T}$$

Solutions

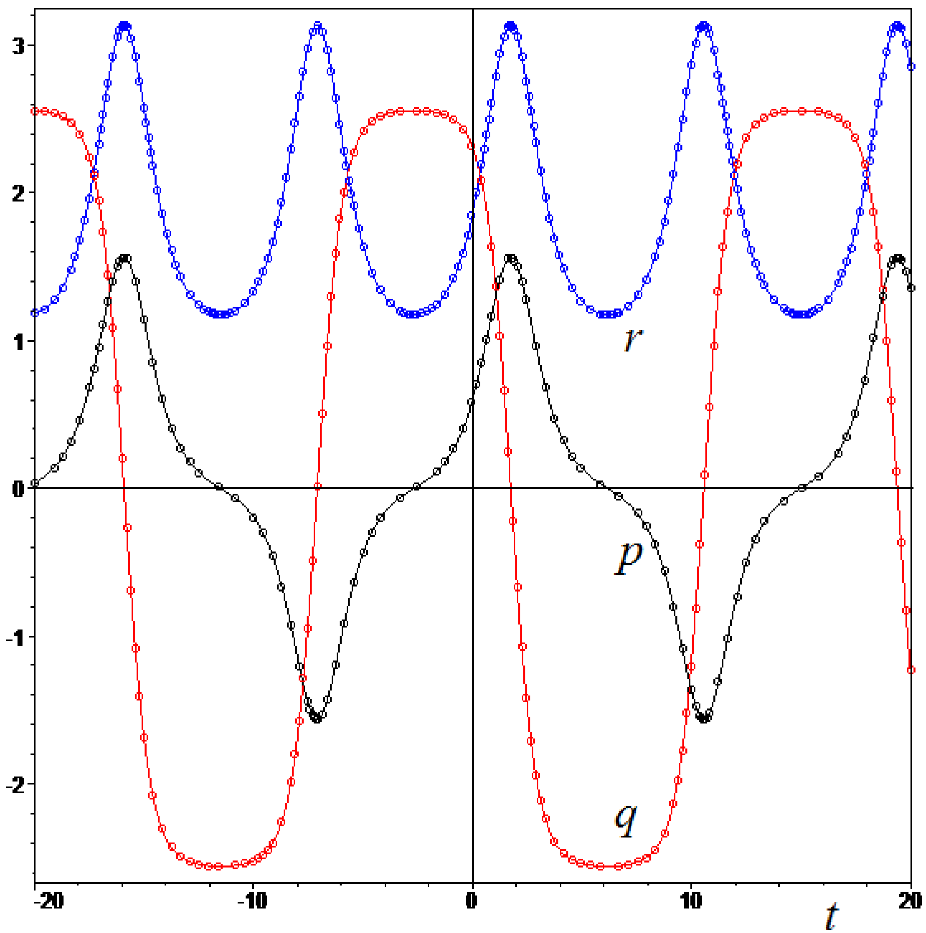

$$\begin{cases} q(t) = \pm\sqrt{\dfrac{1}{B(A-B)}\left[H - C_b(A-C_b)\left(x(t)+\Delta\beta\right)^2\right]}; \\ p(t) = \pm\sqrt{\dfrac{1}{A(A-B)}\left[C_b(B-C_b)x^2(t) - F\right]}; \\ r(t) = \dfrac{\Delta}{A-C_b} \pm \left(x(t) + \Delta\beta - \dfrac{\mu}{(1-\nu)}\alpha\right); \end{cases} \tag{2.4}$$

$$x(t) = e\frac{R/P + \tilde{c}^2\,\mathrm{sn}^2\left[\pm\left(N(1-\nu)(t-t_0)+I_0\right),k\right]}{R/P - \tilde{c}^2\,\mathrm{sn}^2\left[\pm\left(N(1-\nu)(t-t_0)+I_0\right),k\right]};$$

I.9. Hamilton form of equations in the Andoyer-Deprit variables

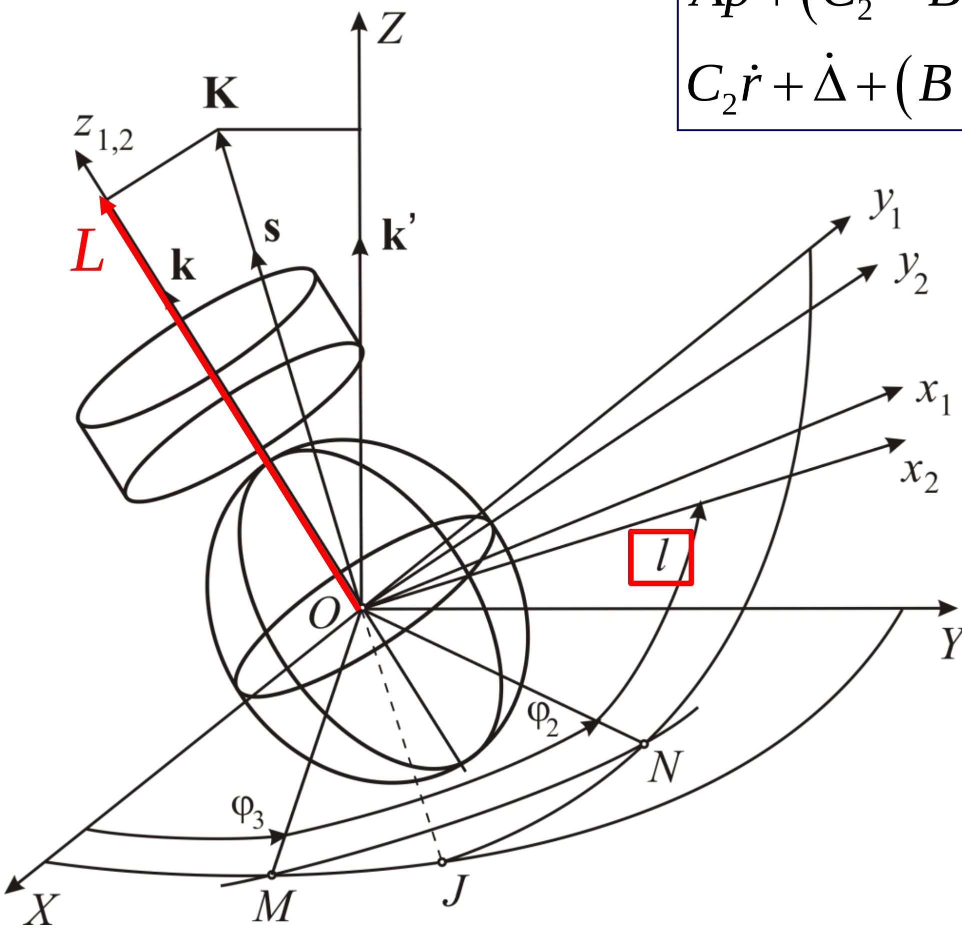

$$\begin{aligned} &A\dot{p}+(C_2-B)qr+q\Delta=0, \qquad B\dot{q}+(A-C_2)pr-p\Delta=0, \\ &C_2\dot{r}+\dot{\Delta}+(B-A)pq=0, \qquad \dot{\Delta}=M_\Delta, \end{aligned} \tag{21}$$

$$\Delta=C_1(r+\sigma); \tag{22}$$

$$A=A_1+A_2,\quad B=A_1+B_2;$$

$$\begin{cases} L=\dfrac{\partial \mathrm{T}}{\partial \dot{l}}=\mathbf{K}\cdot\mathbf{k};\; I_2=\dfrac{\partial \mathrm{T}}{\partial \dot{\varphi}_2}=\mathbf{K}\cdot\mathbf{s}=|\mathbf{K}|=K; \\ I_3=\dfrac{\partial \mathrm{T}}{\partial \dot{\varphi}_3}=\mathbf{K}\cdot\mathbf{k}'; \quad L\le I_2 \end{cases} \tag{23}$$

$$\begin{cases} K_{x_2}=Ap=\sqrt{I_2^2-L^2}\sin l; \\ K_{y_2}=Bq=\sqrt{I_2^2-L^2}\cos l; \\ K_{z_2}=C_2 r+\Delta=L. \end{cases} \tag{24}$$

$$H=H_0+\varepsilon H_1; \quad H_0=\frac{I_2^2-L^2}{2}\left[\frac{\sin^2 l}{A_1+A_2}+\frac{\cos^2 l}{A_1+B_2}\right]+\frac{1}{2}\left[\frac{\Delta^2}{C_1}+\frac{(L-\Delta)^2}{C_2}\right] \tag{25}$$

I.10. Poincaré sections $\left(t \bmod (1/\nu)\right)$

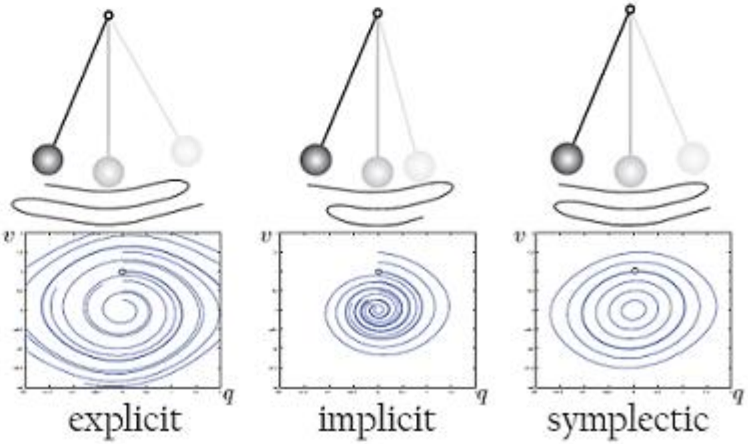

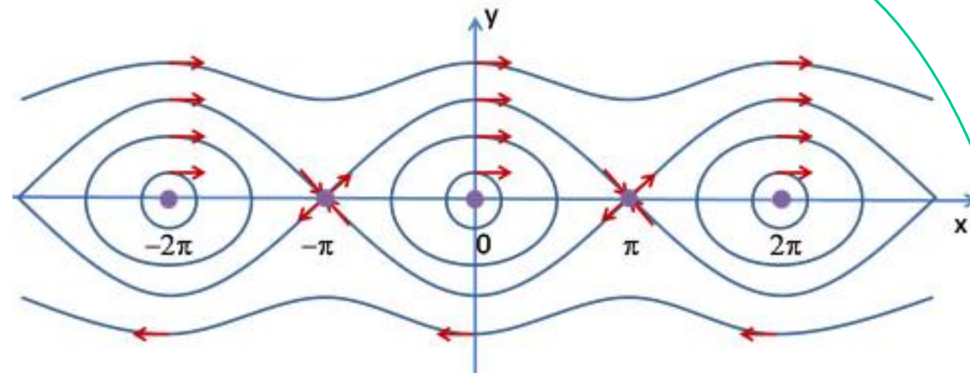

Andoyer-Deprit canonical variables

$$L = \frac{\partial \mathrm{T}}{\partial \dot{l}} = \mathbf{K}\cdot\mathbf{k}, \quad G = \frac{\partial \mathrm{T}}{\partial \dot{\varphi}_2} = \mathbf{K}\cdot\mathbf{s} = K, \quad H = \frac{\partial \mathrm{T}}{\partial \dot{\varphi}_3} = \mathbf{K}\cdot\mathbf{k}', \quad \Delta_{ij} = \frac{\partial \mathrm{T}}{\partial \dot{\delta}_{ij}} = \frac{\partial \mathrm{T}}{\partial \sigma_{ij}}$$

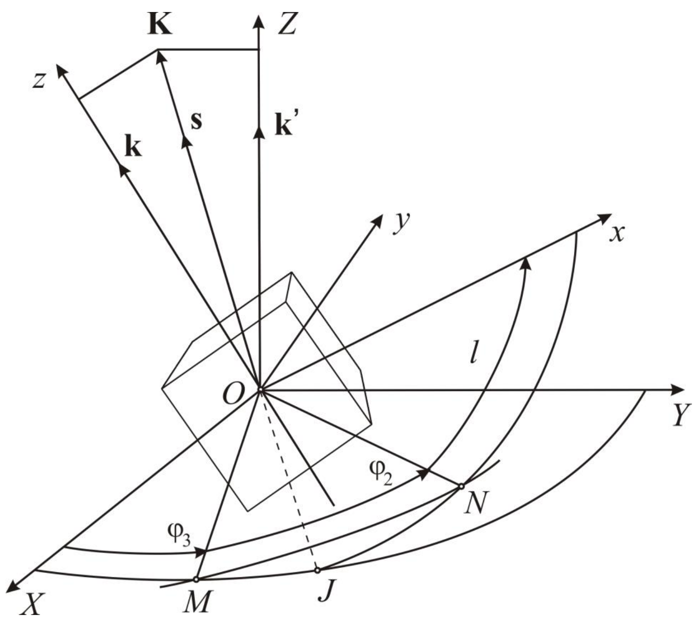

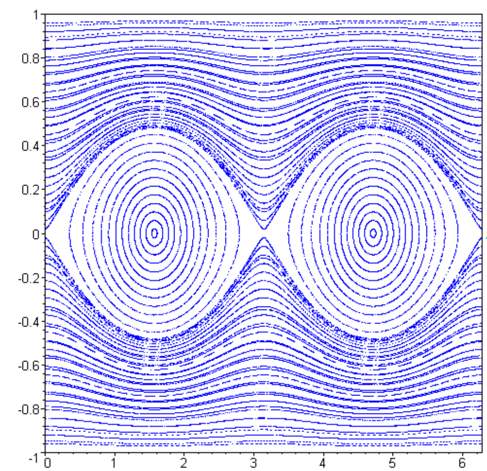

$$\left\{ x = l, \;\; y = L / I_2 \right\}$$

Hamilton form of equations:

$$\begin{cases} \dot{L} = f_L(l,L) + \varepsilon g_L(t); \quad \dot{l} = f_l(l,L) + \varepsilon g_l(t); \\ f_L(l,L) = \alpha\left(I_2^2 - L^2\right)\sin l \cos l; \; f_l(l,L) = L\left[\dfrac{1}{C_2} - \dfrac{\sin^2 l}{(A_1 + A_2)} - \dfrac{\cos^2 l}{(A_1 + B_2)}\right] - \dfrac{\Delta}{C_2}, \end{cases} \quad (26)$$

$$A_2 > B_2 > C_2 > A_1 > C_1.$$

$$\alpha = (A_1 + B_2)^{-1} - (A_1 + A_2)^{-1}.$$

Assumption : $\Delta = 0$

Equations (21) have heteroclinic solutions :

$$\bar{p}(t) = \frac{p_0}{\operatorname{ch} \lambda t}; \quad \bar{q}(t) = b \operatorname{th} \lambda t; \quad \bar{r}(t) = \frac{r_0}{\operatorname{ch} \lambda t}; \quad \Delta \equiv 0; \quad b^2 = \frac{(C_2 - A)A}{(C_2 - B)B} p_0^2, \quad \lambda^2 = \frac{(B - A)(C_2 - A)}{C_2 B} p_0^2, \quad (27)$$

Perturbation: $M_\Delta = \mu \cdot \cos(\nu t)$

From (21) $\Rightarrow$ $\Delta(t) = (\mu / \nu) \sin \nu t \quad \Rightarrow \Rightarrow \quad g_L(t) = 0, \; g_l(t) = -\varepsilon \sin \nu t, \; \varepsilon = \mu / (\nu C_2).$

Melnikov function:

$$M(t_0) = \int_{-\infty}^{+\infty} f_L\left(\bar{l}(t), \bar{L}(t)\right) g_l(t + t_0)\, dt,$$

$$M(t_0) = \{(25),(26),(27)\} = \alpha \int_{-\infty}^{+\infty} A\bar{p}(t) B\bar{q}(t) \sin\left(\nu(t + t_0)\right) dt = \alpha b p_0 AB\left[\cos \nu t_0 J_1 + \cos \nu t_0 J_2\right] = R \cos \nu t_0, \quad (28)$$

$$J_1 = \int_{-\infty}^{+\infty} \frac{\operatorname{th} \lambda t}{\operatorname{ch} \lambda t} \cdot \sin(\nu t)\, dt = \text{const} \neq 0, \quad J_2 = \int_{-\infty}^{+\infty} \frac{\operatorname{th} \lambda t}{\operatorname{ch} \lambda t} \cdot \cos(\nu t)\, dt = 0, \quad R = \alpha b p_0 A B J_1.$$

Melnikov function has infinite number of simple roots. This proves the fact of the motion chaotization at presence of small harmonical perturbation torques between the coaxial bodies.

Perturbations and the Melnikov's function

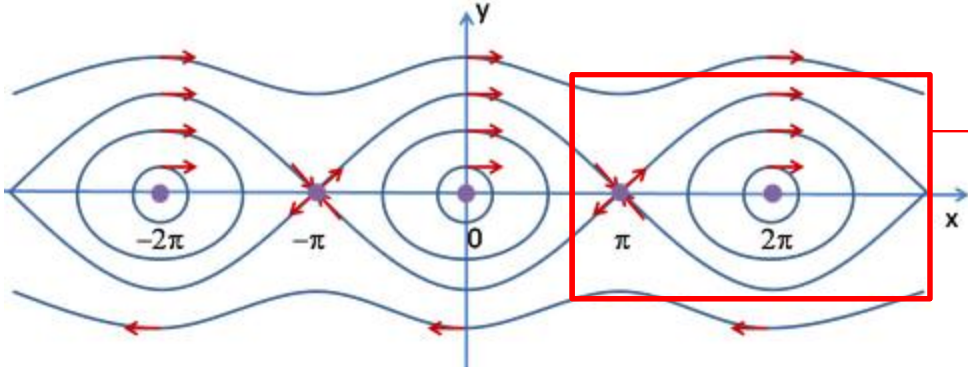

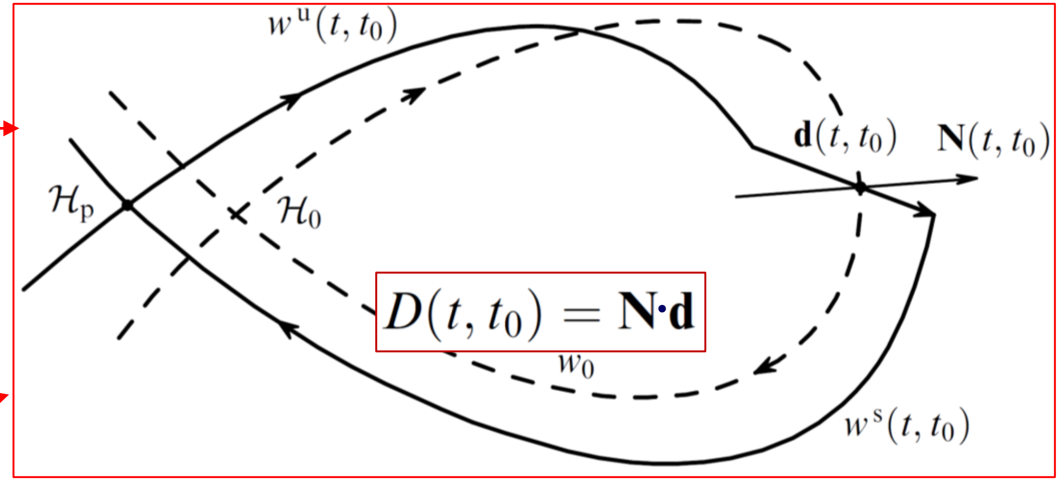

$$M_\Delta = m_\Delta \cos \nu_\Delta t;$$

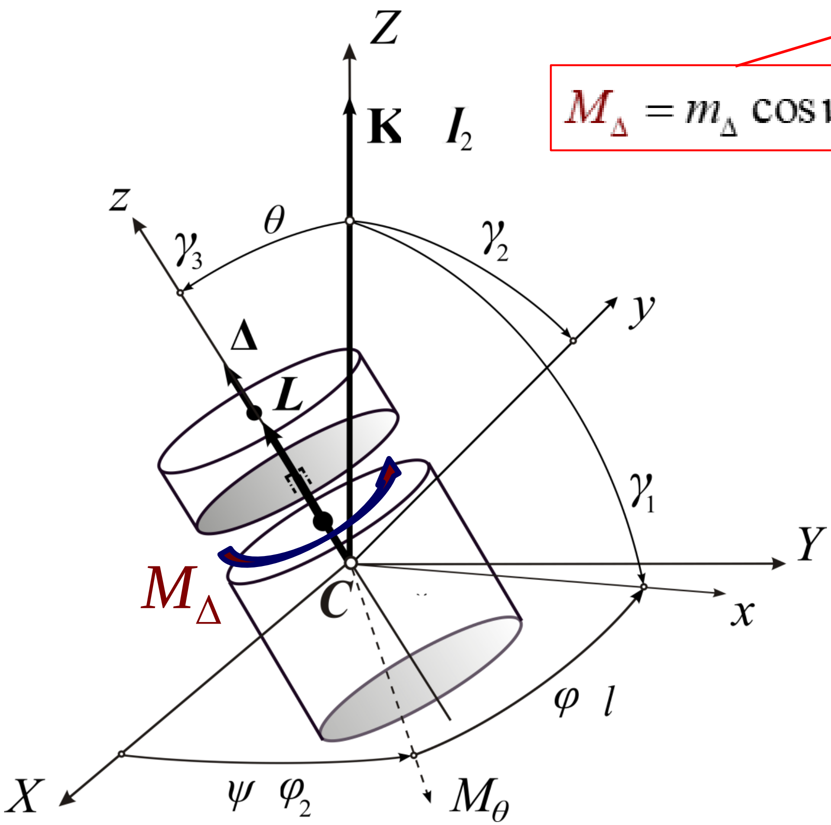

$$M(t_0) = D(t, t_0) =$$

$$= \varepsilon \int_{-\infty}^{+\infty} \left[\frac{\partial \mathcal{H}_0}{\partial l} \frac{\partial \mathcal{H}_1}{\partial L} - \frac{\partial \mathcal{H}_0}{\partial L} \frac{\partial \mathcal{H}_1}{\partial l} \right]_{\left(\bar{l}(t), \bar{L}(t), t+t_0\right)} dt$$

1. **Мельников В.К. (1963)** Об устойчивости центра при периодических по времени возмущениях. Труды Московского математического общества, Т.12, с.3-52.

4. **Holmes P. J., Marsden J. E. (1983)** Horseshoes and Arnold diffusion for Hamiltonian systems on Lie groups, Indiana Univ. Math. J. 32, pp. 273-309.

4. **Wiggins S. (1988)** Global Bifurcations and Chaos : Analytical Methods (Applied mathematical sciences: vol. 73). Springer-Verlag..

Perturbed motion

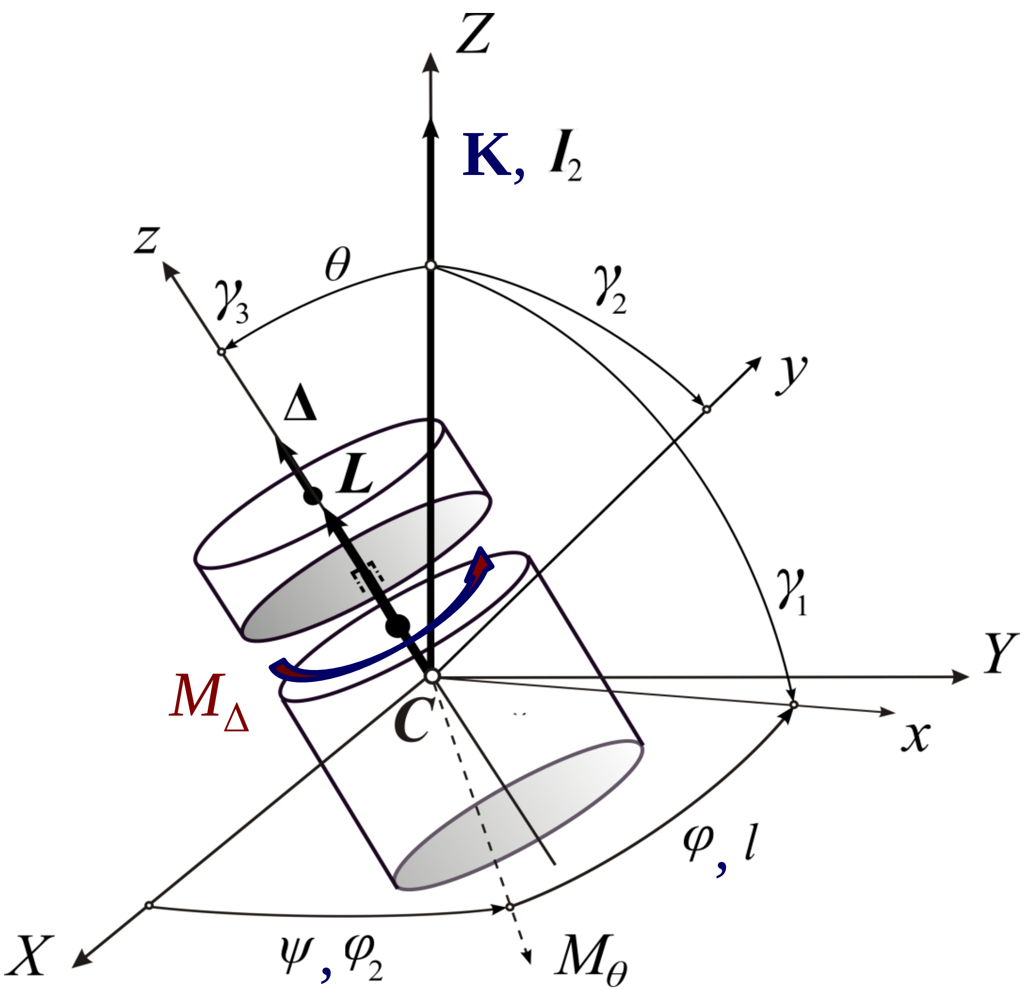

$$\begin{cases} M_\Delta = m_\Delta \cos \nu_\Delta t; \quad \mathcal{H} = \mathcal{H}_0 + \varepsilon \mathcal{H}_1 \\ \mathcal{H}_1 = -L\nu_\Delta \sin \nu_\Delta t; \quad \varepsilon = \dfrac{m_\Delta}{C_2 \nu_\Delta^2} \end{cases} \tag{3.1}$$

Melnicov's function:

$$M(t_0) = \varepsilon \int_{-\infty}^{+\infty} \left[\frac{\partial \mathcal{H}_0}{\partial l} \frac{\partial \mathcal{H}_1}{\partial L} - \frac{\partial \mathcal{H}_0}{\partial L} \frac{\partial \mathcal{H}_1}{\partial l} \right]_{\left(\bar{l}(t), \bar{L}(t), t+t_0\right)} dt$$

$$\boxed{M(t_0) = m_\Delta \pi \sqrt{\frac{AB}{(A-C_2)(B-C_2)}} \operatorname{sech} \frac{\nu_\Delta \pi}{2\lambda} \cos(\nu_\Delta t_0) = \\ = \text{harmonic}(t_0) \qquad (3.2)}$$

CHAOS

$\left\{l, L/I_2\right\}$

I.10. Poincaré sections $\left(t \bmod \left(1/\nu\right)\right)$

$\left\langle\left(\nu_\Delta t \bmod 2\pi\right)=0\right\rangle$

$\varepsilon = 0.0$

$\nu_\Delta = 1$

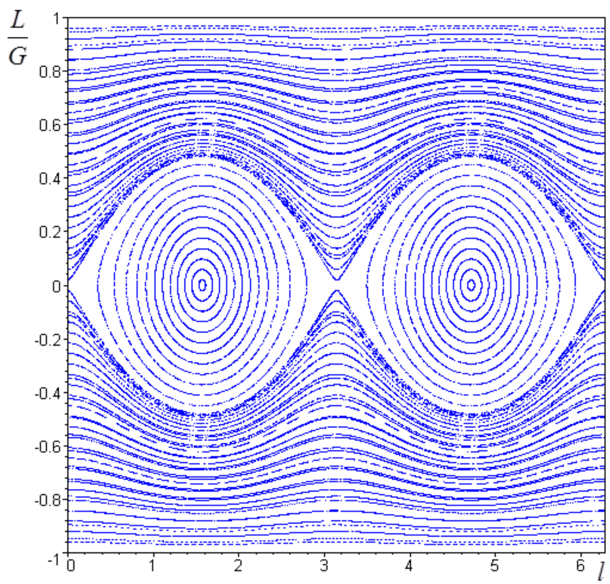

$\varepsilon = 0.1$

$\nu_\Delta = 1$

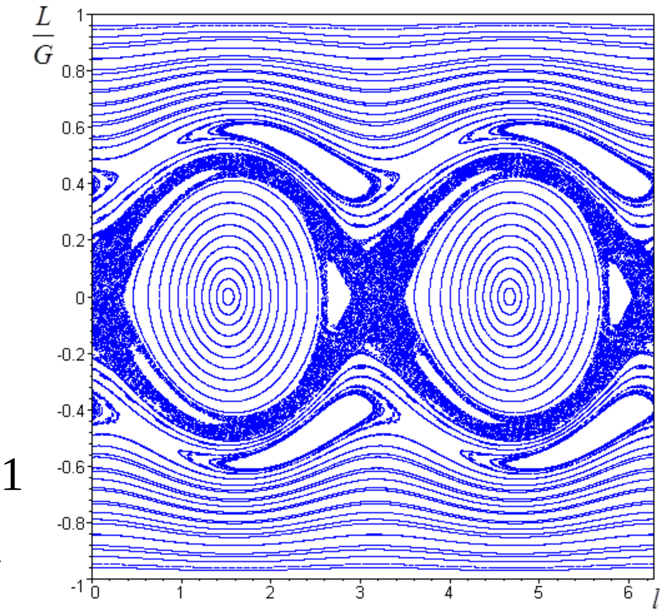

$A_b = 15$
$B_b = 8$
$C_b = 6$
$A_r = 5$
$C_r = 4$
$K = 10$
$\Delta = 0$

Small perturbation

Big perturbation

$\varepsilon = 0.4$

$\nu_\Delta = 2$

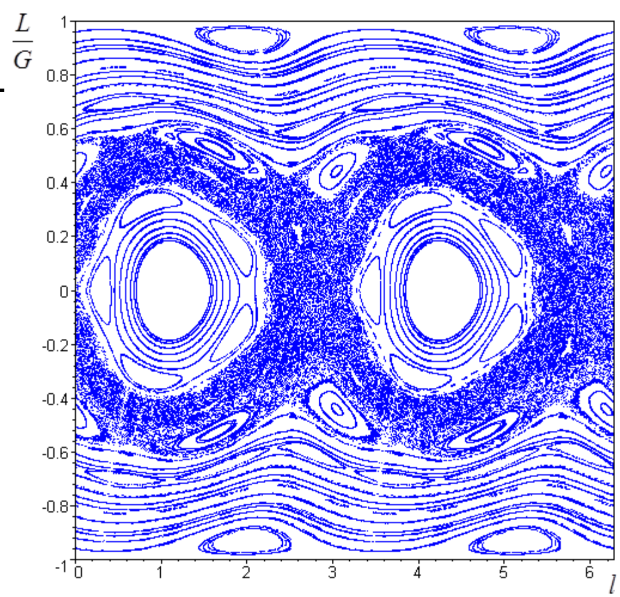

$\varepsilon = 0.8$

$\nu_\Delta = 2$

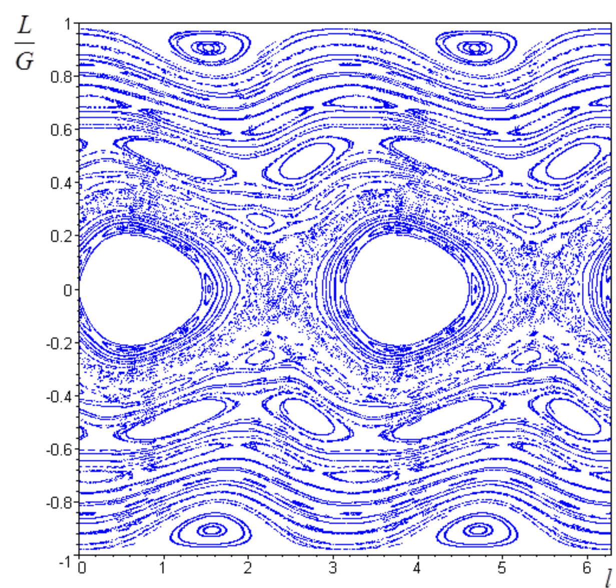

$A_b = 15$
$B_b = 8$
$C_b = 6$
$A_r = 5$
$C_r = 4$
$K = 10$
$\Delta = 0$

Poincare section $\quad \left\langle \left(\nu_{\Delta} t \bmod 2\pi \right) = 0 \right\rangle$

Heteroclinic nets

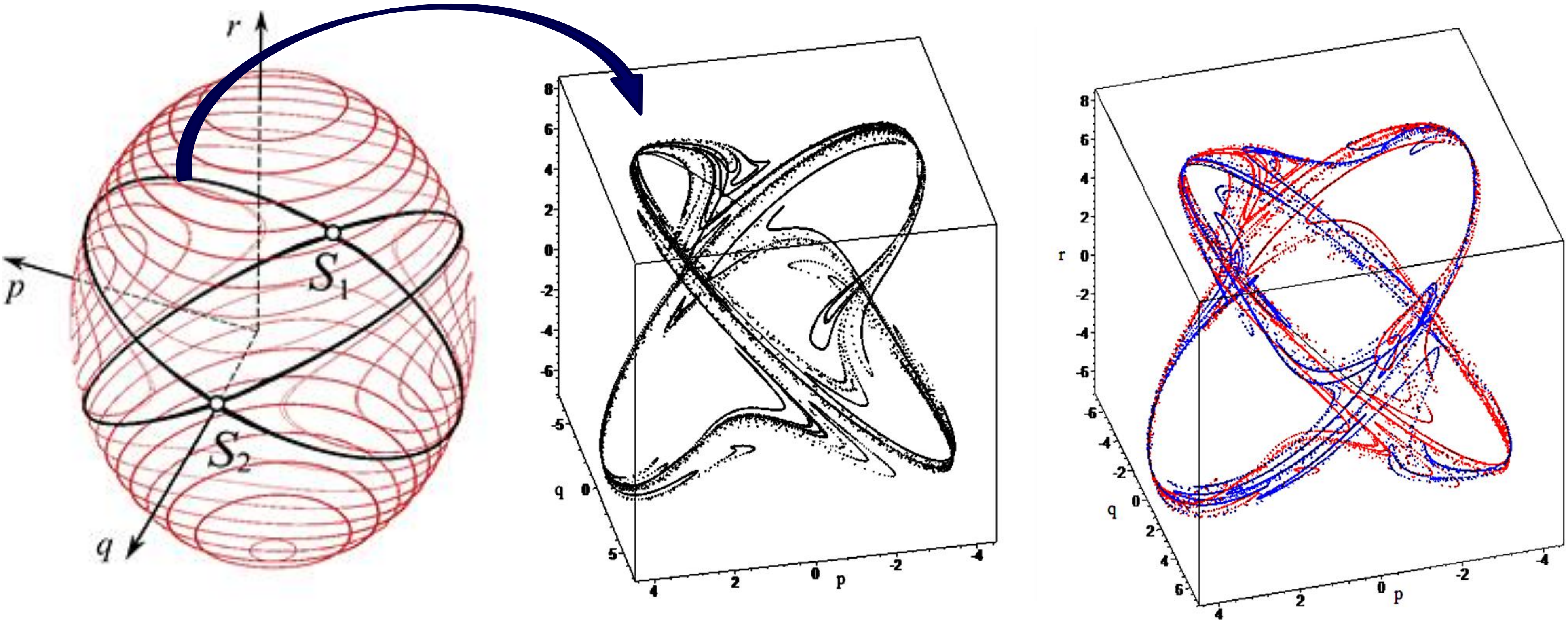

Cases of chaotization

HUGHES 376

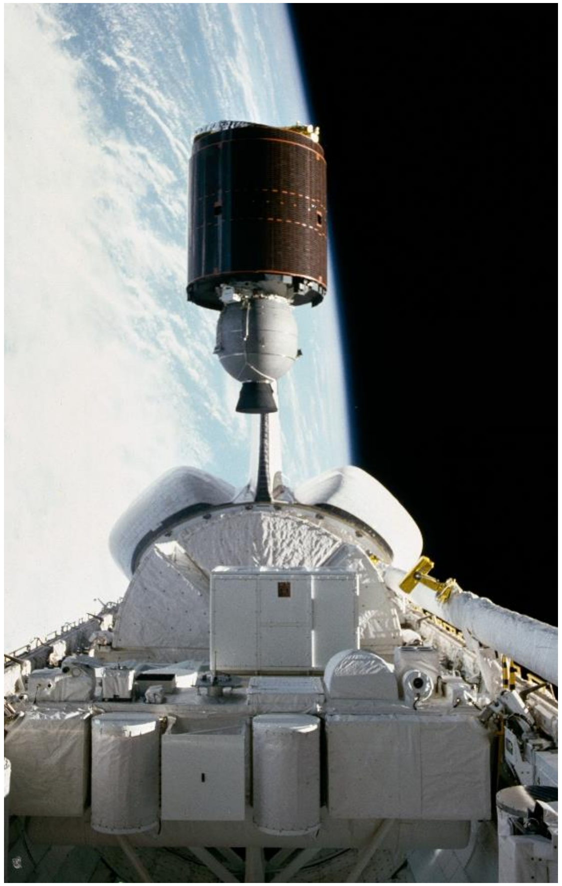

DSSC is placed into an orbit

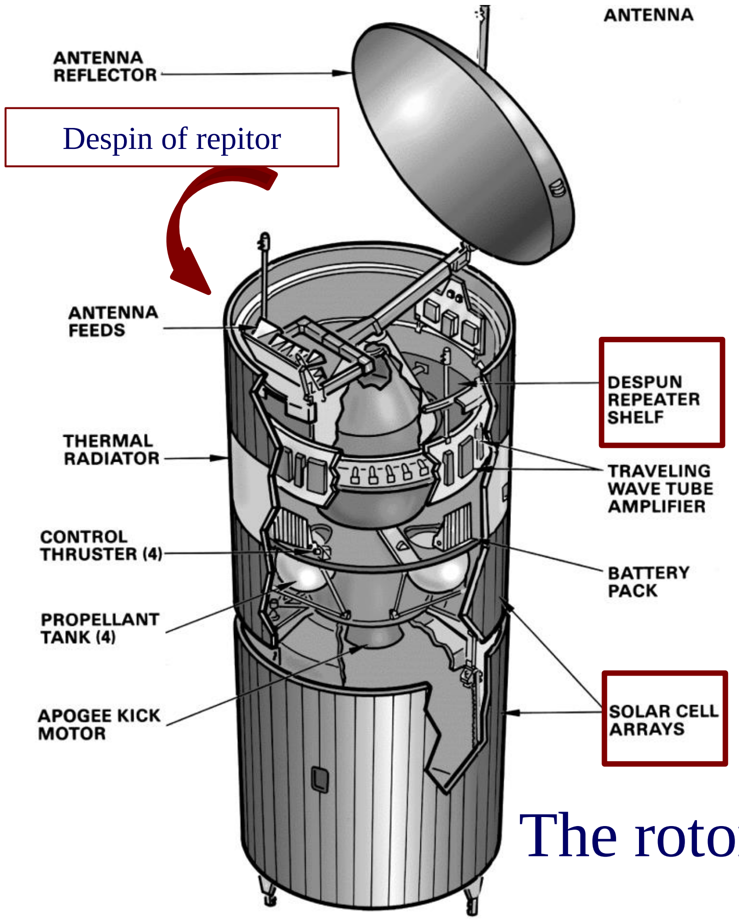

The spin-up of the rotor (M_Δ =const → Δ↑)

[Hall C. D. (1998), Escape from gyrostat trap states, J. Guidance Control Dyn. 21, pp. 421-426].

⇕

CHAOS

The chaotization of the DSSC at the spin-up of the rotor (M_Δ =const)

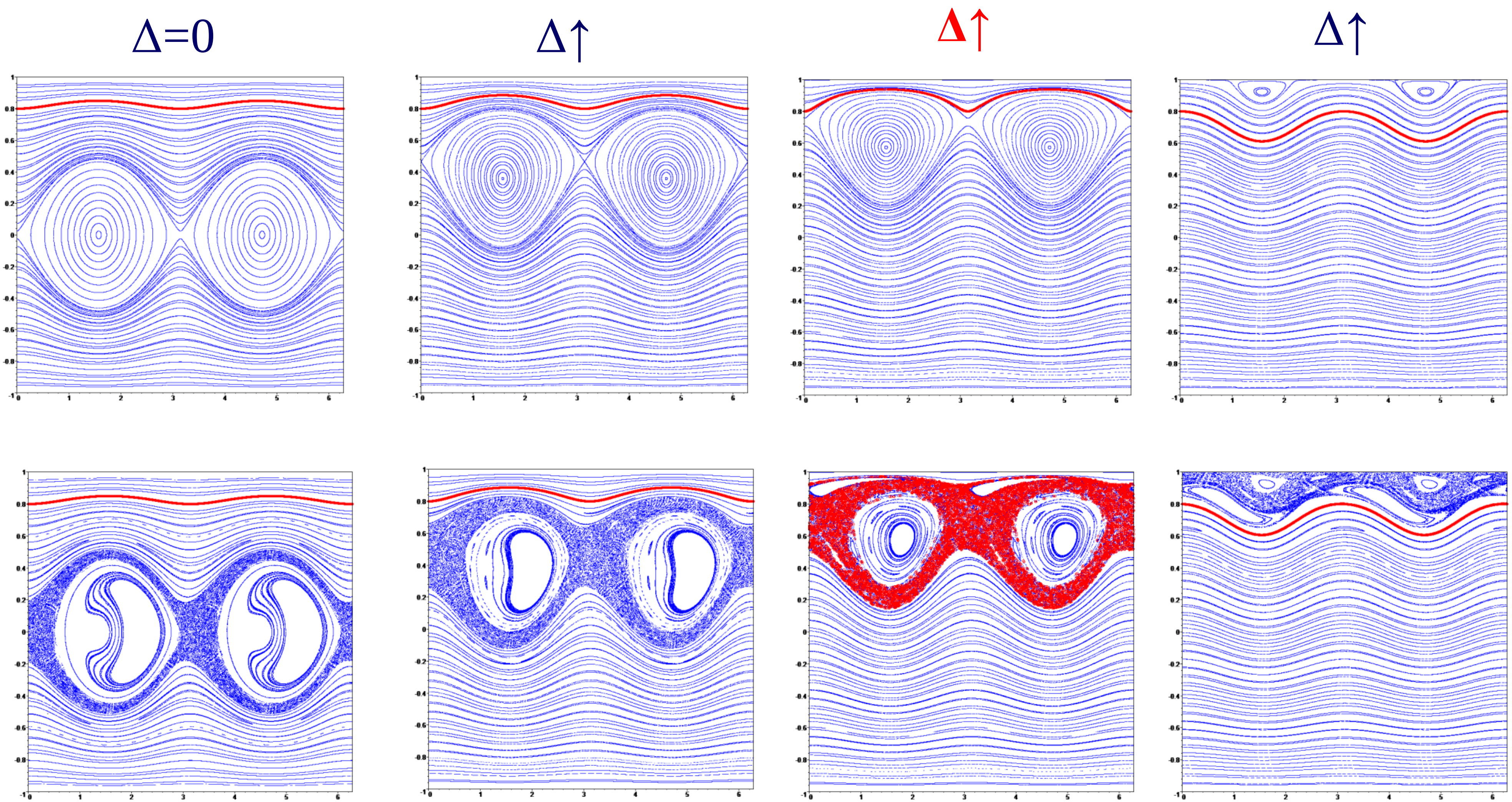

$\tilde{M}_\Delta = m_\Delta \cos \nu_\Delta t;$

here we go through chaos

Cases of attitude motion

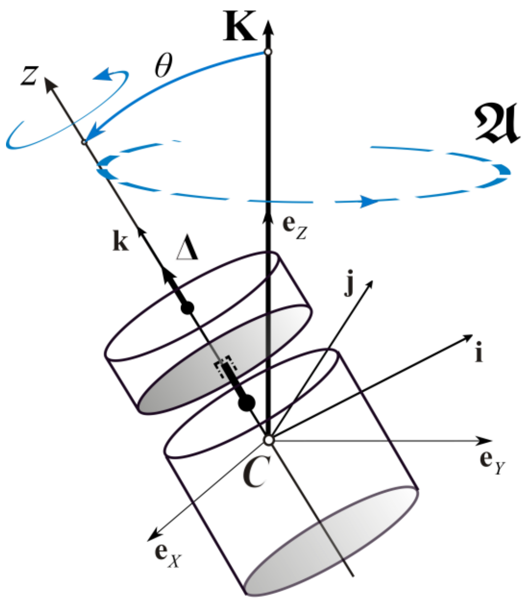

$$\begin{cases} \left| r(t) - \dfrac{\Delta(t)}{B-C_b} \right| > \left| p(t) \cdot \sqrt{\dfrac{A(A-B)}{C_b(B-C_b)}} \right|; \\ r(t) - \dfrac{\Delta(t)}{B-C_b} > 0 \end{cases} \qquad (4.2)$$

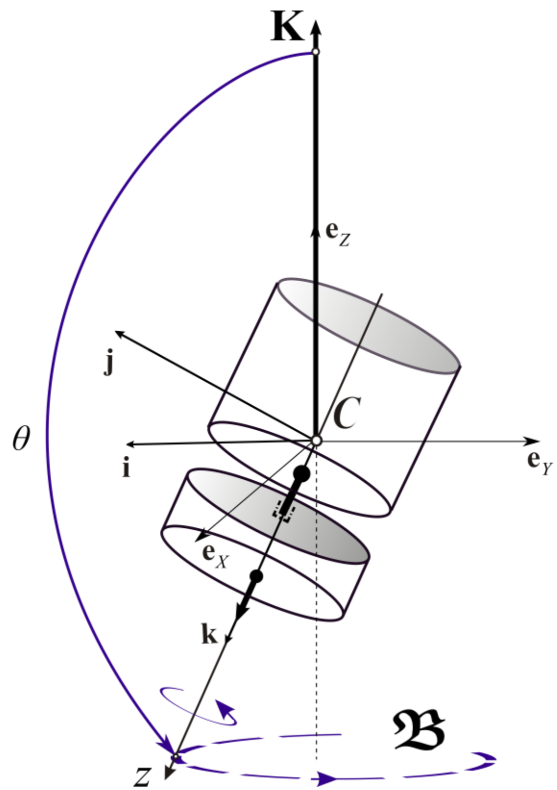

$$\begin{cases} \left| r(t) - \dfrac{\Delta(t)}{B-C_b} \right| > \left| p(t) \cdot \sqrt{\dfrac{A(A-B)}{C_b(B-C_b)}} \right|; \\ r(t) - \dfrac{\Delta(t)}{B-C_b} < 0 \end{cases} \qquad (4.3)$$

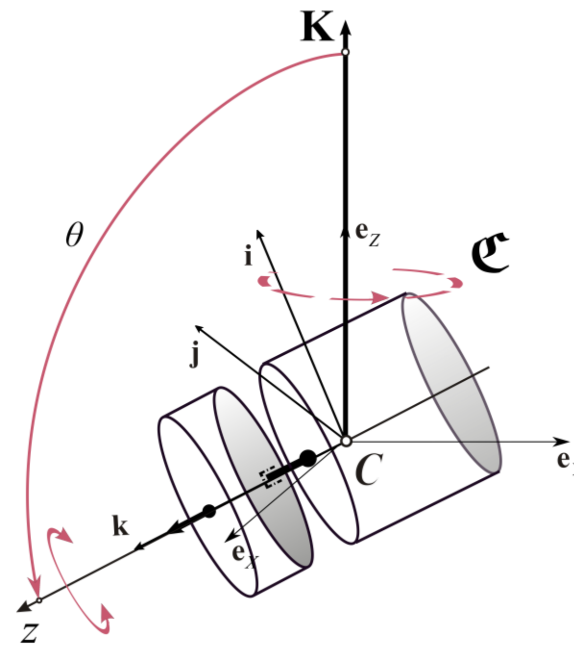

$$\begin{cases} \left| r(t) - \dfrac{\Delta(t)}{B-C_b} \right| > \left| p(t) \cdot \sqrt{\dfrac{A(A-B)}{C_b(B-C_b)}} \right|; \\ r(t) - \dfrac{\Delta(t)}{B-C_b} < 0 \end{cases} \qquad (4.4)$$

The chaotic reorientation – the positive implementation

$$\begin{cases} \dot{\Delta} = M_{\Delta} \cdot \left(H\left(t - t_{ini}\right) - H\left(t - t_{hetero}\right) \right) \\ if \left\{ \left\| r(t) - \dfrac{\Delta(t)}{B - C_b} \right| - \left| p(t) \cdot \sqrt{\dfrac{A(A-B)}{C_b\left(B - C_b\right)}} \right\| \le \xi \right\} \;\; then \;\; t \to t_{hetero} \end{cases} \qquad (4.1)$$

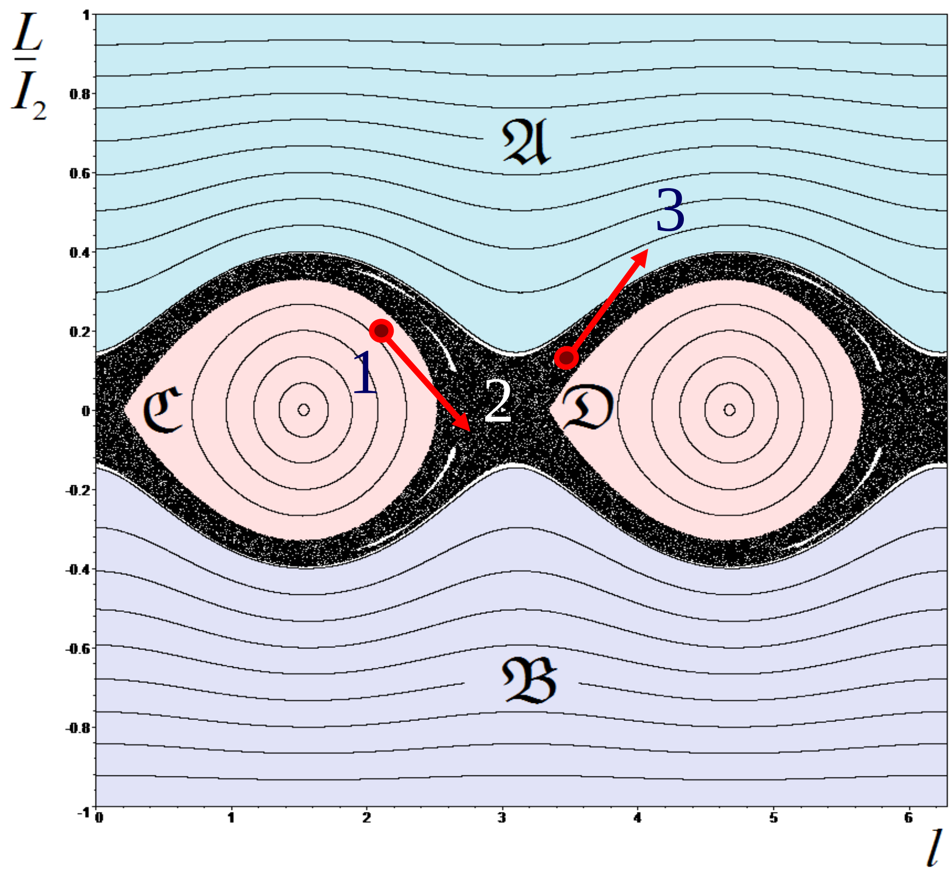

The chaotic reorientation

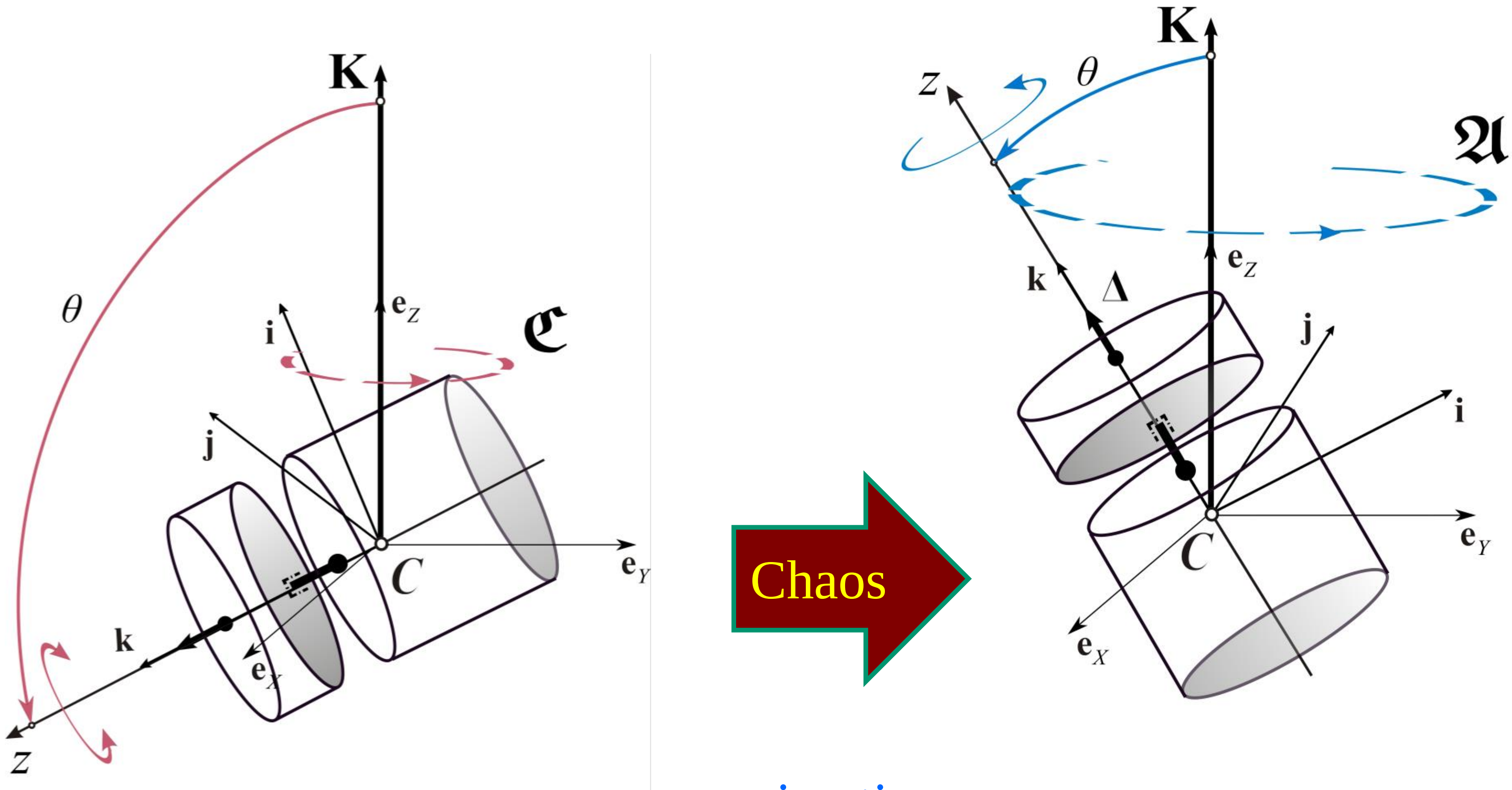

animation

[19] *Doroshin A.V.* CHAOS AS THE HUB OF SYSTEMS DYNAMICS. THE PART I – THE ATTITUDE CONTROL OF SPACECRAFT BY INVOLVING IN THE HETEROCLINIC CHAOS // Communications in Nonlinear Science and Numerical Simulation. 2018. Vol. 59

II. The spider-type systems motion

II.1 Angular momentum of the system in projections onto axes of the frame *Oxyz*

$$\mathbf{K} = \mathbf{K}_m + \mathbf{K}_r$$

$$\mathbf{K}_m = \begin{bmatrix} \tilde{A}p \\ \tilde{B}q \\ \tilde{C}r \end{bmatrix} + (4J + 2I) \begin{bmatrix} p \\ q \\ r \end{bmatrix}, \quad \mathbf{K}_r = I \begin{bmatrix} \sigma_1 + \sigma_2 \\ \sigma_3 + \sigma_4 \\ \sigma_5 + \sigma_6 \end{bmatrix} \qquad (1)$$

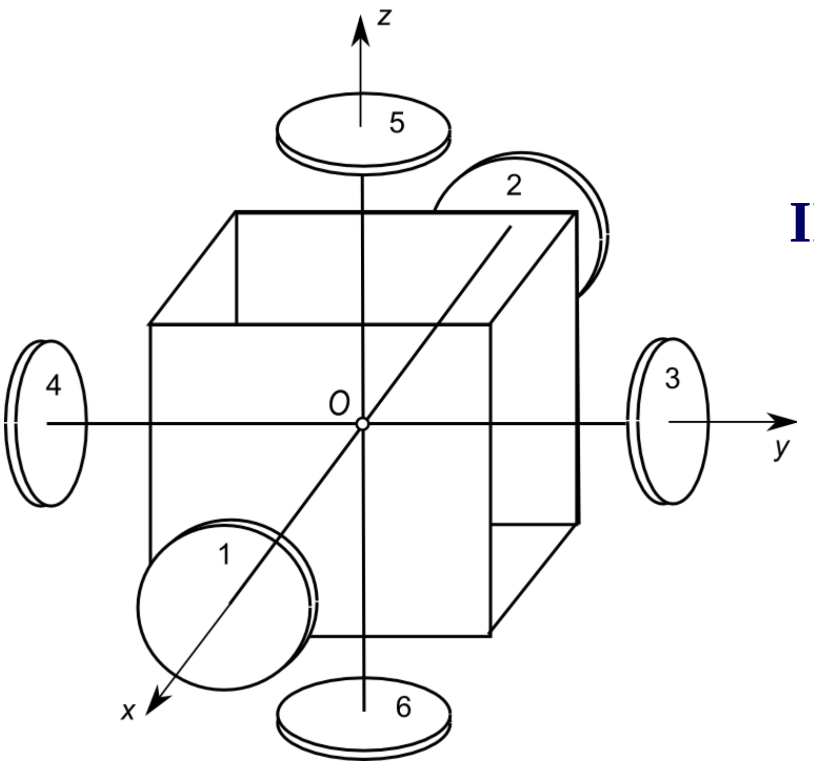

$$\sigma^{ij} = \sigma_i + \sigma_j, \qquad A = \tilde{A} + 4J + 2I$$

$$B = \tilde{B} + 4J + 2I, \quad C = \tilde{C} + 4J + 2I$$

II.2. The motion equations of the multirotor system

$$\frac{d\mathbf{K}}{dt} + \boldsymbol{\omega} \times \mathbf{K} = \mathbf{M}^e \qquad (2)$$

$$\begin{cases} A\dot{p} + I\dot{\sigma}^{12} + (C - B)qr + I\left(q\sigma^{56} - r\sigma^{34}\right) = M_x^e \\ B\dot{q} + I\dot{\sigma}^{34} + (A - C)pr + I\left(r\sigma^{12} - p\sigma^{56}\right) = M_y^e \\ C\dot{r} + I\dot{\sigma}^{56} + (B - A)pq + I\left(p\sigma^{34} - q\sigma^{12}\right) = M_z^e \end{cases} \qquad (3)$$

$$\begin{cases} I\left(\dot{p} + \dot{\sigma}_1\right) = M_1^i + M_{1x}^e; \; I\left(\dot{p} + \dot{\sigma}_2\right) = M_2^i + M_{2x}^e \\ I\left(\dot{q} + \dot{\sigma}_3\right) = M_3^i + M_{3y}^e; \; I\left(\dot{q} + \dot{\sigma}_4\right) = M_4^i + M_{4y}^e \\ I\left(\dot{r} + \dot{\sigma}_5\right) = M_5^i + M_{5z}^e; \; I\left(\dot{r} + \dot{\sigma}_6\right) = M_6^i + M_{6z}^e \end{cases} \qquad (4)$$

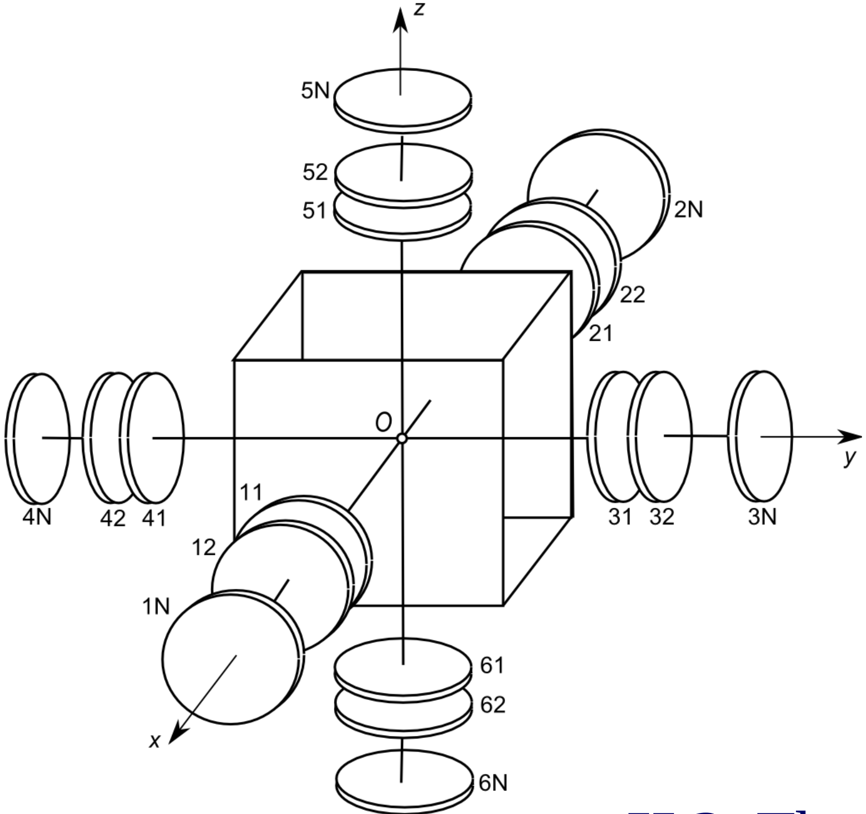

$$\sigma^{ij}=\sum_{l=1}^{N}\left(\sigma_{il}+\sigma_{jl}\right),\qquad A=\tilde{A}+4\sum_{l=1}^{N}J_l+2NI$$

$$B=\tilde{B}+4\sum_{l=1}^{N}J_l+2NI,\quad C=\tilde{C}+4\sum_{l=1}^{N}J_l+2NI$$

$$\begin{cases} I\left(\dot{p}+\dot{\sigma}_{1l}\right)=M_{1l}^{i}+M_{1lx}^{e};\; I\left(\dot{p}+\dot{\sigma}_{2l}\right)=M_{2l}^{i}+M_{2lx}^{e} \\ I\left(\dot{q}+\dot{\sigma}_{3l}\right)=M_{3l}^{i}+M_{3ly}^{e};\; I\left(\dot{q}+\dot{\sigma}_{4l}\right)=M_{4l}^{i}+M_{4ly}^{e} \\ I\left(\dot{r}+\dot{\sigma}_{5l}\right)=M_{5l}^{i}+M_{5lz}^{e};\; I\left(\dot{r}+\dot{\sigma}_{6l}\right)=M_{6l}^{i}+M_{6lz}^{e} \end{cases} \qquad (4')$$

II.3. The Euler parameters

$$\begin{cases} \lambda_0=\cos\dfrac{\chi}{2}; \\ \lambda_1=\cos\alpha\sin\dfrac{\chi}{2} \\ \lambda_2=\cos\beta\sin\dfrac{\chi}{2} \\ \lambda_3=\cos\gamma\sin\dfrac{\chi}{2} \end{cases}$$

$$2\dot{\boldsymbol{\lambda}}=\boldsymbol{\Theta}\cdot\boldsymbol{\lambda}\qquad (5)$$

$$\boldsymbol{\lambda}=\begin{bmatrix}\lambda_0\\ \lambda_1\\ \lambda_2\\ \lambda_3\end{bmatrix},\qquad \boldsymbol{\Theta}=\begin{bmatrix}0 & -p & -q & -r\\ p & 0 & r & -q\\ q & -r & 0 & p\\ r & q & -p & 0\end{bmatrix}$$

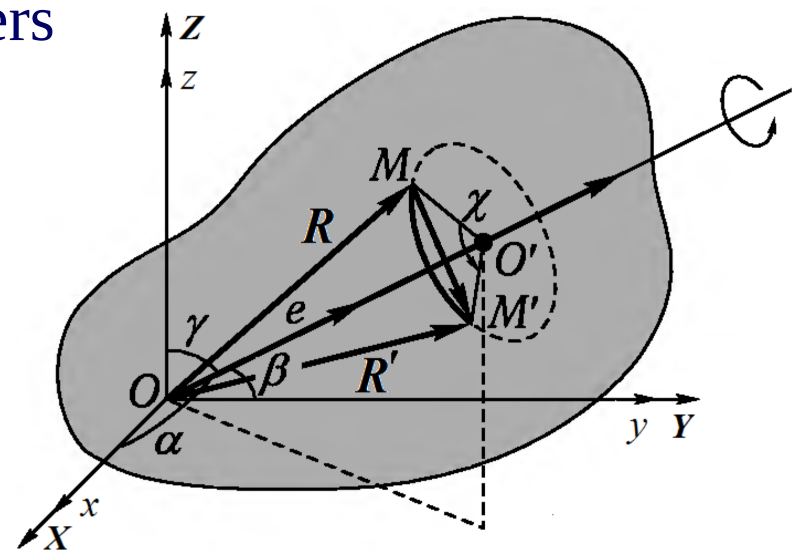

II.4. The conjugate spinups and captures

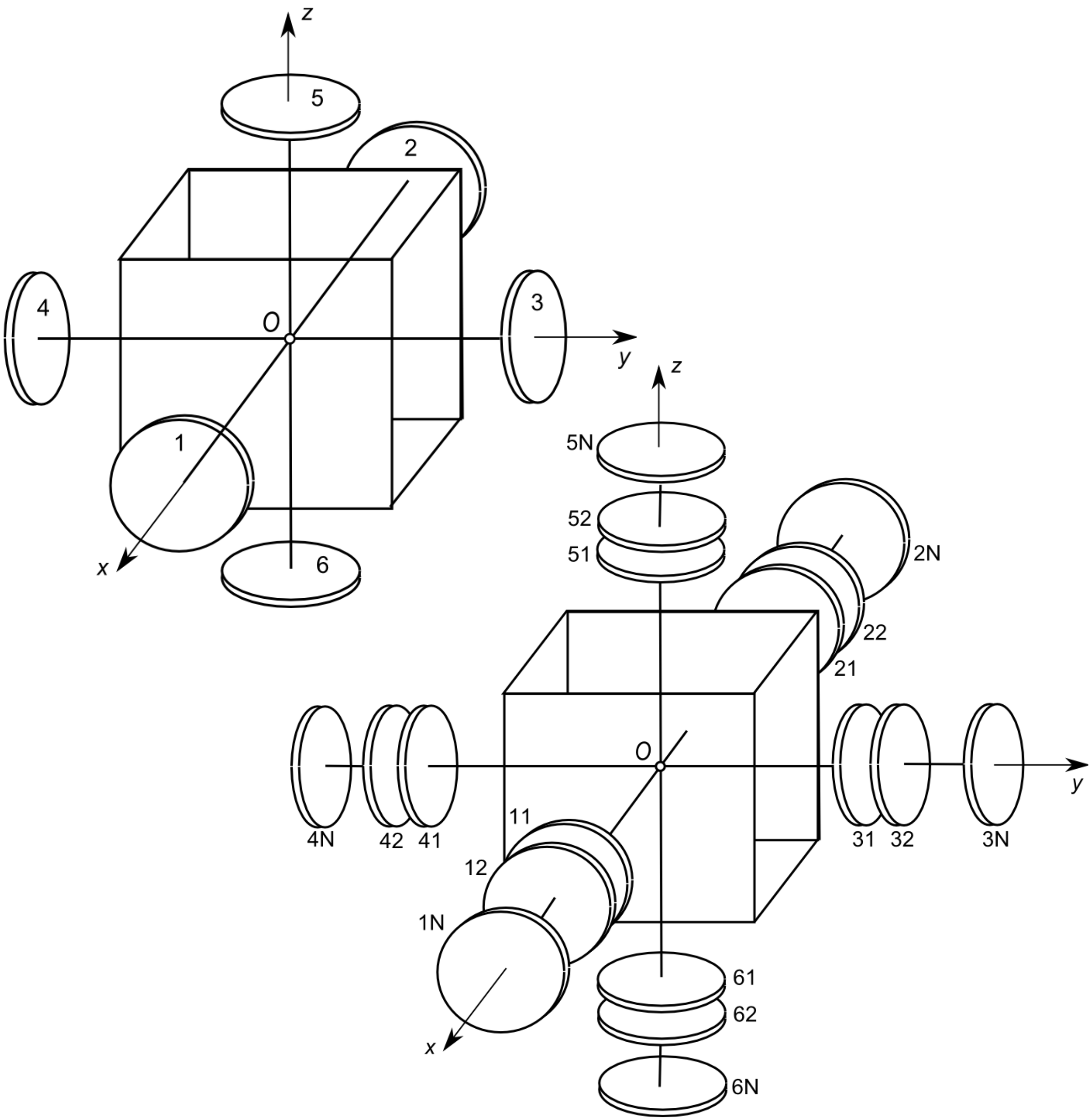

Def.1. Conjugate rotors are paired rotors located in the same layer on the opposite rays. For example, rotor 3N and rotor 4N are conjugate rotors (also rotor 12 and rotor 22, etc.).

Def.2. Conjugate spinup mean a process of spinning up conjugate rotors in opposite directions up to a desired value of relative angular velocity with the help of internal moments from main body. Velocities of conjugate rotors will be equal in absolute value and opposite in sign.

Def.3. Rotor capture is an immediate deceleration of rotor relative angular velocity with the help of internal moment from the main body. So, rotor capture means an "instantaneous freezing" of rotor with respect to the main body. The capture can be performed with the help of gear meshing, friction clutch or other methods.

II.5. Method of attitude reorientation of multiple-rotor system

Conjugate rotors → *Conjugate spinups* → *Rotor captures*

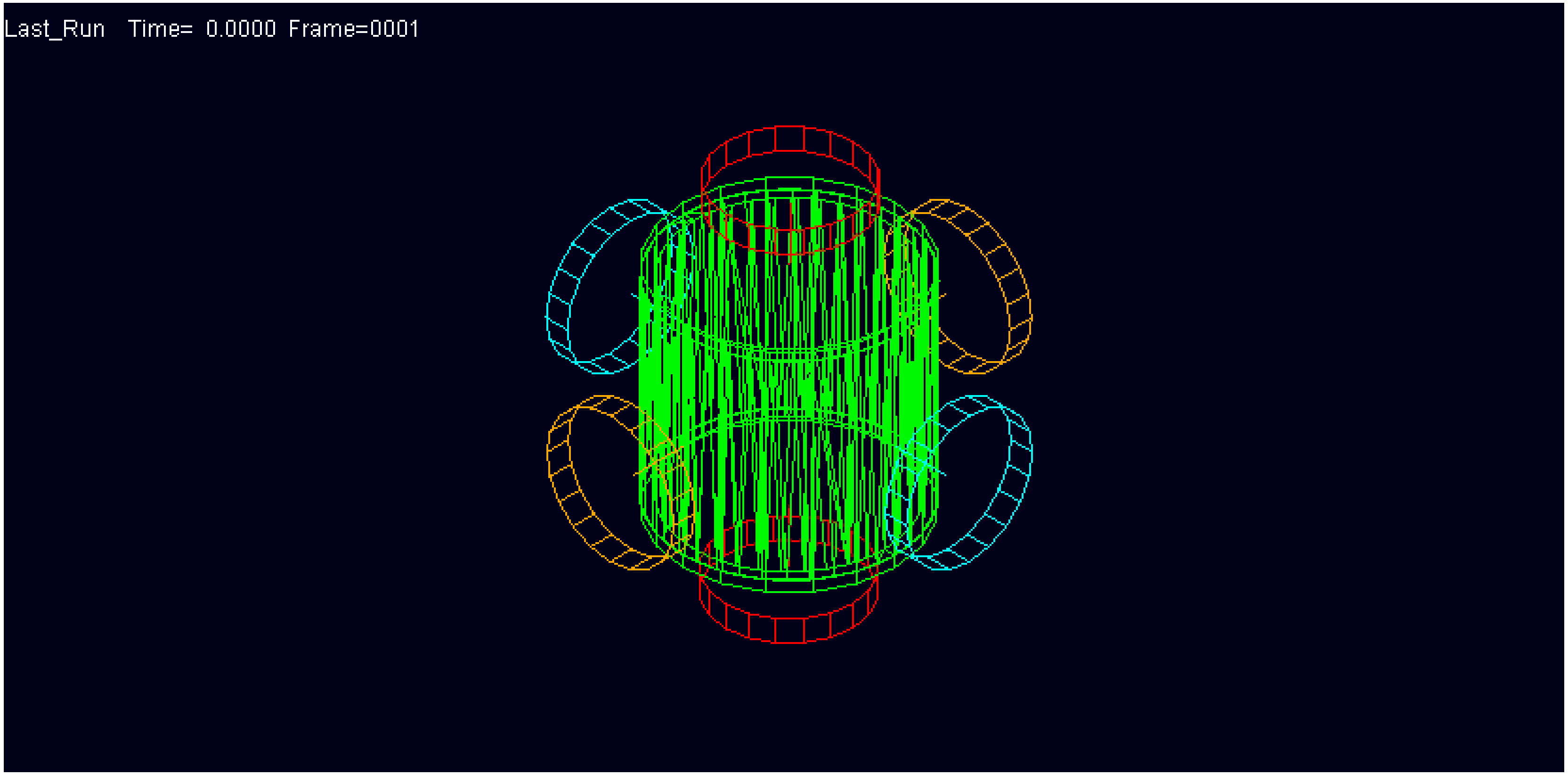

Patent: RU 2009115267/11 – 21 april 2009 – Doroshin A.V.

II.6. Analytical solutions of motion equations

$$\left(M_x^e = M_y^e = M_z^e = 0\right)$$

$$A = B = C = D$$

Conjugate spinup of rotors #1, 2

$$M_1^i = \begin{cases} M_{12}, & if \quad t \in \left[0, t_{12}^s\right] \\ 0, & otherwise \end{cases}$$

$$M_2^i = \begin{cases} -M_{12}, & if \ t \in \left[0, t_{12}^s\right] \\ 0, & otherwise \end{cases} \qquad (6)$$

$$\sigma_1 = S_{12}, \ \sigma_2 = -S_{12}$$

$$S_{12} = M_{12} \cdot t_{12}^s / I$$

Rotor #1 capture

$$t_1^c \quad \left(t_1^c > t_{12}^s\right) \longrightarrow \sigma_1' = 0$$

$$\sigma_1' = 0$$

$$p = \frac{IS_{12}}{A - I}$$

$$\sigma_2' = -\frac{AS_{12}}{A - I}$$

Rotor #2 capture

$$t_2^c \quad \left(t_2^c > t_1^c\right)$$

Two serial captures of conjugate rotors bring to piecewise constant angular velocity of the main body

$$p = \begin{cases} 0, & t \in \left[0, t_1^c\right) \cup \left(t_2^c, \infty\right) \\ P = \dfrac{IS_{12}}{A - I}, & t \in \left[t_1^c, t_2^c\right] \end{cases}$$

The main body performed the rotation about *Ox* axis by finite angle

$$\varphi_x = \frac{IS_{12}\left(t_2^c - t_1^c\right)}{A - I}$$

Let's assume synchronically captures of coresponded conjugate rotors {1, 2}, {3, 4}, {5, 6} and coincidence of the frame *Oxyz* initial position and the fixed frame *OXYZ*

$$t_1^c = t_3^c = t_5^c = t_{start}^c; \quad t_2^c = t_4^c = t_6^c = t_{finish}^c$$

$$\lambda_0\left(t_{start}^c\right) = 1;\ \lambda_1\left(t_{start}^c\right) = \lambda_2\left(t_{start}^c\right) = \lambda_3\left(t_{start}^c\right) = 0 \qquad (18)$$

Angular velocities between conjugate captures of rotors

$$t \in \left[t_1, t_2\right]: \quad p = P;\ q = Q;\ r = R \qquad (19)$$

Solutions of kinematic equations (5)

$$\lambda_0(t) = \cos\frac{\Omega\cdot\left(t - t_{start}^c\right)}{2}; \qquad \lambda_1(t) = \frac{P}{\Omega}\sin\frac{\Omega\cdot\left(t - t_{start}^c\right)}{2}$$

$$\lambda_2(t) = \frac{Q}{\Omega}\sin\frac{\Omega\cdot\left(t - t_{start}^c\right)}{2}; \quad \lambda_3(t) = \frac{R}{\Omega}\sin\frac{\Omega\cdot\left(t - t_{start}^c\right)}{2} \qquad (20)$$

$$\Omega = \sqrt{P^2 + Q^2 + R^2}; \quad t \in \left[t_{start}^c, t_{finish}^c\right]; \quad T = t_{finish}^c - t_{start}^c$$

The main body performed finite rotation about vector **e** by angle χ

$$\mathbf{e} = \left[\cos\alpha = \frac{P}{\Omega},\ \cos\beta = \frac{Q}{\Omega},\ \cos\gamma = \frac{R}{\Omega}\right]^T \qquad (21)$$

$$\chi = \Omega T$$

II.7. Numerical simulation of reorientation process

$$M_j^i = M_{jj*} \cdot \left[H(t) - H\left(t - t^s\right) \right] - \nu \sigma_j \cdot H\left(t - t_j^c\right)$$

$$M_{j*}^i = -M_{jj*} \cdot \left[H(t) - H\left(t - t^s\right) \right] - \nu \sigma_{j*} \cdot H\left(t - t_{j*}^c\right)$$

$$M_{jj*} = \text{const} > 0; \quad \nu >> 1; \quad j = 1,3,5; \quad j* = 2,4,6$$

$H(t)$ is Heaviside function

Two sets of results of numerical simulation

Fig.A - zero value of angular momentum and different inertia moments of main body.

Fig.4 - reorientation process at nonzero system angular momentum:

$$\boldsymbol{\omega}(0) = \sigma_1(0) = \ldots = \sigma_4(0) = 0; \quad \sigma_5(0) = 100 \quad 1/s$$

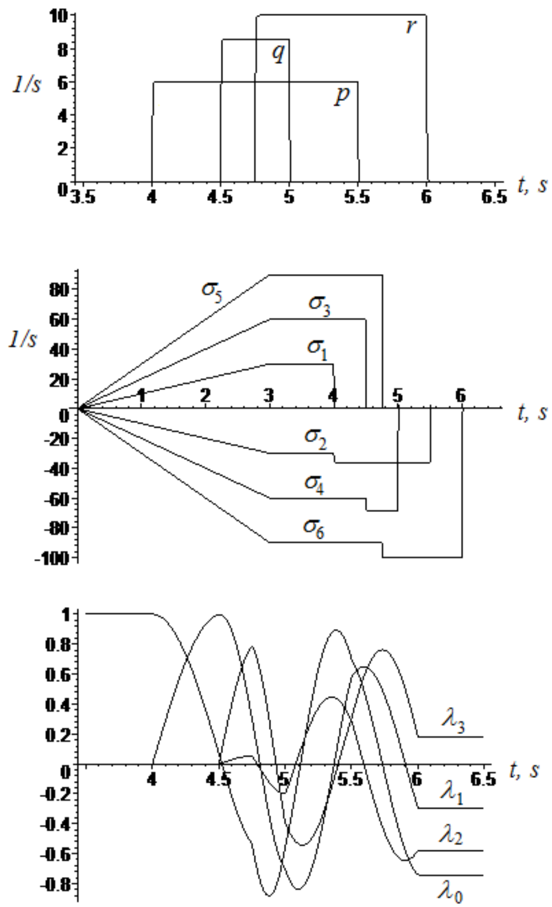

Fig. A

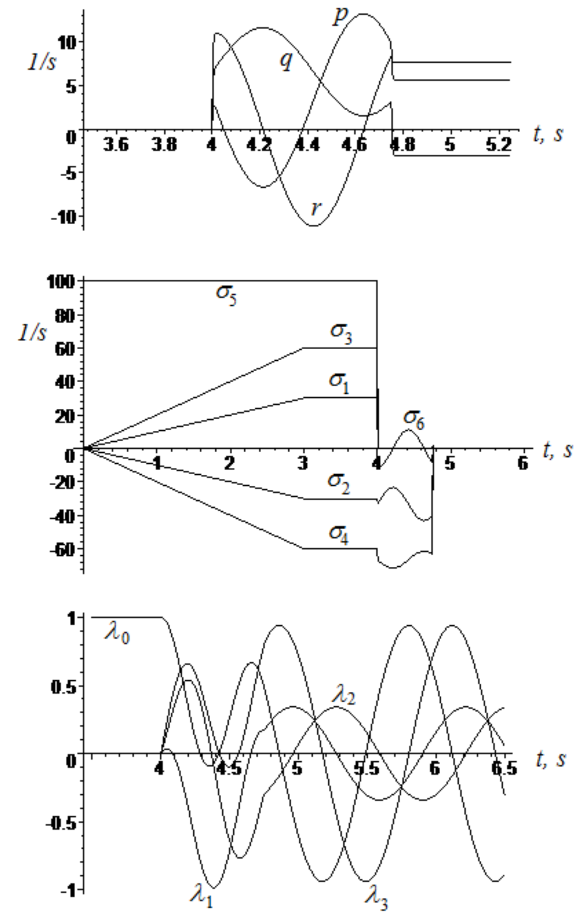

Fig. B

$\nu = 300\ N \cdot m \cdot s$

Table I. *Numerical parameters for calculations*

	A, $kg \cdot m^2$	B, $kg \cdot m^2$	C, $kg \cdot m^2$	I, $kg \cdot m^2$	t_1^c, s	t_2^c, s	t_3^c, s	t_4^c, s	t_5^c, s	t_6^c, s	M_{12}, $N \cdot m$	M_{34}, $N \cdot m$	M_{56}, $N \cdot m$
Fig. A	60	80	100	10	4.0	5.5	4.5	5.0	4.75	6.0	10	20	30
Fig. B	100	100	100	10	4.0	4.75	4.0	4.75	4.0	4.75	10	20	0

II.8. ADAMS motion animations

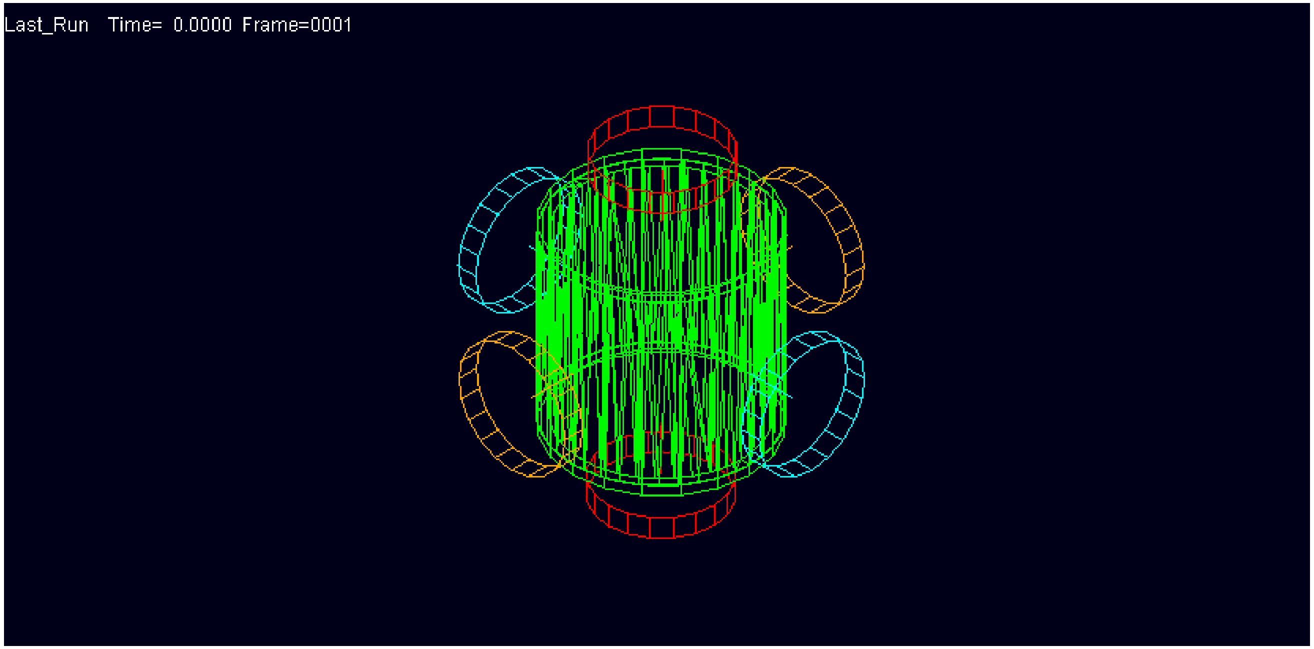

← Case of motion with zero initial value angular momentum of system.

Case of motion with non-zero initial value angular momentum of system→

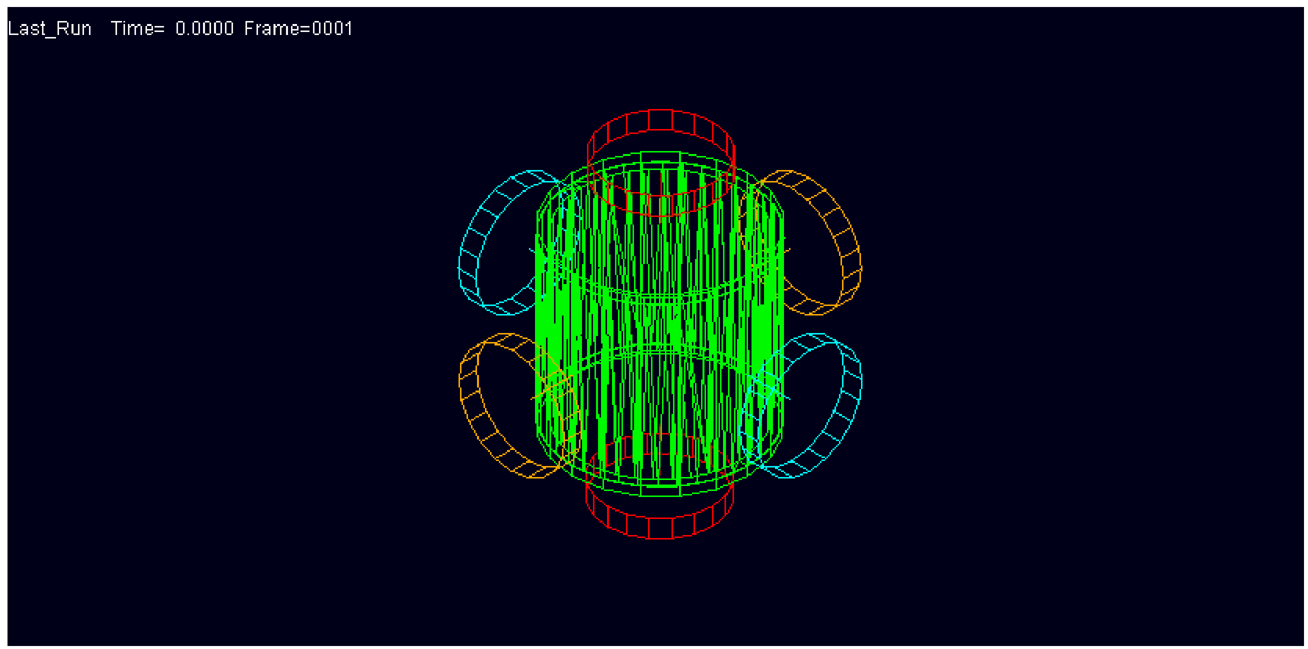

II.9. Hamiltonian form of equations

Kinetic energies of six rotors in j-layer are

$$2T_{1j} = J_j\left(q^2 + r^2\right) + I_j\left(p + \sigma_{1j}\right)^2; \quad 2T_{2j} = J_j\left(q^2 + r^2\right) + I_j\left(p + \sigma_{2j}\right)^2$$

$$2T_{3j} = J_j\left(p^2 + r^2\right) + I_j\left(q + \sigma_{3j}\right)^2; \quad 2T_{4j} = J_j\left(p^2 + r^2\right) + I_j\left(q + \sigma_{4j}\right)^2 \qquad (6)$$

$$2T_{5j} = J_j\left(p^2 + q^2\right) + I_j\left(r + \sigma_{5j}\right)^2; \quad 2T_{6j} = J_j\left(p^2 + q^2\right) + I_j\left(r + \sigma_{6j}\right)^2$$

Kinetic energy of the system has the following expression

$$T = T_0 + \sum_{j=1}^{N} T_j; \qquad 2T_0 = \tilde{A}p^2 + \tilde{B}q^2 + \tilde{C}r^2; \qquad T_j = \sum_{i=1}^{6} T_{ij}; \qquad (7)$$

$$2T_j = \left(2I_j + 4J_j\right)\left(p^2 + q^2 + r^2\right) +$$

$$+2I_j\left(p\left[\sigma_{1j} + \sigma_{2j}\right] + q\left[\sigma_{3j} + \sigma_{4j}\right] + r\left[\sigma_{5j} + \sigma_{6j}\right]\right) + I_j\sum_{i=1}^{6}\sigma_{ij}^2$$

II.10. Andoyer-Deprit canonical variables

$$L = \frac{\partial \mathrm{T}}{\partial \dot{l}} = \mathbf{K}\cdot\mathbf{k}, \quad G = \frac{\partial \mathrm{T}}{\partial \dot{\varphi}_2} = \mathbf{K}\cdot\mathbf{s} = K, \quad H = \frac{\partial \mathrm{T}}{\partial \dot{\varphi}_3} = \mathbf{K}\cdot\mathbf{k}', \quad \Delta_{ij} = \frac{\partial \mathrm{T}}{\partial \dot{\delta}_{ij}} = \frac{\partial \mathrm{T}}{\partial \sigma_{ij}} \qquad (8)$$

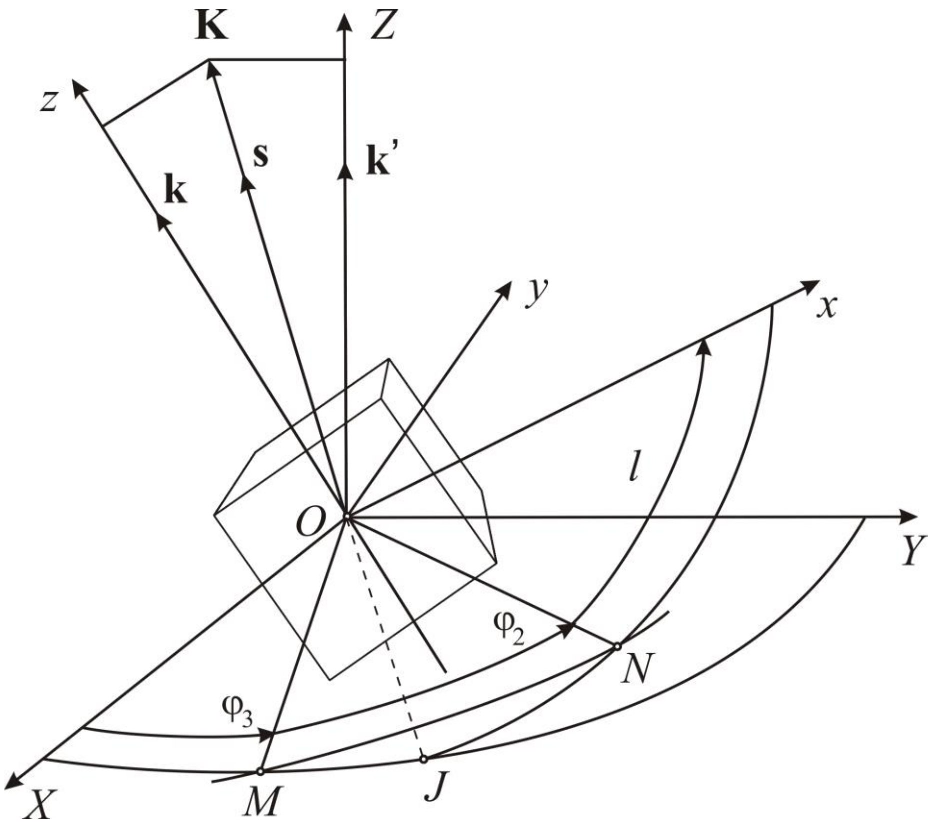

$$K_x = \sqrt{G^2 - L^2}\sin l = Ap + \sum_{j=1}^{N} I_j\left(\sigma_{1j} + \sigma_{2j}\right)$$

$$K_y = \sqrt{G^2 - L^2}\cos l = Bq + \sum_{j=1}^{N} I_j\left(\sigma_{3j} + \sigma_{4j}\right) \qquad (9)$$

$$K_z = L = Cr + \sum_{j=1}^{N} I_j\left(\sigma_{5j} + \sigma_{6j}\right), \qquad \left(L \le G\right)$$

$$\Delta_{1j} = I_j\left(p + \sigma_{1j}\right); \quad \Delta_{2j} = I_j\left(p + \sigma_{2j}\right)$$

$$\Delta_{3j} = I_j\left(q + \sigma_{3j}\right); \quad \Delta_{4j} = I_j\left(q + \sigma_{4j}\right) \qquad (10)$$

$$\Delta_{5j} = I_j\left(r + \sigma_{5j}\right); \quad \Delta_{6j} = I_j\left(r + \sigma_{6j}\right)$$

$$\sum_{j=1}^{N} I_j\left(\sigma_{1j} + \sigma_{2j}\right) = \sum_{j=1}^{N}\left(\Delta_{1j} + \Delta_{2j}\right) - 2p\sum_{j=1}^{N} I_j \qquad \sum_{j=1}^{N} I_j\left(\sigma_{3j} + \sigma_{4j}\right) = \sum_{j=1}^{N}\left(\Delta_{3j} + \Delta_{4j}\right) - 2q\sum_{j=1}^{N} I_j \qquad (11)$$

$$\sum_{j=1}^{N} I_j\left(\sigma_{5j} + \sigma_{6j}\right) = \sum_{j=1}^{N}\left(\Delta_{5j} + \Delta_{6j}\right) - 2r\sum_{j=1}^{N} I_j$$

The angular velocity components in the Andoyer-Deprit variables

$$p=\frac{1}{\hat{A}}\left[\sqrt{G^2-L^2}\sin l-\sum_{j=1}^{N}\left(\Delta_{1j}+\Delta_{2j}\right)\right] \qquad q=\frac{1}{\hat{B}}\left[\sqrt{G^2-L^2}\cos l-\sum_{j=1}^{N}\left(\Delta_{3j}+\Delta_{4j}\right)\right]$$

$$r=\frac{1}{\hat{C}}\left[L-\sum_{j=1}^{N}\left(\Delta_{5j}+\Delta_{6j}\right)\right] \qquad (12)$$

$$\hat{A}=A-2\sum_{j=1}^{N}I_j;\ \ \hat{B}=B-2\sum_{j=1}^{N}I_j;\ \ \hat{C}=C-2\sum_{j=1}^{N}I_j$$

Kinetic energy in Andoyer-Deprit variables:

$$\begin{aligned}2T=&\left(G^2-L^2\right)\left[\frac{\sin^2 l}{\hat{A}}+\frac{\cos^2 l}{\hat{B}}\right]+\frac{1}{\hat{C}}\left(L-\sum_{j=1}^{N}\left[\Delta_{5j}+\Delta_{6j}\right]\right)^2-\\ &-2\sqrt{G^2-L^2}\left\{\frac{\sin l}{\hat{A}}\cdot\sum_{j=1}^{N}\left[\Delta_{1j}+\Delta_{2j}\right]+\frac{\cos l}{\hat{B}}\cdot\sum_{j=1}^{N}\left[\Delta_{3j}+\Delta_{4j}\right]\right\}+\\ &+\frac{1}{\hat{A}}\left(\sum_{j=1}^{N}\left[\Delta_{1j}+\Delta_{2j}\right]\right)^2+\frac{1}{\hat{B}}\left(\sum_{j=1}^{N}\left[\Delta_{3j}+\Delta_{4j}\right]\right)^2+\sum_{j=1}^{N}\sum_{i=1}^{6}\frac{\Delta_{ji}^2}{I_j}\end{aligned} \qquad (13)$$

Hamiltonian of the system takes the form

$$H = T = \frac{G^2 - L^2}{2}\left[\frac{\sin^2 l}{\hat{A}} + \frac{\cos^2 l}{\hat{B}}\right] + \frac{1}{2\hat{C}}\left(L - D_{56}\right)^2 - \tag{14}$$

$$-\sqrt{G^2 - L^2}\left\{\frac{D_{12}\sin l}{\hat{A}} + \frac{D_{34}\cos l}{\hat{B}}\right\} + \frac{D_{12}^2}{2\hat{A}} + \frac{D_{34}^2}{2\hat{B}} + T_R = h = \text{const},$$

$$D_{12} = \sum_{j=1}^{N}\left[\Delta_{1j} + \Delta_{2j}\right], \quad D_{34} = \sum_{j=1}^{N}\left[\Delta_{3j} + \Delta_{4j}\right]$$

$$D_{56} = \sum_{j=1}^{N}\left[\Delta_{5j} + \Delta_{6j}\right], \quad T_R = \frac{1}{2}\sum_{j=1}^{N}\sum_{i=1}^{6}\frac{\Delta_{ji}^2}{I_j}. \tag{15}$$

$$\dot{Q} = \frac{\partial H}{\partial P}; \quad \dot{P} = -\frac{\partial H}{\partial Q} \tag{16}$$

$$Q = \left\{l, \varphi_2, \varphi_3, \delta_{ij}\right\}, \quad P = \left\{L, G, H, \Delta_{ij}\right\}$$

The canonical equations for Andoyer-Deprit variables

$$\dot{L} = -\frac{\partial H}{\partial l} = -\frac{G^2 - L^2}{2}\left[\frac{1}{\hat{A}} - \frac{1}{\hat{B}}\right]\sin 2l - \sqrt{G^2 - L^2}\, D \sin\left(l - s\right) \tag{17}$$

$$\dot{l} = \frac{\partial H}{\partial L} = L\left[\frac{1}{\hat{C}} - \left(\frac{1}{2\hat{A}} + \frac{1}{2\hat{B}}\right) - \left(\frac{1}{2\hat{B}} - \frac{1}{2\hat{A}}\right)\cos 2l + \frac{D\cos\left(l - s\right)}{\sqrt{G^2 - L^2}}\right] - \frac{D_{56}}{\hat{C}}$$

$$D = \sqrt{\frac{D_{12}^2}{\hat{A}^2} + \frac{D_{34}^2}{\hat{B}^2}}, \quad \cos\left(s\right) = \frac{D_{34}}{\hat{B}D}$$

II.11. Investigation of motion modes

II.11.1. Case of motion of the system with dynamically symmetrical main body : $\hat{A} = \hat{B}$

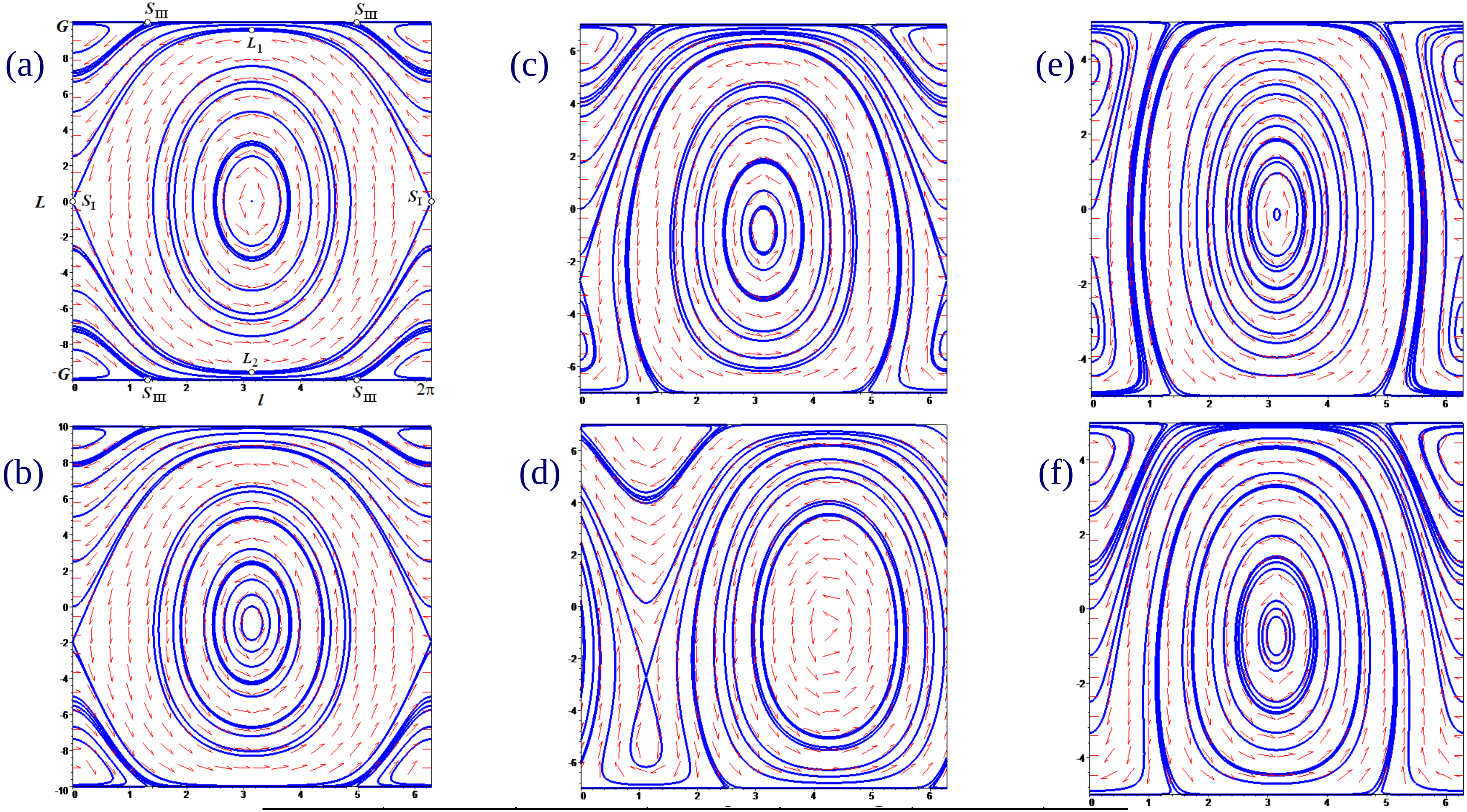

Momentum	Case (a)	(b)	(c)	(d)	(e)	(f)
G, N·m·s	10	10	7	7	5	5
D_{12}, N·m·s	0	0	0	0.9	0	0
D_{34}, N·m·s	1	1	1	0.44	1	1
D_{56}, N·m·s	0	0.5	0.5	0.5	0.1	0.5

$\hat{A} = \hat{B} = 0.5$

$\hat{C} = 0.7$

II.11.2. Case Of Triaxial Main Body : $\hat{A} < \hat{B} < \hat{C}$ and $D_{12} = D_{56} = 0$

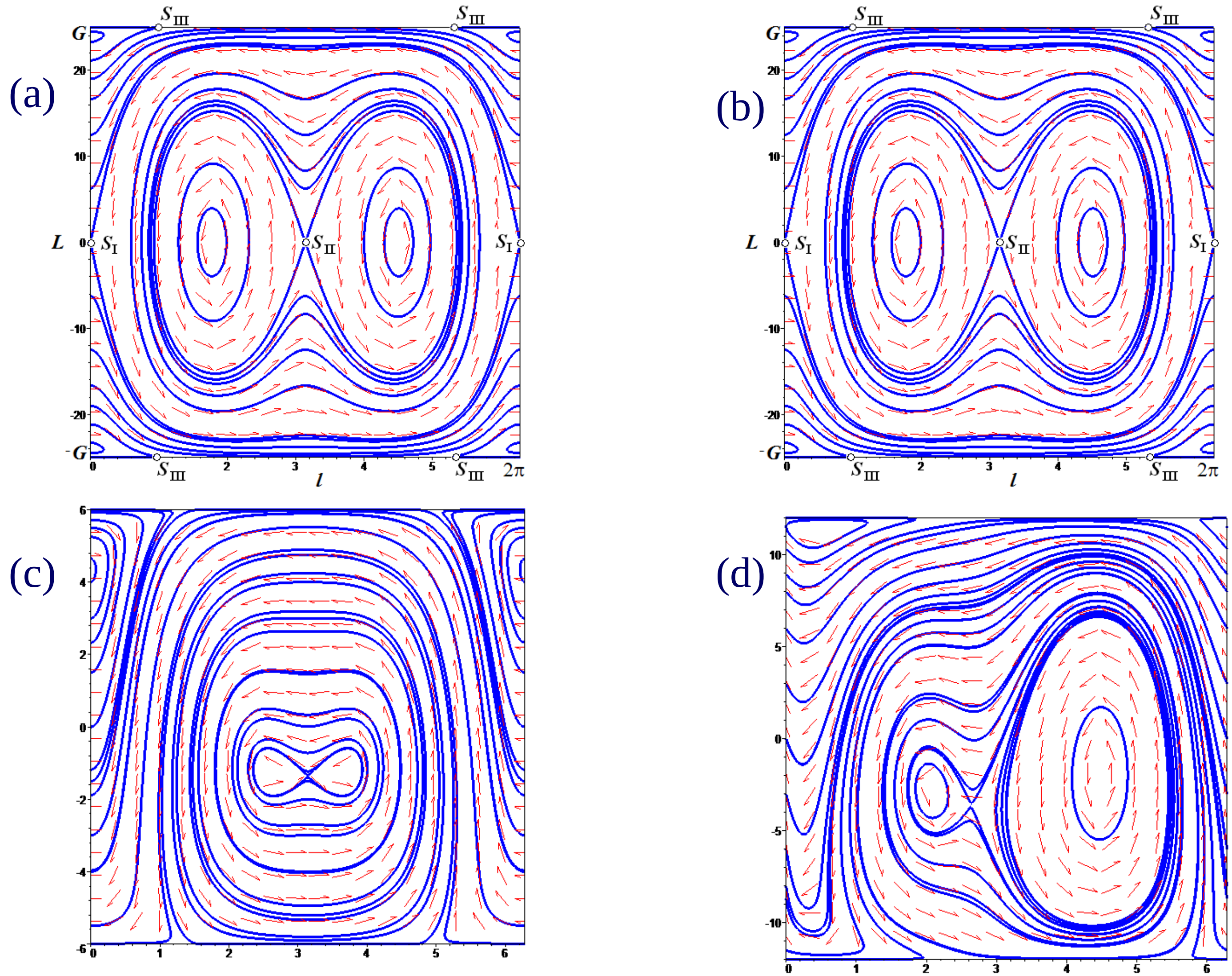

$\hat{A} = 0.5$

$\hat{B} = 0.6$

$\hat{C} = 0.7$

Momentum	Case (a)	(b)	(c)	(d)
G, N·m·s	25	12	6	12
D_{12}, N·m·s	0	0	0	0.6
D_{34}, N·m·s	1	1	1	0.7
D_{56}, N·m·s	0	0	0.5	0.9

II.12. Modelling results of the chaotic motion

Perturbations of rotors angular velocities:

$$D_{12} = \varepsilon \sin(\nu_{12} t); \quad D_{34} = \varepsilon \sin(\nu_{34} t); \quad D_{56} = \varepsilon \sin(\nu_{56} t)$$

Puancare intersections: $\{L/G,\, l\}$; $\quad \nu_{12} t \bmod 2\pi$

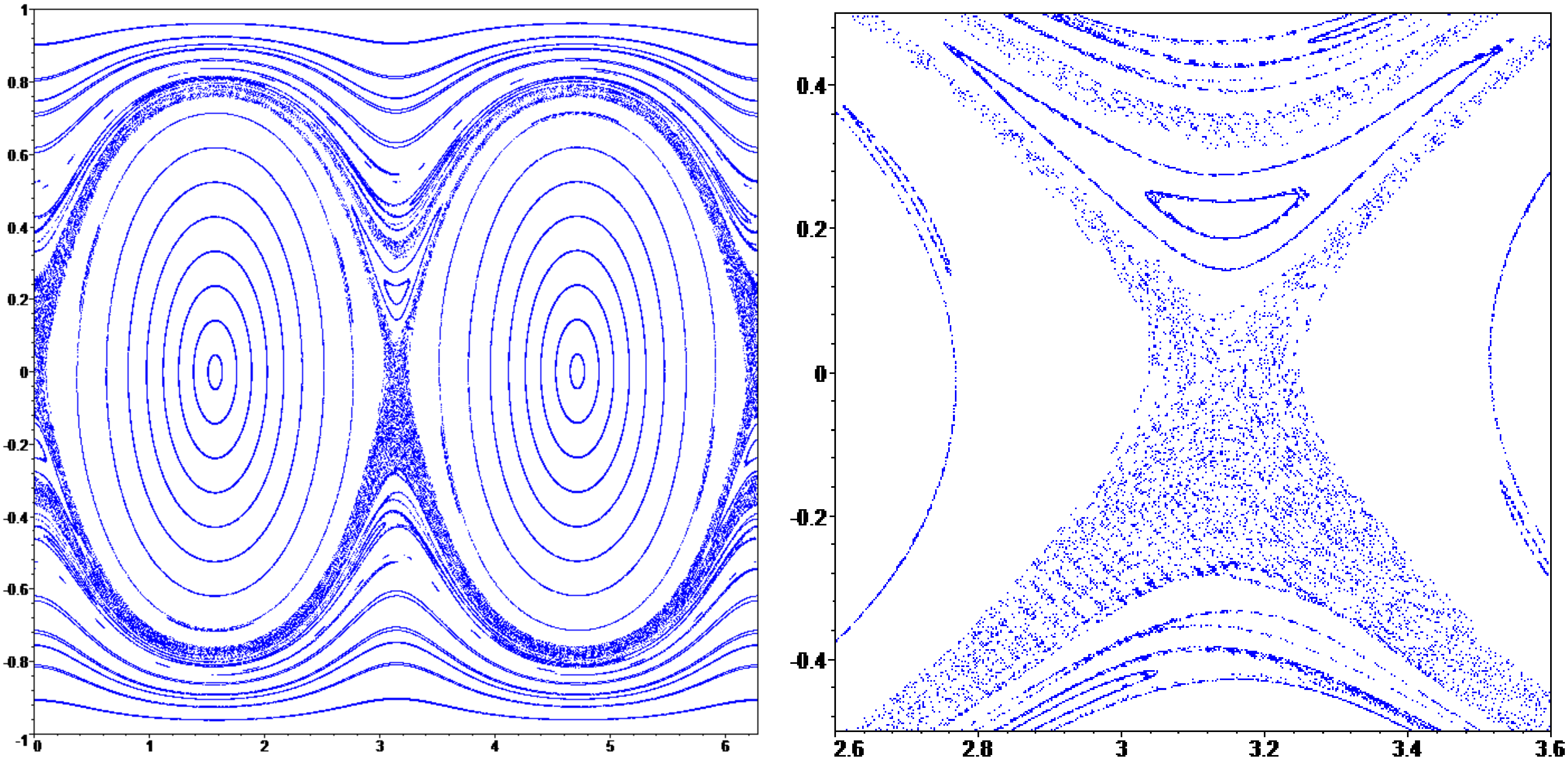

A_=0.5; B_=0.6; C_=0.7; $\quad \varepsilon = 0.025; \quad \nu_{12} = 2; \quad \nu_{12} = 8; \quad \nu_{12} = 16;$

A_=0.5; B_=0.6; C_=0.7; $\varepsilon = 0.025$; $v_{12} = 2$; $v_{12} = 4$; $v_{12} = 8$;

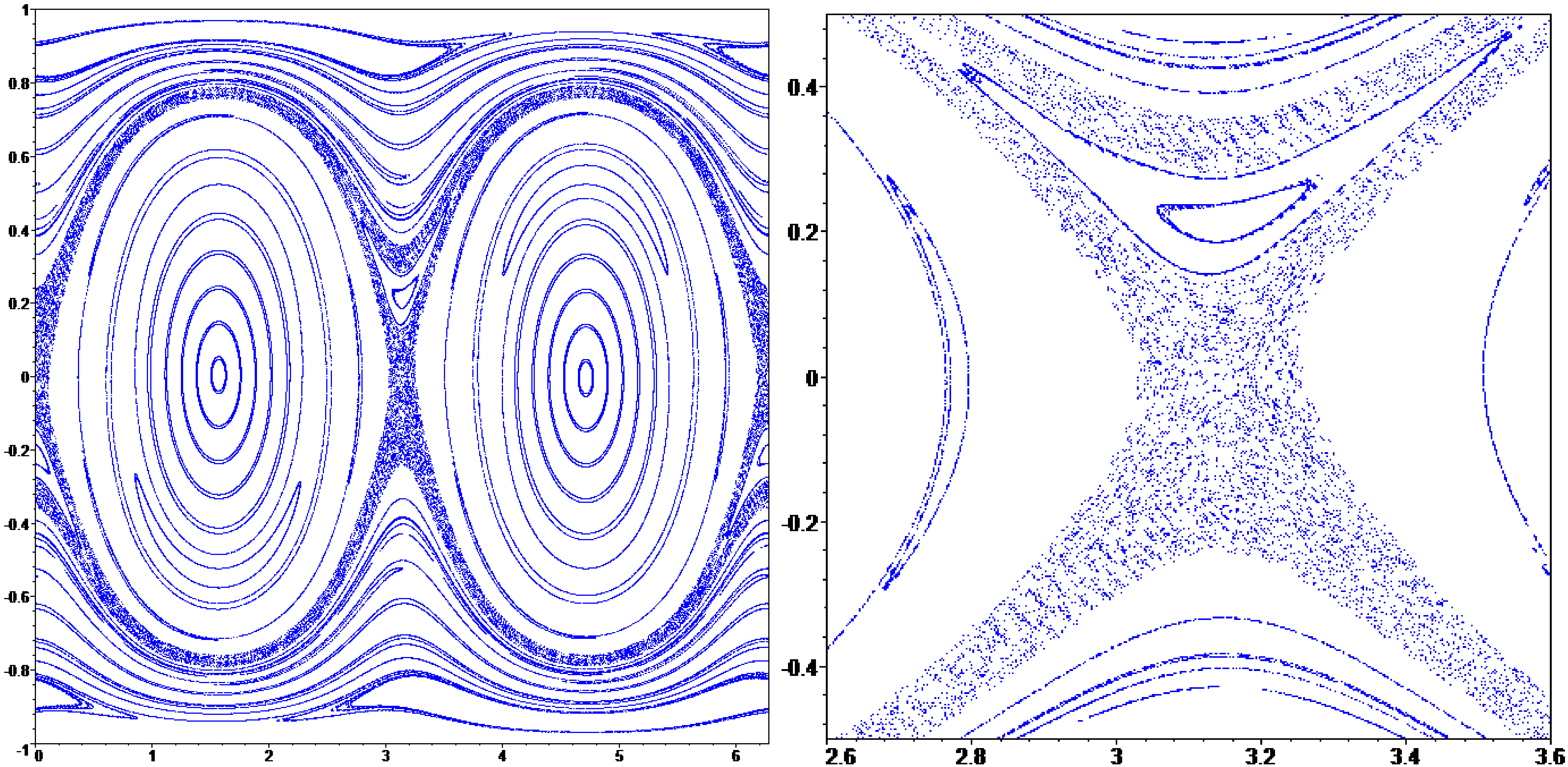

A_=0.5; B_=0.6; C_=0.7; $\varepsilon = 0.025$; $v_{12} = 2$; $v_{12} = 5.1$; $v_{12} = 7.5$;

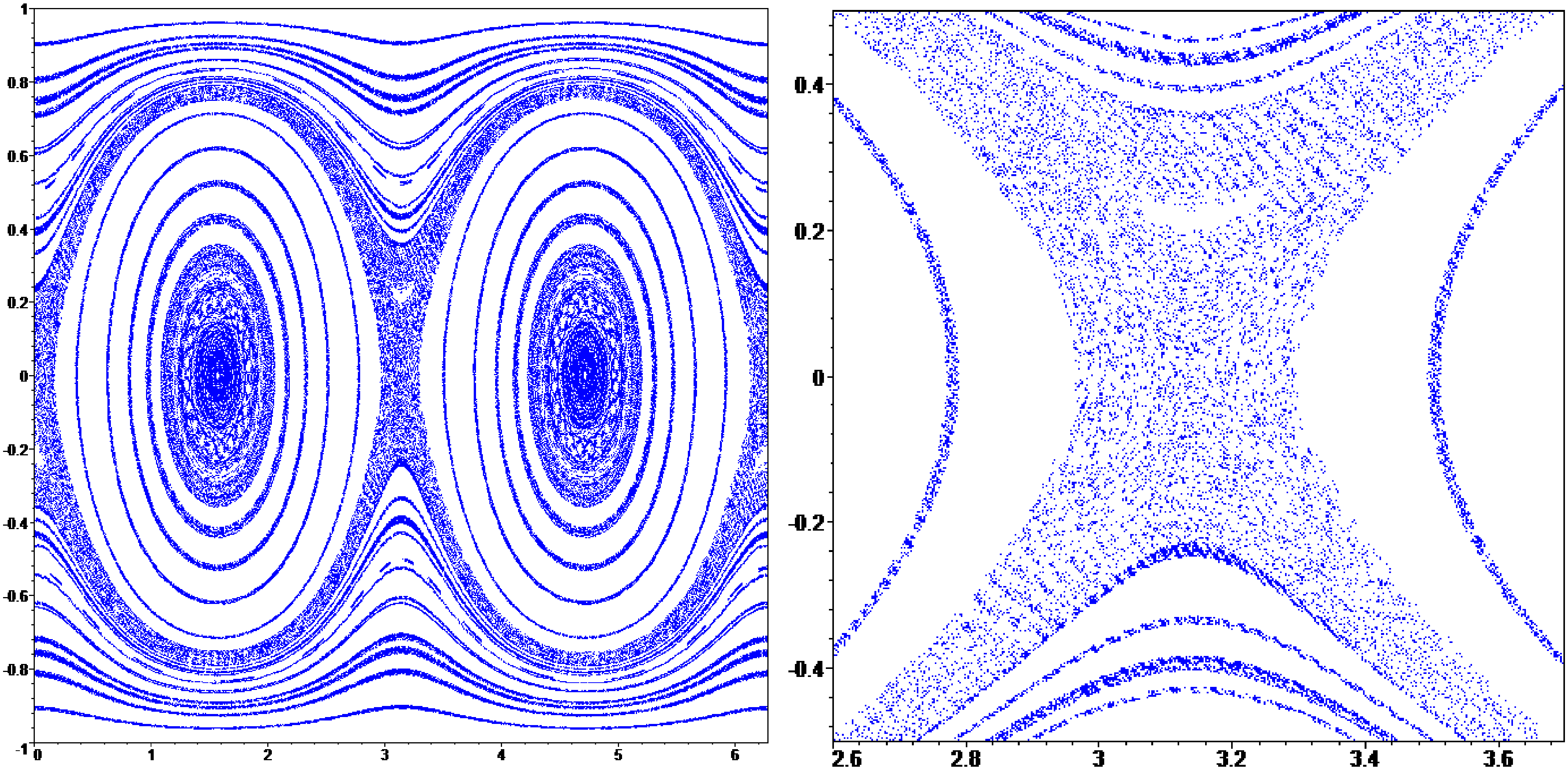

III. ADAMS motion animations of multirotor Roll-Walking Robots

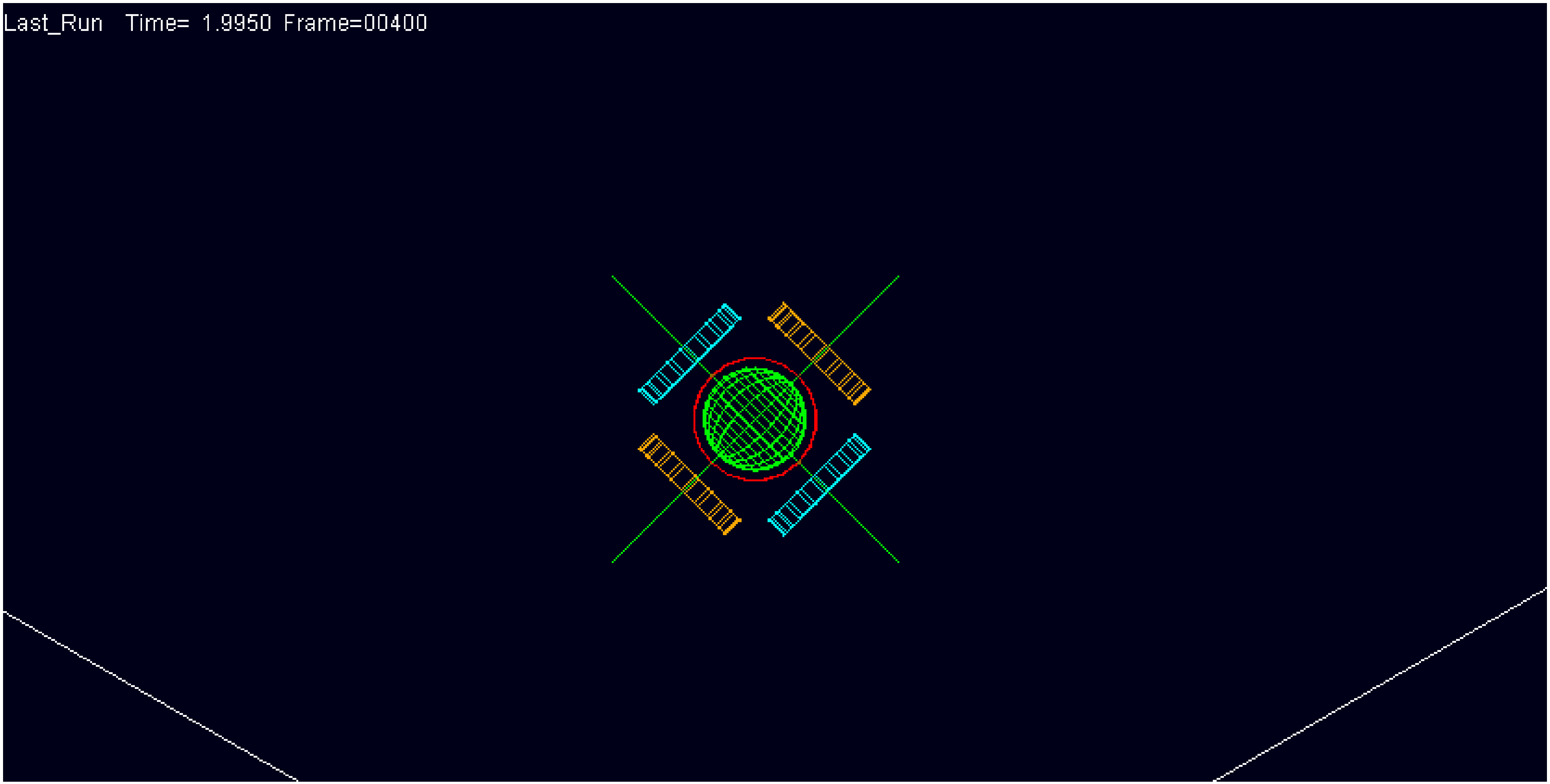

Conclusion

The main properties of the attitude stabilization and control of SC (and multirotor systems) have been examined.

Research into attitude motion of the one-body-SC, dual-spin SC and spider-type-SC is very complicated.

Nontrivial and chaotic modes are possible in the SC attitude motion.

Acknowledgments:

This work is supported by the Russian Science Foundation (# **19-19-00085**).